HIGHWAY RESEARCH RECORD

Number 329

Design and Performance of Rigid and Flexible Pavements

6 Reports

Subject Areas

25 Pavement Design
40 Maintenance, General

HIGHWAY RESEARCH BOARD
DIVISION OF ENGINEERING NATIONAL RESEARCH COUNCIL
NATIONAL ACADEMY OF SCIENCES—NATIONAL ACADEMY OF ENGINEERING
WASHINGTON, D.C. 1970

ISBN 0-309-01832-3

Price: $3.20

Available from

Highway Research Board
National Academy of Sciences
2101 Constitution Avenue
Washington, D.C. 20418

Department of Design

W. B. Drake, Chairman
Kentucky Department of Highways, Lexington

L. F. Spaine
Highway Research Board Staff

PAVEMENT DIVISION

Milton E. Harr, Chairman
Purdue University, Lafayette, Indiana

COMMITTEE ON RIGID PAVEMENT DESIGN

(As of December 31, 1969)

F. H. Scrivner, Chairman
Texas Transportation Institute, Texas A&M University, College Station

W. Ronald Hudson, Secretary
University of Texas at Austin

Henry Aaron
Phillip P. Brown
John E. Burke
B. E. Colley
E. A. Finney
Phil Fordyce
William S. Housel
F. N. Hveem
W. H. Jacobs
Wallace J. Liddle
B. F. McCullough
Phillip L. Melville
Lionel T. Murray
L. Frank Pace
Thomas J. Pasko, Jr.
Thomas B. Pringle
Emery L. Shaw
M. D. Shelby
W. T. Spencer
William Van Breemen
K. B. Woods

COMMITTEE ON FLEXIBLE PAVEMENT DESIGN

(As of December 31, 1969)

Stuart Williams, Chairman
Federal Highway Administration, Washington, D.C.

John A. Bishop
W. H. Campen
Bonner S. Coffman
Robert A. Crawford
James M. Desmond
W. B. Drake
Charles R. Foster
John M. Griffith
Frank B. Hennion
Raymond C. Herner
William S. Housel
Wallace J. Liddle
R. E. Livingston
Alfred W. Maner
Chester McDowell
C. E. Minor
Carl L. Monismith
William M. Moore
Frank P. Nichols, Jr.
R. L. Peyton
Donald R. Schwartz
Emery L. Shaw
George B. Sherman
Eugene L. Skok, Jr.
Richard L. Stewart
John H. Swanberg
B. A. Vallerga

Department of Maintenance

J. F. Andrews, Chairman
New Jersey Department of Transportation, Trenton

Adrian G. Clary
Highway Research Board Staff

COMMITTEE ON MAINTENANCE OF PORTLAND CEMENT CONCRETE PAVEMENTS

(As of December 31, 1969)

Francis C. Staib, Chairman
Ohio Turnpike Commission, Berea

J. D. Geesaman, Secretary
Portland Cement Association, Skokie, Illinois

William J. Buglass
Lloyd G. Byrd
R. J. Ervin
Israel Narrow
John P. Pendleton
Keith M. Saville
Donald R. Schwartz
Chris Siebel, Jr.
Richard K. Shaffer
Ronald L. Zook

Foreword

Those interested in the design of pavement systems should be aware of continuing changes and advancements in technology. The 6 papers in this RECORD address the subject of design and performance of both rigid and flexible pavement systems. Investigations on the subject include analytical and laboratory techniques as well as field testing and observations.

The validity of an analytical method can be applied with confidence when its solutions are confirmed with actual test results. Agarwal and Hudson report on the verification of discrete-element solutions for pavement slabs by use of tests with small-dimension aluminum slabs resting on saturated clay subgrades. They conclude that this analytical method can be used to provide satisfactory solutions for pavement slabs.

The paper by Treybig, Hudson, and McCullough describes a sensitivity analysis using an extended AASHO Interim Guide Mathematical Model to determine the change in rigid pavement service life caused by unit changes in independent design variables. The analysis determined the relative importance of and significant interaction among the design variables and also evaluated the stochastic variation for each variable.

Teng's paper covers an observation study of continuously reinforced concrete pavements constructed in Mississippi since 1961. Reported are failure investigations, repair procedures, and a preliminary review of design and construction statistics related to crack spacing. Also presented and discussed are design features and measurements made on experimental projects constructed in 1961 and 1962.

Fredrickson, Diethelm, and Zwiers report on the development of a new flexible pavement design from results of the Minnesota Department of Highways AASHO Satellite Test Program on 50 selected roadways. The design emanated from the study of the effects of pavement section characteristics, subgrade soil strength, climate, and loading and distribution of traffic on the performance of flexible pavements. A design chart is presented that shows the required gravel equivalent thickness dependent on embankment stabilometer R-value and equivalent 18,000-lb single-axle loads.

The investigation reported by Coffman, Ives, and Edwards was conducted to determine whether asphaltic concrete will respond isotropically to surface forces when used in relatively large volumes such as in structural pavement. Core and block specimens were secured from a contract-constructed pavement in 3 orthogonal directions and tested in unconfined compression and bending. A comparison of the resulting linear complex moduli indicated that, on an engineering basis, the differences found were not considered significant for predicting strains and deflections for a layered pavement structural system.

The final paper by Vaswani covers results of a quantitative evaluation of the thickness equivalences of materials on Interstate, primary, secondary, and subdivision roads in Virginia and a qualitative model study of layered systems. Among other things, the investigation showed that the structural strength of a pavement decreases when a weaker layer lies over a stronger layer or when a weaker layer is sandwiched between 2 stronger layers.

Contents

Experimental Verification of Discrete-Element Solutions for Pavement Slabs

SOHAN L. AGARWAL and W. RONALD HUDSON,
Center for Highway Research, University of Texas at Austin

The validity of any analytical method can best be proved by comparing its solutions with actual test results. To obtain specific test results for use in verification of the discrete-element methods, a study of small-dimension slab-on-foundation under controlled conditions was conducted. An instrumented aluminum slab 9 by 9 by $\frac{1}{8}$ in. was tested resting on a specially prepared saturated clay subgrade under 2 loading positions. Plate-load tests were performed to determine linear and nonlinear characteristics of the soil for representing the subgrade according to the Winkler assumption. These characteristics were also determined from stress-strain relations of the soil, obtained from unconfined compression tests. A comparison of discrete-element solutions and experimental results was made for deflections, principal stresses, and stresses along the edge for different loads. The tests confirm that the discrete-element solutions can be used with confidence to obtain satisfactory solutions for pavement slabs.

•PRIOR TO 1963, the Westergaard solutions for pavement slabs (17, 18, 19, 20) were the best available. Since that time a discrete-element method develop by Hudson and others (3, 4, 5, 6, 10, 14) has overcome many of the limitations of previous methods.

Matlock and Haliburton (10) presented a discrete-element model that satisfied the differential equation for a beam column. The model is a system of rigid bars connected by springs that represent the stiffness of the beam. Hudson and Matlock (3, 4, 5) extended this bar spring model to a slab by using an alternating direction iterative method to solve for the deflected shape of the slab. Stelzer and Hudson (14, 6) utilized a direct matrix manipulation technique to obtain the deflections. For most problems this has been shown to be more efficient computationally than the alternating-direction technique.

In the discrete-element model of the slab as suggested by Hudson and others (3, 4, 5, 6, 14), the slab is replaced by an analogous mechanical model representing all stiffness and support properties of the actual slab (Fig. 1). The joints of the model (Fig. 2) are connected by rigid bars that are in turn interconnected by torsion bars representing the twisting stiffness. The flexible joint models the concentrated bending stiffness and the effects of Poisson's ratio. The soil support is represented by independent elastic springs, i.e., the Winkler foundation, concentrated at the joints.

The deflection at each joint is unknown. The basic equilibrium equations are derived from the free body of the slab joint with all appropriate internal and external forces and reactions. These equations include summing the vertical forces at each joint and summing the moments about each individual bar. A complete derivation of these equations can be found elsewhere (14). The stiffness matrix thus generated is partitioned into submatrices. A back-and-forth recursive technique analogous to Matlock's method of solving beam columns (10) is applied to the submatrices to solve for the deflections; and the slopes, moments, shears, and reactions are computed by using

Paper sponsored by Committee on Rigid Pavement Design and presented at the 49th Annual Meeting.

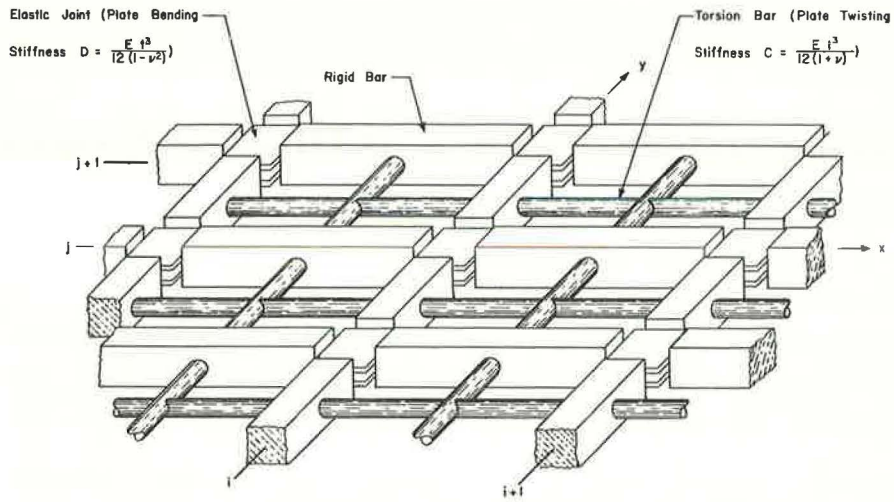

Figure 1. Discrete-element model of a plate or slab (19).

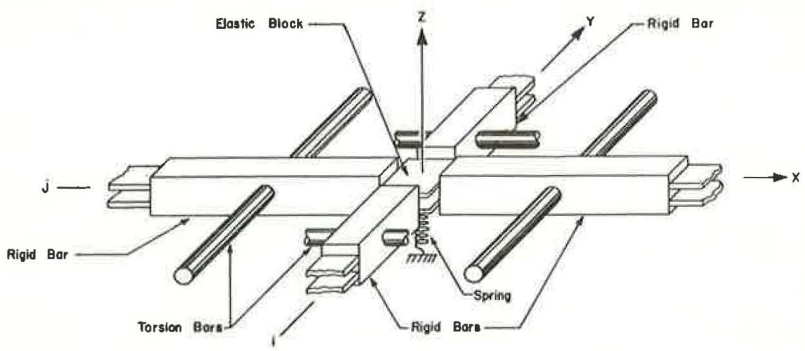

Figure 2. Typical joint i-j taken from discrete-element slab model (19).

the difference-equation relations. Computer programs DSLAB 5 and DSLAB 30 (14 and 11 respectively) have been developed for a slab resting on linearly elastic foundation springs. They are written in FORTRAN computer language for the Control Data Corporation 6600 digital computer. Subsequently the method has been modified by Kelly (7) using nonlinear support characteristics. Salient features of DSLAB 5, DSLAB 30, and DSLAB 26 are given in the Appendix. The method was checked by comparing solutions with data existing for problems in the literature, but more complete checks were needed.

The validity of analytical solutions can best be proved by comparing them with results of carefully controlled tests. To obtain test results for use in verifying discrete-element methods for slabs on foundation, a study was developed in two parts, one to check the modeling and method of solution for plates on simple supports for a variety of stiffness and load conditions, and the second to investigate the modeling of a slab on soil foundation using linear and nonlinear Winkler foundation models (1, 2). Tests were conducted on an instrumented aluminum slab resting on a clay subgrade for a

center load and two-point corner loads. Characteristics of the soil subgrade, for use in the computer program, were determined by tests conducted on circular rigid plates (12), and from stress-strain relationships of the soil obtained from unconfined compression tests. This paper briefly describes the second portion of the study including development of the test procedure, various tests conducted, representation of the soil by linear and nonlinear characteristics, and comparison of analytical and experimental solutions for the tests under static loading.

SOIL PREPARATION AND PROPERTIES

Taylor Marl clay from near Austin, Texas, was used as the subgrade material. The clay was thoroughly dried at 130 F, crushed, redried, and pulverized. It was then mixed with water in a mechanical mixer to get an approximate water content of 38 percent, and the mixed soil was placed in plastic bags and stored in a moisture-controlled room to avoid evaporation. Storing of the prepared soil for a month helped to achieve uniform moisture content throughout the soil mass. After one test was performed, the soil was stored in a similar way until the next test.

The properties of Taylor Marl as determined in the laboratory were liquid limit, 59; plasticity index, 29; optimum water content, 17.5 percent; and maximum dry density, 106.5 lb/ft^3. The in situ properties in the test box were average density, 116 lb/ft^3; water content, 38 percent; average degree of saturation, 96 percent; average shear strength from unconfined compression test, 177 lb/ft^2 (1.23 lb/in.^{2}); and modulus of subgrade reaction (tangent) k, 160 lb/in^3.

TEST BOX AND SLAB SIZES

A 2 by 2 by 2 ft box, made of plywood $\frac{3}{4}$ in. thick, stiffened by 2 by 4 in. lumber with detachable top and bottom covers that could be bolted on, was used in the tests. Based on work by Lee (8), a slab of 9 by 9 in. was chosen so that there would be little restraining effect due to the container walls and bottom. This size also agreed with the rough criterion that the zone of influence extend to at least twice the width of the slab (15). The thickness of the slab, $\frac{1}{8}$ in., was chosen so that increasing the horizontal dimensions of the slab would have a negligible effect on the behavior of the slab.

Elastic properties, i.e., modulus of elasticity E and Poisson's ratio ν, were determined by testing a 2 by 18 in. strap of the material in tension. Longitudinal and transverse strains were measured by using foil strain gages oriented at 90 deg. The slab properties determined are as follows: modulus of elasticity E, 10.5×10^6 lb/in.^{2}; Poisson's ratio ν, 0.34; bending stiffness $D_x = D_y$, 1.930×10^3 lb/in.; twisting stiffness $C_x = C_y$, 1.280×10^3 lb/in.; and radius of relative stiffness ℓ, 1.87 in.

Method of Placing Soil and Slab in the Test Box

The top and bottom covers of the test box were detached. To position the slab on the inside of the bottom cover, 4 plywood planks were fixed so that a 9 by 9 in. space was left in the center. This space was filled with plaster of paris, but the top $\frac{1}{8}$-in. portion was left for the slab, which was positioned with the side having rosettes facing downward and the other side flush with the plywood planks. To reduce friction between soil and the slab, the top face of the slab, which would be in contact with the soil, was covered with a thin film of grease. A polyethylene sheet was spread on the planks, and the greased slab was left uncovered. The body of the box was then fixed to this assembly by bolts. The soil was prepared by mixing and was extruded in a 3 by 3 in. cross section in convenient lengths under a vacuum of about 20 psi. The soil blocks, cut in different lengths, were placed in the box until one row was completed. Several precautions were taken to ensure close contact between adjacent blocks by staggering the joints in the adjacent blocks with fingers and compacting each layer by a 10-lb drop hammer with a compacting surface of 6 by 6 in. falling 18 in. with 2 blows at each position. This procedure was continued until the whole box was filled. Then a polyethylene sheet was placed over it, and the top cover was attached. The box was taken to the testing bed, where it was lifted by 2 small hoists and supported from the

ceiling. The box was then turned over, bringing the slab to the top, and the top cover in the new position was then removed. The plaster of paris block was also removed, leaving the slab and the rosettes exposed to the room temperature. The soil was covered by a polyethylene sheet and wooden planks until arrangements for loading and measurement were completed.

LOADING

Load was applied by a mechanical screw jack, measured by a load cell, and recorded in a digital voltmeter. The output was read on the digital scanning system as well as on the digital voltmeter. The details and specifications of these devices are given elsewhere (1, 2). Tests were performed under 2 loading positions: center load and 2-point corner loads.

DEFLECTION AND STRAIN MEASUREMENT

Deflections of slab were measured by 0.0001-in. dial gages and LVDT's (linear variable differential transducers). An independent frame consisting of vertical, horizontal, and diagonal members was made to support the dial gages and LVDT's. The frame did not touch the box or the loading unit during the testing. Strains were measured by 4 rosettes for center loading and by 3 rosettes and 2 strain gages along one edge for corner loading.

TEST PROCEDURE

After the box was turned upside down, it was positioned under the loading frame, the level of the top of the slab was checked, and the verticality of the applied load was ensured. All the LVDT's and dial gages were fixed at their respective places. The connections of the LVDT's, strain gages, and load cells to the 40-channel voltmeter were completed. Alternate channels were used for load to aid in getting the LVDT output and strain gages output to correspond to exact loads separately. When all the test arrangements were completed, the LVDT's and strain gages were calibrated. The screw jack was set to produce a movement of the loading rod of about 0.0124 in./min. After the initial readings of all the measuring devices were recorded, the load was applied continuously and data were obtained at regular intervals. The loading continued until the maximum load, 255 lb for center loading and 208 lb for corner loading, was reached. The slab was then unloaded and readings were again taken at regular intervals.

After the test the slab was removed. The plate load test was conducted on a rigid plate ½-in. thick and 9 in. in diameter according to ASTM specifications. Tests on rigid plates of 1, 2, 4, and 6 in. in diameter were also conducted, as reported by Siddiqi (12). Vane shear tests were conducted at 8 locations and up to 5 in. from the surface, and torvane shear tests were also conducted. Samples were taken for moisture content, density, and degree of saturation and for unconfined compression tests during the soil placement and after the test. The unconfined compression tests were performed at the same loading rate as the slab testing and also at several moisture contents.

TESTS CONDUCTED

Tests were conducted in a 3-phase program. Phase 1 was preliminary slab testing under center load to establish a suitable test procedure. Two preliminary series (series 300 and 320) were conducted, one on an uninstrumented slab and the other on an instrumented slab. Both series were conducted under small loads producing deflections within linear characteristics of the soil. Test data, analysis, and difficulties encountered in these preliminary series are reported by Agarwal and Hudson (1, 2). Phase 2 (series 330) was the testing of the instrumented slab with center load. The testing was done under loads producing deflections within linear and nonlinear soil characteristics, first under static and then under cyclic loads. Phase 3 was the testing on the instrumented slab under 2-point corner loads (series 340), producing deflec-

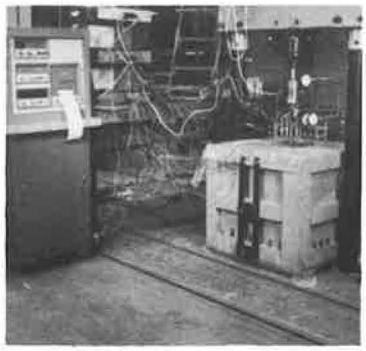

test setup

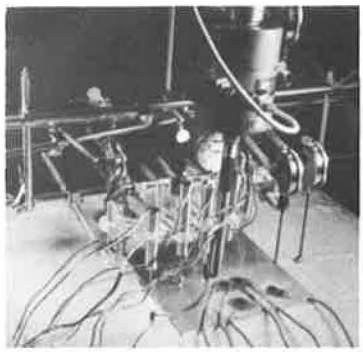

loading and measurement devices

Figure 3. Center-load slab test.

tions within linear and nonlinear soil characteristics, first under static and then under cyclic loads. Slab series 330 and 340 were the main test series and are analyzed here for the static case. The chief findings of the preliminary series are also included wherever helpful. Test data of series 330 and 340 under cyclic loading are discussed elsewhere (1, 2).

CENTER-LOAD SLAB TEST (SERIES 330)

Load was applied by the mechanical jack (Fig. 3) through a $^{3}/_{4}$-in. diameter loading rod and transmitted to the slab by a ball so as to apply only a vertical component of load.

Soil Properties

Soil subgrade was represented by the Winkler foundation, which was determined from the pressure versus deflection characteristics obtained from plate load tests. From the preliminary series, as reported in detail by Siddiqi (12), it was observed that these characteristics were influenced by the plate size. Therefore, it was decided to use the data of the 9-in. diameter rigid plate in analysis of the 9 by 9 in. slab. The pressure versus average deflection data are shown in Figure 4 along with 2 sets of test data; one for a preliminary series (series 320), and the other for corner-load slab test (series 340). The curves for the material used in series 330 and 340 are almost identical, but the behavior in series 320 was significantly different. Curve I for the main series and Curve II for the preliminary series were used in subsequent linear and nonlinear analyses.

The soil properties as determined after the slab test are discussed in detail by Agarwal and Hudson (1, 2), and the average properties have already been given.

Test Results

Deflections and strains were calculated for different loads during loading and unloading. The method of reduction is described by Agarwal and Hudson (1, 2).

Dial gages on the slab served as checks for LVDT's at identical positions. The deflections at all the points increased nonlinearly with the increase in load (Fig. 5). At all points, deflections were downward up to a 55-lb load and then upward at the corner for the rest of the loading. During unloading the curves did not follow the loading curves, but had permanent sets of different magnitudes at various points at zero load. The deflection data of the 3 dial gages serving as checks for the LVDT's at identical position showed that nonlinear behavior, following different paths during loading and unloading and having different permanent sets, was similar to that for LVDT's

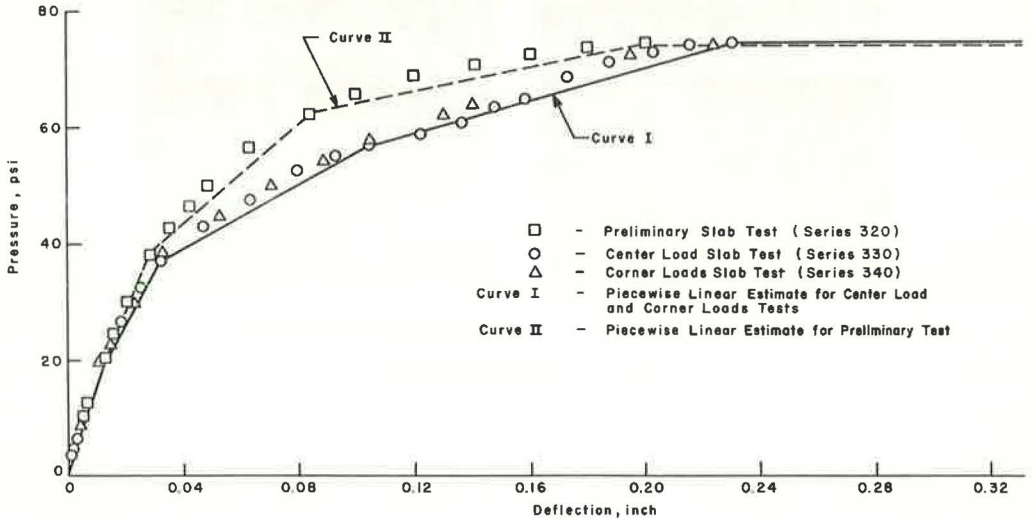

Figure 4. Pressure versus deflection data of 9-in. diameter rigid plate.

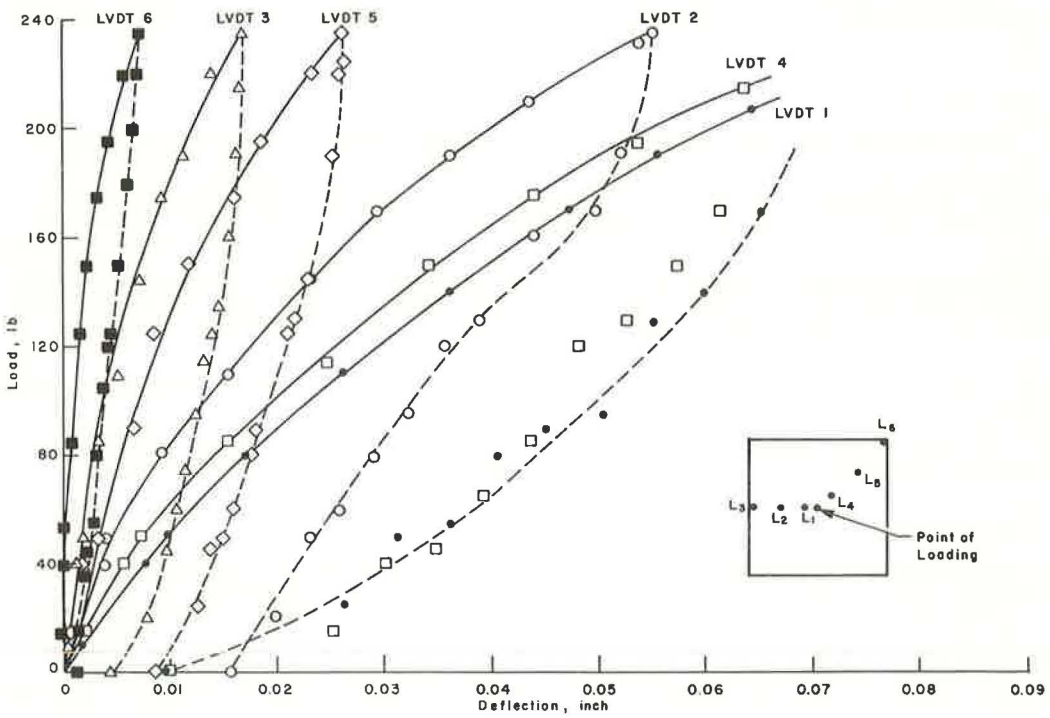

Figure 5. Load versus deflection curves for LVDT's for center-load slab test (series 300).

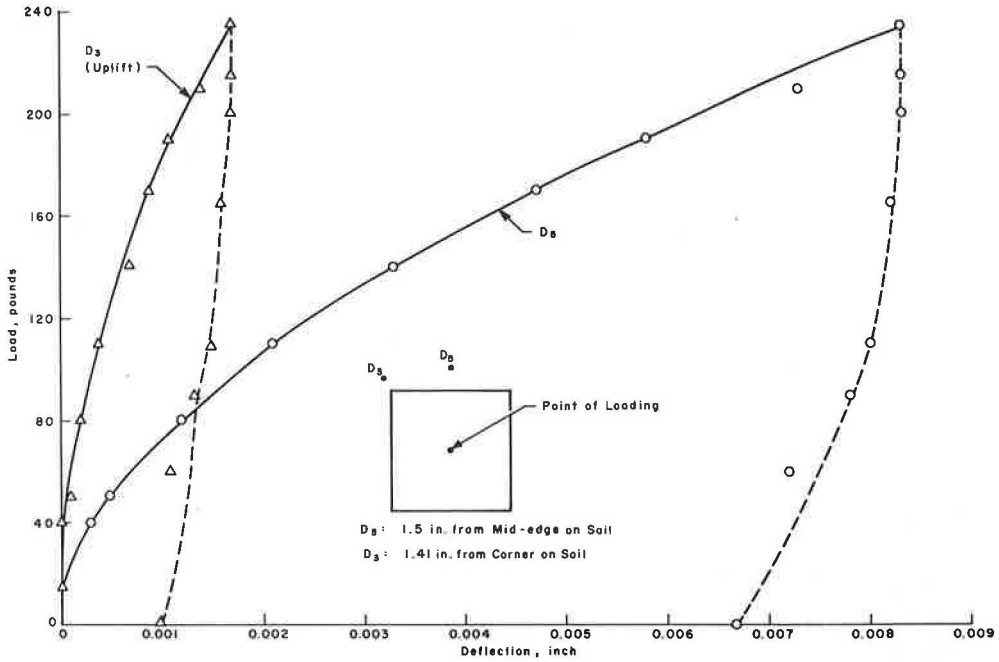

Figure 6. Load versus deflection curves for dial gages on soil for center-load slab test (series 330).

(1, 2). For 2 points on the soil near the slab periphery, the nonlinear behavior and large permanent sets on unloading indicate that the adjoining soil was affected as the slab was loaded (Fig. 6).

The method of getting largest principal stresses and their directions from the strain reading of the rosette is described elsewhere (1, 2). The behavior of nonlinear variations, having different paths during loading and unloading, and different residual stresses at various locations on unloading, was similar to that for deflections (Fig. 7).

Comparison of Experimental and Analytical Deflections

Analytical solutions based on the discrete-element model were found by using DSLAB 30 (11), with soil represented by linear springs; and DSLAB 26 (7), with soil represented by nonlinear springs. Salient features of DSLAB 30 and DSLAB 26 are given in the Appendix. The linear and nonlinear soil springs below the slab were obtained by the following methods:

1. Linear springs from 9-in. diameter rigid plate test data corresponding to 0.01-in. deflection (tangent modulus);
2. Linear springs from 9-in. diameter rigid plate test data corresponding to 0.02-in. deflection (secant modulus);
3. Nonlinear springs using the entire pressure versus deflection curve of the 9-in. diameter plate test; and
4. Nonlinear springs using Skempton's recommendation for unconfined compression test data (derivation given in 1 and 2).

The different soil representations outlined in the preceding are shown in Figure 8. The linear springs act in tension as well as compression. The nonlinear springs act in compression only. As clays can take small amounts of tension (16), these springs were made active in tension also, with the same slope as that in compression for the earlier portion of the curve.

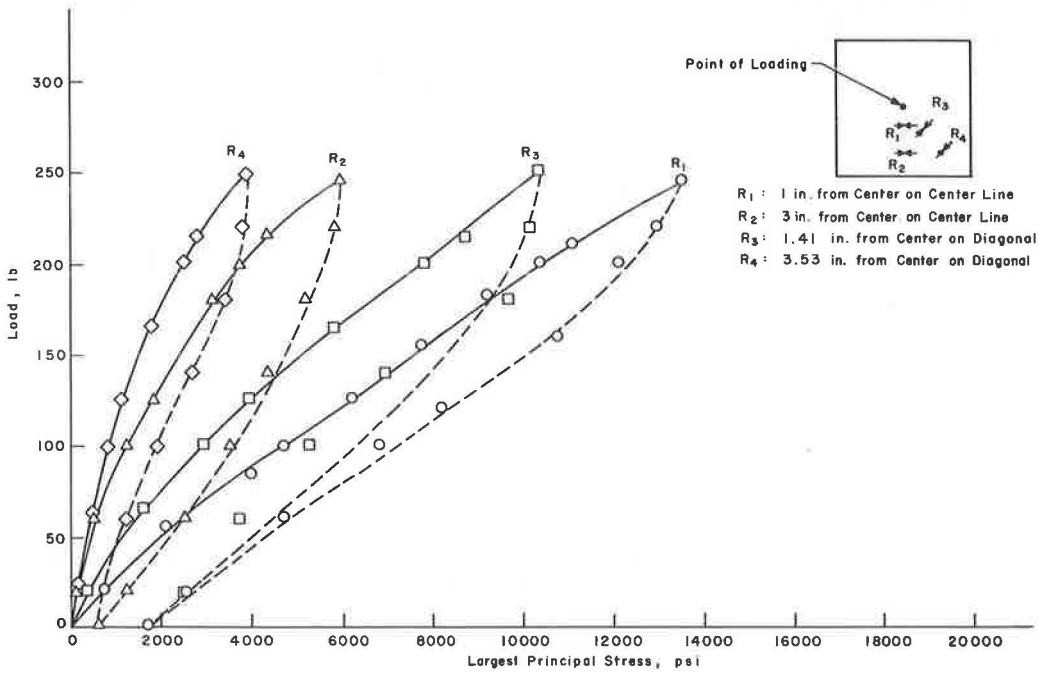

Figure 7. Load versus largest principal stress for rosettes for center-load slab test (series 330).

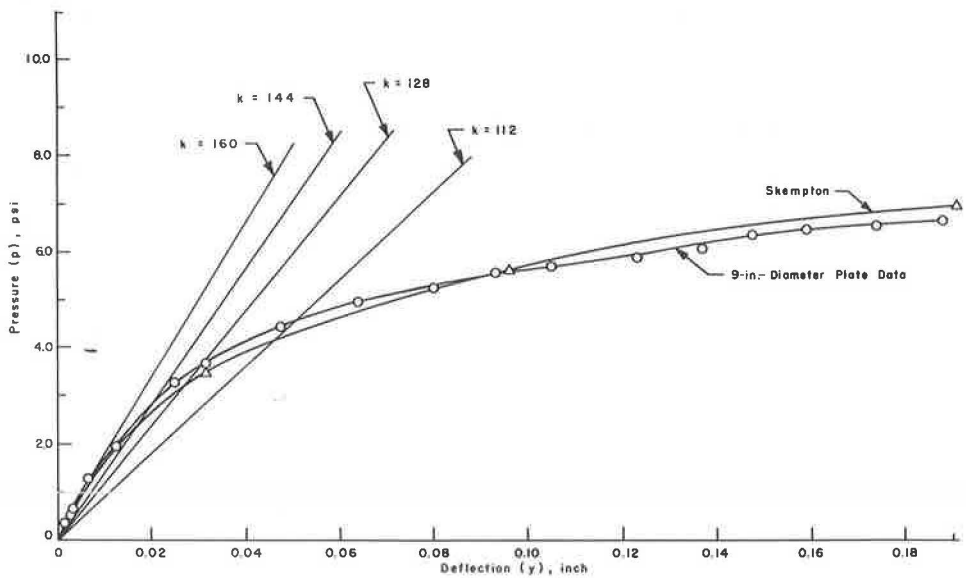

Figure 8. Linear and nonlinear soil representation.

The measured and computed deflections using linear and nonlinear springs for soil for a particular load on the slab were compared, and the error was calculated as percentage of maximum measured deflection, i.e.,

$$\text{Percentage error} = \frac{w_{mi} - w_{ci}}{(w_{max})_m} \times 100 \quad (1)$$

where

w_{mi} = measured deflection at point i,
w_{ci} = computed deflection at point i, and
$(w_{max})_m$ = maximum measured deflection for the load under consideration.

For a load of 100 lb (categorized as a load producing small deflections), the plots along centerline and diagonal for measured and analytical deflections using different linear and nonlinear springs (Figs. 9 and 10) and the percentage errors (1, 2) indicated there was good correlation between the experimental and DSLAB solutions using springs B, C, and D. The error was within 5 percent near the loaded area, 7 percent near the midedge, and 22 percent near the corner. The difference in error at the corresponding checkpoints, using dial gages, was within 2 percent. The results obtained by using linear springs (secant modulus corresponding to maximum deflection) were almost the same as those using nonlinear springs. Similar comparisons in both preliminary slab tests were observed (1, 2).

From the plots for measured and analytical deflections along the centerline and diagonal (Figs. 11 and 12 respectively), for a load of 200 lb (categorized as a load producing large deflections), and percentage errors (1, 2), it was observed that good correlation existed using nonlinear springs only. Percentage error using C and D springs was within 8 percent near the load, 3 percent near the midedge, and 14 percent near the corner. The difference in error at the corresponding checkpoints, using dial gages, was within 2 percent. Solutions using linear springs (A and B) did not

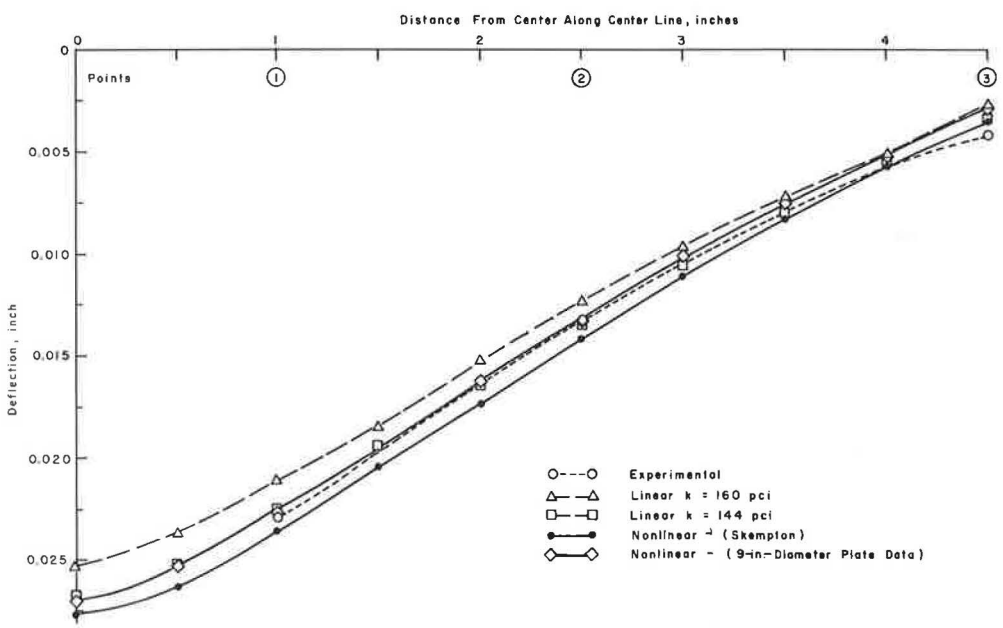

Figure 9. Experimental and analytical deflections on centerline under center load of 100 lb (series 330).

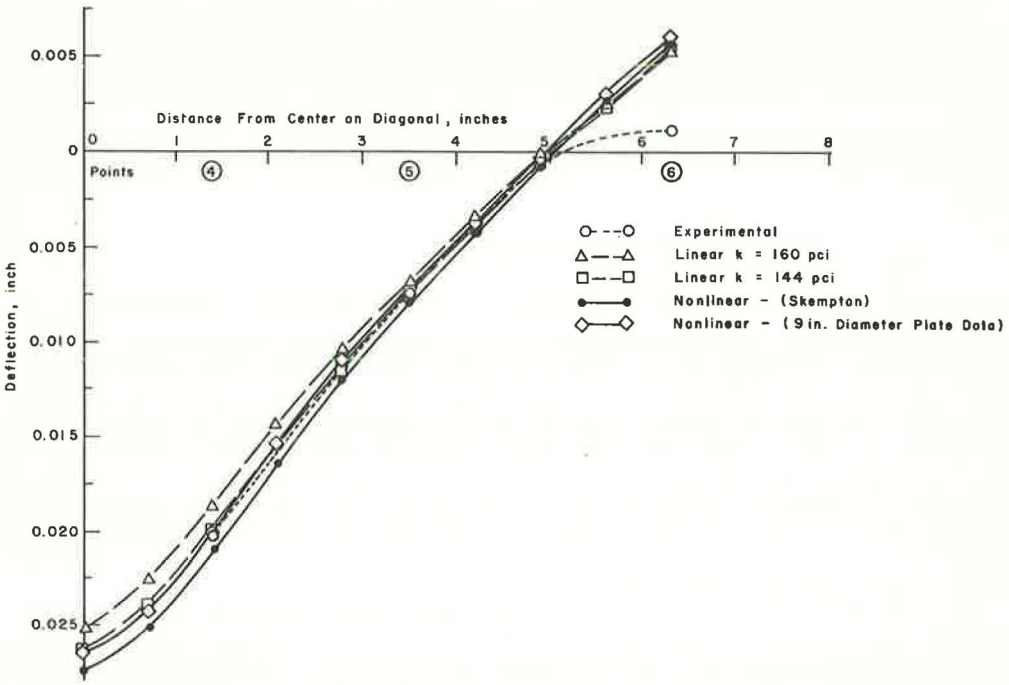

Figure 10. Experimental and analytical deflections on diagonal under center load of 100 lb (series 330).

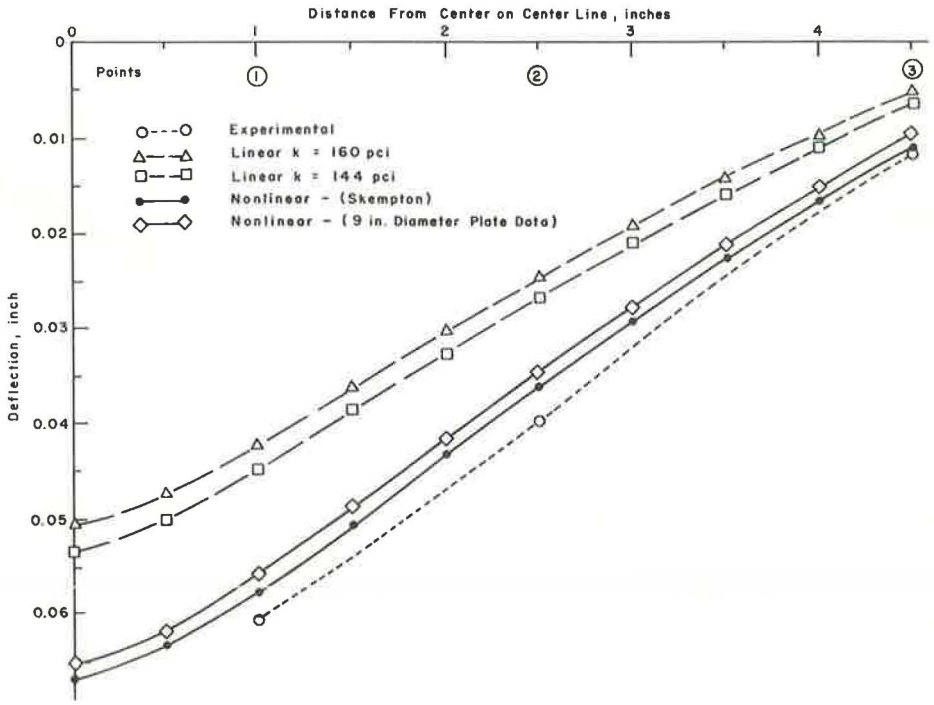

Figure 11. Experimental and analytical deflections on centerline under center load of 200 lb (series 330).

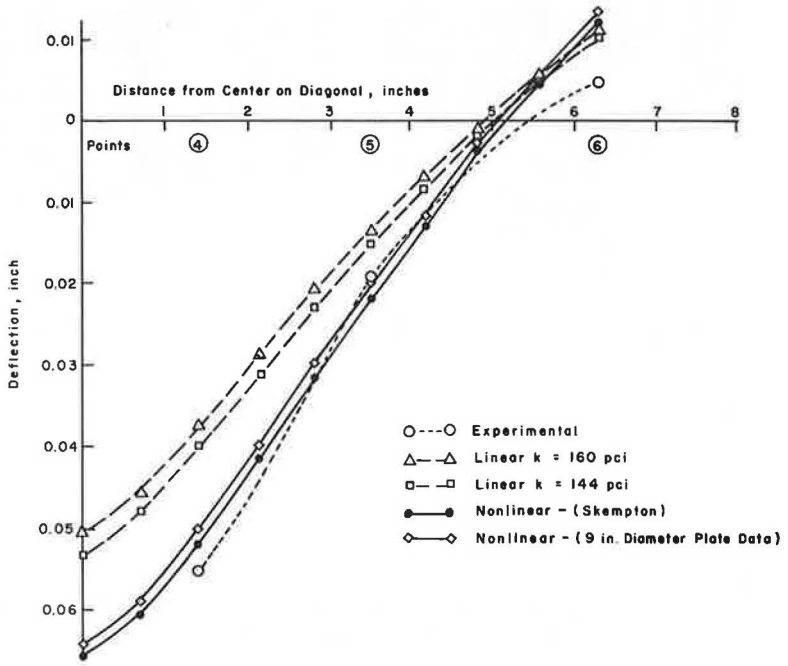

Figure 12. Experimental and analytical deflections on diagonal under center load of 200 lb (series 330).

yield good agreement if the deflections on the slab were large and lay on the nonlinear part of the pressure versus deflection curve for the soil.

Comparison of Experimental and Analytical Principal Stresses

The largest principal stresses for loads of 100 and 200 lb on the slab were calculated from the strains of the rectangular rosettes (1, 2). The measured principal stresses corresponded to the top of the slab, whereas those obtained by using DSLAB corresponded to the bottom. This difference was kept in mind, as a comparison was made of the measured and DSLAB largest principal stresses with the absolute values and percentage errors calculated as a function of the maximum measured largest principal stress.

$$\text{Percentage error} = \frac{\sigma_{im} - \sigma_{ic}}{(\sigma_{max})_m} \times 100 \qquad (2)$$

where

σ_{im} = measured largest principal stress at point i,
σ_{ic} = DSLAB largest principal stress at point i, and
$(\sigma_{max})_m$ = maximum measured largest principal stress for the load under consideration.

For a 100-lb load on the slab, the comparison of measured largest principal stresses with the DSLAB solutions, using the linear and nonlinear springs (1, 2), showed that the maximum percentage error was within 7 percent and that there was small difference in percentage errors for solutions using linear and nonlinear springs. Similar observations were made for the preliminary series 320 (1, 2). A similar comparison of largest principal stresses for 200 lb showed that agreement was within 7 percent between experimental measurements and DSLAB solutions using nonlinear springs; linear spring did not yield good agreement (1, 2).

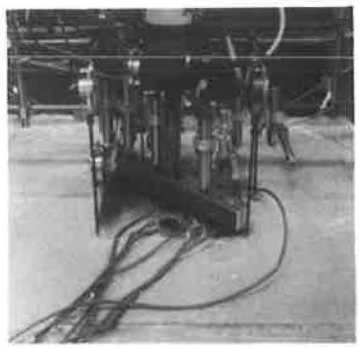

test setup

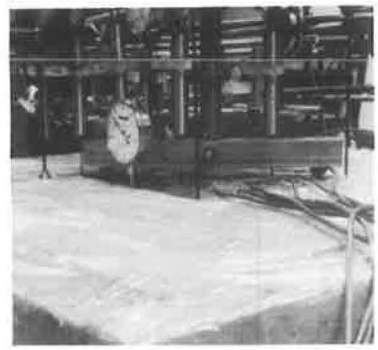

loading beam

Figure 13. Corner-load slab test (series 340).

CORNER-LOAD SLAB TEST (SERIES 340)

Load was transferred to the slab near the opposite corners through a loading beam (Fig. 13). To ensure equal loads at both ends, the beam was joined to the loading rod by a pin connection. As it was desired to measure deflections along the diagonal itself, ¼-in. diameter holes were made in the beam for the cores of the LVDT's to pass through. Identical holes were made on both sides of the center of the beam, so that equal loads were transmitted at the 2 ends. The testing procedure was exactly the same as for the center-load slab test. The soil properties as determined after the slab test are discussed in detail elsewhere (1, 2), and the average values have also been given.

Test Results

Deflections and strains were calculated for different loads (1, 2). For all the LVDT's, except 6 and 7, the deflections increased with load nonlinearly (Fig. 14). LDVT 6, placed at the unloaded corner, and LVDT 7, measuring the smallest deflections, showed almost linear variation. The deflections were upward at the unloaded corner, and downward at all the other points. The results, which showed different paths during unloading and permanent sets, were similar to center-load slab test results. The deflection data for the 4 dial gages on the slab that served as checkpoints for 4 LVDT's showed that the nonlinear behavior during loading and unloading was similar to that of LVDT's.

The deflection data for 2 points on the soil near the slab periphery showed that the deflections at both points were nonlinear and downward, with large permanent sets on unloading (1, 2). This indicates that the adjacent soil was affected as the slab was loaded. The data for largest principal stresses (1, 2) and stresses along the edge (Fig. 15) showed that nonlinear behavior with permanent sets in unloading was similar to that for deflections.

Comparison of Experimental and Analytical Solutions

Analytical solutions were obtained by using DSLAB 30 (11), for linear soil springs, and DSLAB 26 (7), for nonlinear springs, for total loads of 100 and 200 lb (50 and 100 lb at each point respectively). The following soil springs were used: linear springs A and nonlinear springs C and D were the same as for the center-load test. Linear springs B were calculated from 9-in. diameter rigid plate test data for deflections of 0.02, 0.03, and 0.04 in. Secant moduli thus obtained were 144, 128, and 112 lb/in.^{3} respectively.

Comparison of measured and analytical solutions for deflections, principal stresses, and stresses along the edge was made, and percentage errors were calculated as a

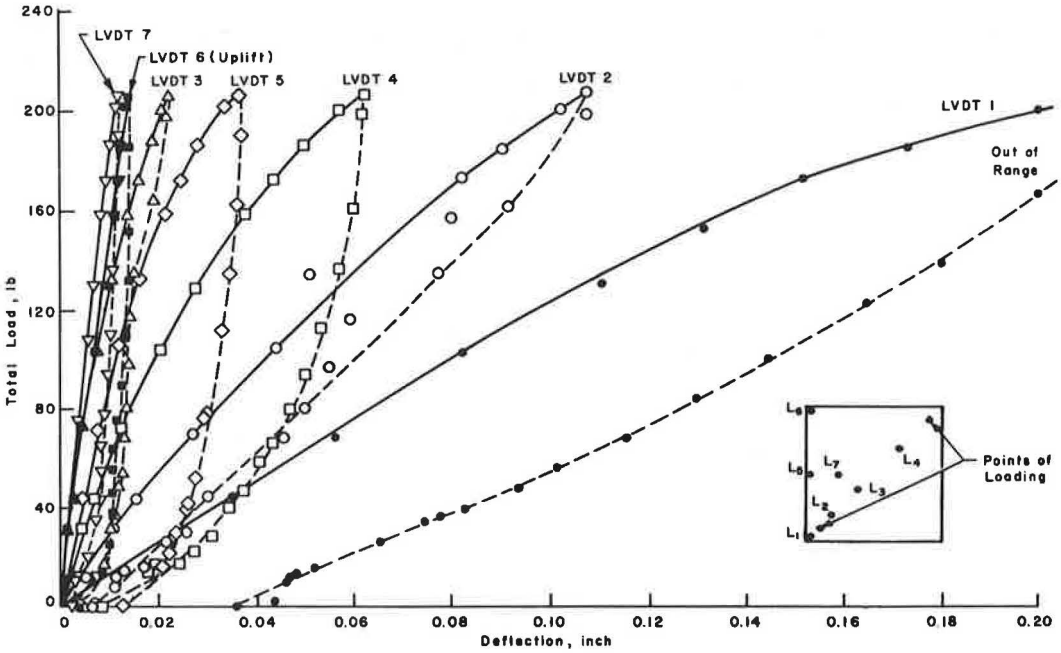

Figure 14. Load versus deflection curves for LVDT's for corner-load slab test (series 340).

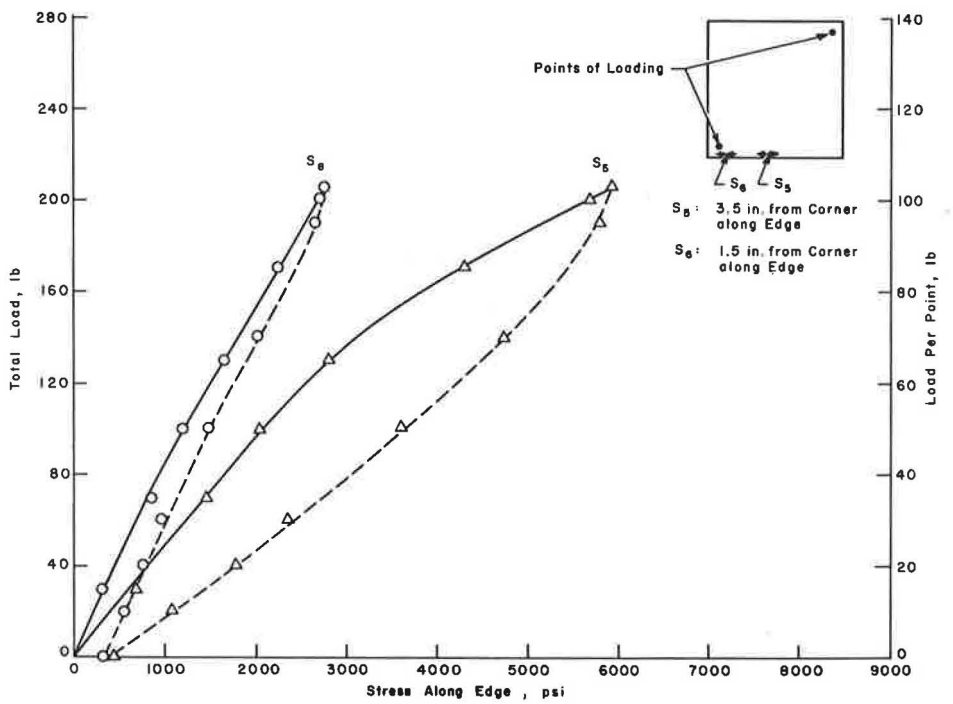

Figure 15. Load versus stresses along edge for corner-load slab test (series 340).

function of the maximum measured value for the load under consideration. The measured and analytical deflections were plotted along the diagonal and the edge. Because the loads were placed symmetrically on the diagonal, the measured values on both sides of the center were taken as the same while plotting the deflections.

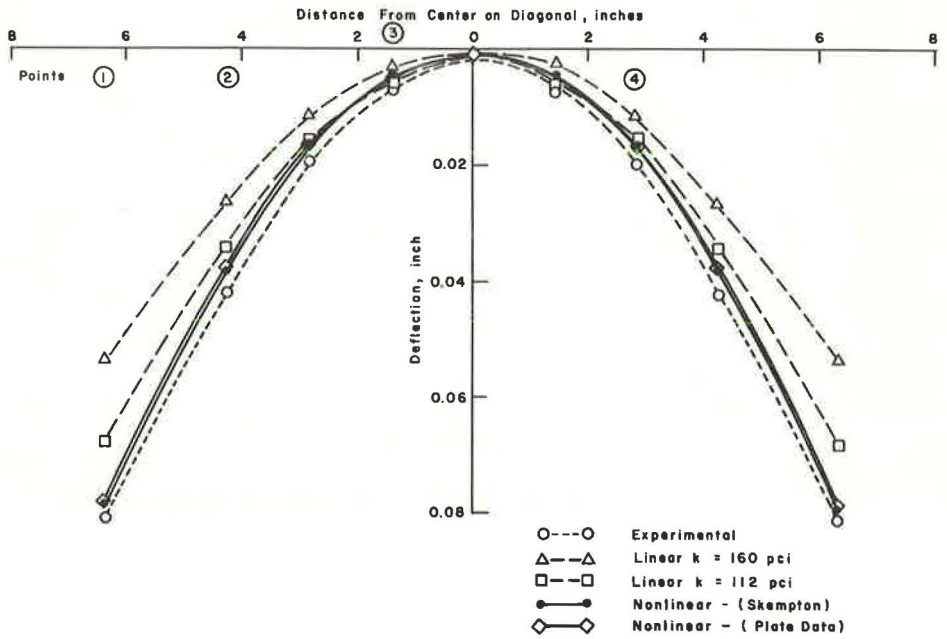

Figure 16. Experimental and analytical deflections on diagonal under corner loads of 100 lb (50 lb at each point).

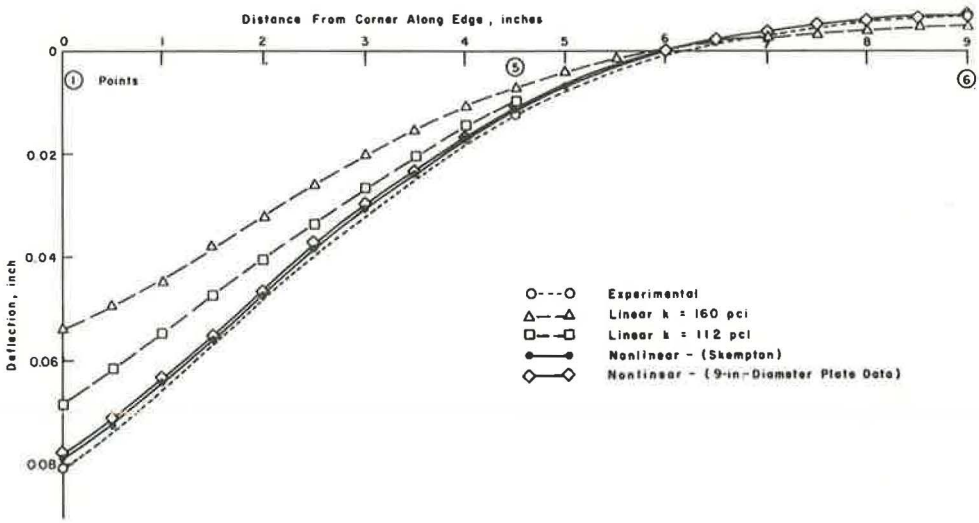

Figure 17. Experimental and analytical deflections on edge under corner loads of 100 lb (50 lb at each point).

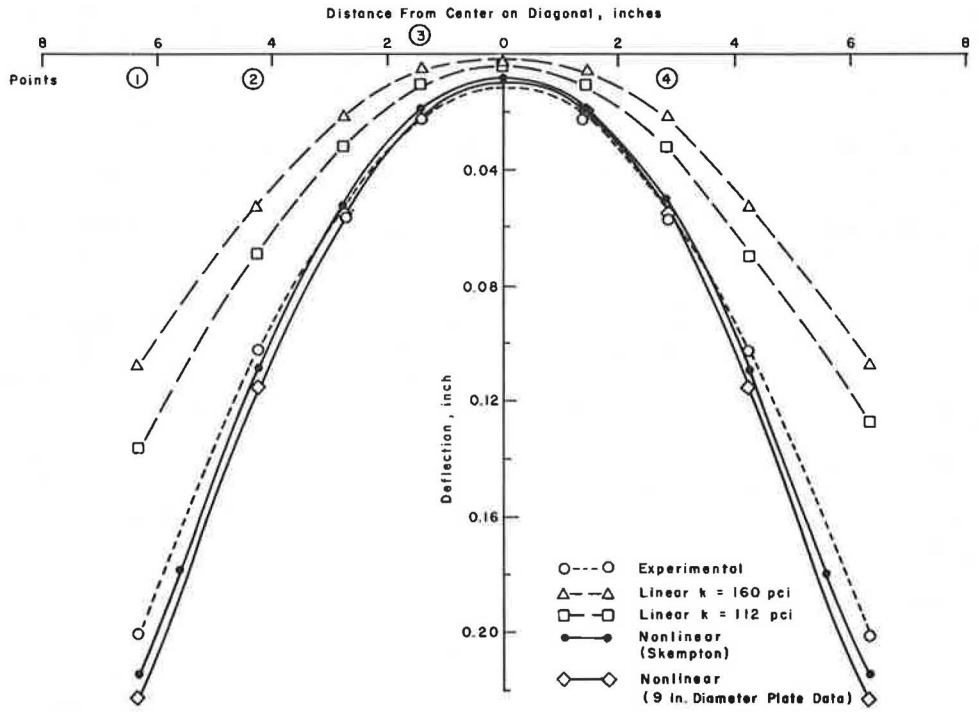

Figure 18. Experimental and analytical deflections on diagonal under corner loads of 200 lb (100 lb at each point).

For a total load of 100 lb, i.e., 50 lb at each point (load producing large deflections), good correlation existed (Figs. 16 and 17) using nonlinear springs only (1, 2). The percentage error using nonlinear springs (C and D) was within 6 percent on the entire slab. The difference in error at checkpoints using dial gages was within 1 percent. Solutions using linear springs (A and B) did not yield good agreement, as the deflections on the slab were large and lay on the nonlinear part of pressure versus deflection characteristics of the soil.

The comparison for largest principal stresses and for stresses along the edge showed that the maximum discrepancy using nonlinear springs (C and D) was within 14 percent and using linear springs (B) was 27 percent (1, 2).

For a total load of 200 lb, i.e., 100 lb at each point (load producing large deflections), good correlation existed (Fig. 18) using nonlinear springs only (1, 2). The percentage error using C and D springs was within 11 percent near the loaded area, 6 percent near the unloaded corner, and 3 percent on the rest of the slab. The percentage error for the corresponding checkpoints using dial gages was 5 percent for points all over the slab. Solutions using linear springs (A and B) did not yield good agreement, as the deflections lay on the nonlinear part of the pressure versus deflection characteristics of soil.

The comparison of largest principal stresses and stresses along the edge (1, 2) showed maximum discrepancy between measured and analytical solutions of 9 percent using nonlinear springs (C and D) and 43 percent using linear springs (B).

CAUSES OF DISCREPANCY

In the slab tests discussed in this paper, the slab was resting on soil, whereas plates tested at another time (1, 2) were resting on rigid supports. From the study of

plates with different stiffness, load, and support conditions, the rigid supports may be represented adequately in the input data in this method of solution. Therefore, the major cause of discrepancy in the slab tests may be in the representation of soil.

From the comparison for deflections, largest principal stresses, and stresses along the edge under the 2 loading conditions, it has been observed that soil can be represented satisfactorily by the Winkler foundation provided that (a) linear or nonlinear springs are input for loads producing small deflections, and (b) only nonlinear springs are used for loads producing large deflections.

It has also been observed that the maximum discrepancy is along the periphery of the slabs. The following factors may be some of the causes of the discrepancy.

1. According to the Winkler foundation, the soil springs act only under the slab, and the adjoining soil is not affected at all. This is in contradiction to the observed deflections of the soil surface during the tests. Deflections were observed at 2 points on the soil each for center-load and corner-load slab tests. From these observations, it seems that the effect of the soil outside the perimeter of the slab may also be included while representing the soil.
2. In the DSLAB input, the properties of the slab and soil are lumped in joints and bars in proportion to the area occupied by each station. This necessitates full values at the interior stations, half values at the edge, and quarter values at the corners. This applies to the slab as well as to the soil, and may be true only if the slab (9 by 9 in.) is resting on 9 by 9 in. soil. If the soil is not represented beyond the dimensions of the slab, the soil springs acting along the periphery may need to be modified. Possible ways to carry out such modifications should be thoroughly investigated.
3. The interaction between the slab and the soil has not been taken into account. The effect of the frictional forces developed because of such interaction should be thoroughly investigated. Because the present DSLAB solutions neglect these frictional forces, the bottom of the slab was lubricated with a thin film of grease before the soil placement, but whether the frictional forces during the testing were completely reduced is not known.
4. The soil is represented by linear and nonlinear independent springs in the DSLAB solutions. The interaction between these springs, in both vertical and horizontal directions, is neglected. Such interaction between the soil springs may be incorporated by introducing coupled springs. A thorough investigation regarding coupled-spring foundation for both linear and nonlinear solutions and the method of representing this parameter needs to be made to understand the phenomenon.
5. Only one nonlinear pressure versus deflection curve, or uniform linear k, that was input for the entire soil surface below the slab may be necessary, as pointed out by Lewis and Harr (10). An experimental investigation with pressure measurements to determine such curves or k variation needs to be made.
6. Great care was taken during the entire test procedure, but the following possible experimental errors could have occurred at various stages of testing:

   (a) The soil placed by extrusion may not have been perfectly homogeneous in moisture content and density. When adjacent blocks, rows, and layers, were placed, perfect jointing may not have been achieved at all the places in the box.
   (b) The method adopted for good contact between slab and soil may not have been perfect enough to ensure such contact at all places.
   (c) A time lag in loading and recording the data may have produced a small error.
   (d) With LVDT's of $1\frac{1}{2}$-inch range used for deflections of ± 0.2 in. or less, it was not possible to obtain a good resolution. LVDT's of smaller range with greater resolution should have been used.
   (e) Slight inaccuracies in fixing gages and rosettes may have led to small error.
   (f) The discrepancies in determining slab properties may have caused a small error, in the same way as for plates (1, 2).

CONCLUSIONS

The experimental evidence in this paper shows that discrete-element solution techniques provide extremely good results in predicting slab stresses and deflections and can be useful tools in the analysis of bridge slabs and pavements. The following specific conclusions can be drawn regarding the results.

For a slab-on-foundation problem, the soil support can be satisfactorily represented as a Winkler foundation by linear and nonlinear springs as determined by plate load tests or from stress-strain data for the soil. A plate load test may not always be feasible in practice; therefore, laboratory testing of the saturated clay sample under triaxial compression test is sometimes recommended. When such soil representation was used for a linearly elastic slab resting on clay soil and tested under 2 different loading configurations, good correlation existed for loads producing small deflections between experimental and analytical results for deflections and stresses using linear springs for the soil. However, for loads producing larger deflections on the slab, nonlinear springs were required.

ACKNOWLEDGMENTS

This investigation was conducted at the Center for Highway Research, University of Texas at Austin. The authors wish to thank the sponsors: the Texas Highway Department and the U.S. Department of Transportation, Federal Highway Administration. Our thanks are extended to Hudson Matlock for his suggestions at various stages of the work. The opinions, findings, and conclusions expressed in this publication are those of the authors and not necessarily those of the Federal Highway Administration.

REFERENCES

1. Agarwal, S. L. Experimental Verification of Discrete-Element Solutions for Two-Dimensional Soil Structure Problems. Univ. of Texas at Austin, PhD dissertation, Aug. 1969.
2. Agarwal, S. L., and Hudson, W. R. Experimental Verification of Discrete-Element Solutions for Plates and Pavement Slabs. Center for Highway Research, Univ. of Texas at Austin, Res. Rept. 56-15, Aug. 1969.
3. Hudson, W. R., and Matlock, Hudson. Discontinuous Orthotropic Plates and Slabs. Center for Highway Research, Univ. of Texas at Austin, Res. Rept. 56-6, May 1966.
4. Hudson, W. R., and Matlock, Hudson. Analysis of Discontinuous Orthotropic Pavement Slabs Subjected to Combined Loads. Highway Research Record 131, 1966, pp. 1-48
5. Hudson, W. R., and Matlock, Hudson. Cracked Pavement Slabs With Nonuniform Support. Jour. Highway Div., Proc. ASCE, Vol. 93, No. HW1, April 1967, pp. 19-42.
6. Hudson, W. R., and Stelzer, C. F., Jr. A Direct Computer Solution for Slabs on Foundation. ACI Jour., Proc. Vol. 65, No. 3, March 1968, pp. 188-200.
7. Kelly, A. E. Dynamic Analysis of Discrete-Element Plates on Nonlinear Foundation. Univ. of Texas at Austin, PhD dissertation, Jan. 1970.
8. Lee, C. E. The Determination of Pavement Deflections Under Repeated Load Applications. Univ. of California, Berkeley, PhD dissertation, 1961.
9. Lewis, K. H., and Harr, M. E. Analysis of Concrete Slabs on Ground and Subjected to Warping and Moving Loads. Paper presented at the HRB 48th Annual Meeting, 1969.
10. Matlock, Hudson, and Haliburton, T. A. A Finite-Element Method of Solution for Linearly Elastic Beam-Columns. Center for Highway Research, Univ. of Texas at Austin, Res. Rept. 56-1, 1965.
11. Panak, J. J., and Matlock, Hudson. A Discrete-Element Method of Multiple-Loading Analysis for Two-Way Bridge Floor Slabs. Center for Highway Research, Univ. of Texas at Austin, Res. Rept. 56-13, Aug. 1968.

12. Siddiqi, Q. S. Experimental Evaluation of Subgrade Modulus and Its Application for Model Slab Studies. Univ. of Texas at Austin, MS thesis, Jan. 1970.
13. Skempton, A. W. The Bearing Capacity of Clays. Building Research Congress, 1951.
14. Stelzer, C. F., Jr., and Hudson, W. R. A Direct Computer Solution for Plates and Pavement Slabs. Center for Highway Research, Univ. of Texas at Austin, Res. Rept. 56-9, 1967.
15. Terzaghi, K. Theoretical Soil Mechanics. John Wiley and Sons, New York, 1943.
16. Tshebotarioff, G. P., Ward, E. R., and DePhillippe, A. A. The Tensile Strength of Disturbed and Recompacted Soils. Proc., Third International Conference on Soil Mechanics and Foundations Engineering, Switzerland, Vol. 1, 1953, pp. 207-212.
17. Westergaard, H. M. Analytical Tools for Judging Results of Structural Tests on Concrete Pavements. Public Roads, Vol. 14, No. 10, 1933.
18. Westergaard, H. M. Computation of Stresses in Concrete Roads. Paper presented at the HRB 5th Annual Meeting, 1926.
19. Westergaard, H. M. New Formulas for Stresses in Concrete Pavements of Airfields. ASCE, Proc. Vol. 73, No. 5, May 1947.
20. Westergaard, H. M. Stresses in Concrete Pavements Computed by Theoretical Analysis. Public Roads, Vol. 7, No. 2, April 1926.
21. Winkler, E. Die Lehre von Elastegatat and Festigkeit/On Elasticity and Fixity. Prague, 1867, pp. 182-184.

Appendix

SALIENT FEATURES OF PREVIOUS REFERENCES USED MOST OFTEN

Slab on Linear Winkler Foundations Model

DSLAB 5 and DSLAB 30 (14 and 11 respectively) are the computer programs developed for the solution of a slab resting on linearly elastic foundation springs based on the discrete-element model and utilizing a direct matrix manipulation technique for the solution. Because DSLAB 30 is a modified version of DSLAB 5 and has more capabilities, DSLAB 30 was used most of the time during the present study.

In the discrete-element solutions for slab (known as DSLAB solutions), the slab is replaced by an analogous mechanical model representing all stiffness and support properties of the actual slab. The joints of the model are connected by rigid bars, which are in turn interconnected by torsion bars representing the twisting stiffness. The effects of bending stiffness and the Poisson's ratio are concentrated at the flexible joint. The soil support, represented by linear Winkler foundation model, is concentrated at the joint.

The deflection at each joint is unknown. The basic equilibrium equations are derived from the free body of the slab joint with all appropriate internal and external forces and reactions. These equations include summing the vertical forces at each joint and summing the moments about each individual bar. The resulting stiffness matrix is symmetrical about its major diagonal, and it is also banded; that is, the terms lie in lines parallel to the major diagonal. This banded matrix has the central band 5 terms wide, the bands on either side of the central band 3 terms wide, and the 2 extreme bands only 1 term wide. The stiffness matrix is partitioned into submatrices. If the slab to be solved has been divided into m increments in the x-direction and n increments in the y-direction, the stiffness matrix will have n + 3 rows and n + 3 columns of submatrices. The submatrices will have m + 3 rows and m + 3 columns of terms. Solution of slab problems involves manipulating the submatrices. A back-and-forth recursive technique analogous to Matlock's method of solving beam columns (11) is applied to the submatrices to solve for the deflections. Slopes, moments, shears, and reactions

are computed by using the difference equation relations. It has been observed that rectangular slab problems will be solved more efficiently if m is larger than n.

Slab on Nonlinear Winkler Foundation Model

DSLAB 26 (8) is a computer program developed for the solution of the slab resting on nonlinear Winkler foundation model. The entire nonlinear support is used, utilizing the piece-wise linear estimate. The solution of the slab gets started with an initial load at each joint, which is accomplished by inputting an initial linear spring (may be tangent modulus). With these initial loads at each joint, the deflections are obtained by using the direct matrix manipulation technique. A correction is applied to the initial loads at the supports by finding the loads corresponding to the deflections obtained from the support nonlinear characteristics. This correction may be applied either in the load or in the spring (secant modulus). The solution for deflections is again obtained with the modified loads. This process is continued until the solution is obtained within a specified tolerance. Slopes, moments, shears, and reactions are computed by using the difference equation relations. The nonlinear springs act in compression only but can be made to act in tension also for clays to take care of the small amount of tension.

Sensitivity Analysis of the Extended AASHO Rigid Pavement Design Equation

HARVEY J. TREYBIG, W. RONALD HUDSON, and B. FRANK McCULLOUGH,
Center for Highway Research, University of Texas at Austin

This paper describes a sensitivity analysis of stochastic rigid pavement design variables. The mathematical model used is that of the extended AASHO interim guide for the design of rigid pavement structures. The sensitivity analysis determined the relative importance of the rigid pavement design variables and also evaluated the effects of stochastic variations for each variable. An analysis of variance was made to determine what interactions among rigid pavement design variables were significant. The sensitivity analysis is for a full factorial of the variables. The variables included are the modulus of elasticity, flexural strength, slab thickness, slab continuity, modulus of subgrade reaction, initial serviceability index, and terminal serviceability index. Each variable was evaluated for 2 levels except that the modulus of subgrade reaction was evaluated at 3 levels and the initial and terminal serviceability indexes were evaluated at 1 level each. In each factorial cell, each variable was evaluated for the effect of perturbations around its mean. In order to compare meaningful variations, the standard deviation was used rather than the standard unit change in the variable. The analysis indicated that flexural strength and thickness were the most important design variables. Others of importance were the slab continuity and terminal and initial serviceability indexes. The modulus of subgrade reaction and modulus of elasticity were the least important of the design variables considered. The analysis of variance indicated the same ordering of variables and showed significant interactions among the variables.

•THE SYSTEMS APPROACH to pavement design has, since 1965, received the attention of many researchers and design engineers. The use of systems engineering has not developed any startling new inputs for the solution of pavement design problems, but rather has organized the various aspects of the total problem into a manageable form. The systems concept emphasizes those factors and ideas that are common to the successful operation of relatively independent parts of the whole pavement problem.

The output response of the pavement system (1) is the serviceability or performance that the pavement experiences. This serviceability-performance concept was first developed by Carey and Irick (2) at the AASHO Road Test. The AASHO Interim Guide for the Design of Rigid Pavement Structures (3) was the first design method that incorporated the performance criteria.

The pavement design variables are of a stochastic nature. Variations occur in the parameters that must be recognized by designers. The effects of these stochastic variations are not always known. The design variables usually considered in rigid pavement design are flexural strength, modulus of elasticity, thickness, type of rigid pavement, environmental conditions, expected traffic, modulus of subgrade reaction,

Paper sponsored by Committee on Rigid Pavement Design and presented at the 49th Annual Meeting.

Poisson's ratio, and subbase. All of these variables affect the pavement problem seriously.

The objectives of this research are (a) to determine the importance of rigid pavement design variables, (b) to determine the interactions among the variables, and (c) to evaluate the effects of stochastic variations of each variable by using an extension of the AASHO Interim Guide (3).

The rigid pavement design variables considered are the modulus of elasticity, flexural strength, slab thickness, slab continuity, modulus of subgrade reaction, initial serviceability index, and terminal serviceability index. Each variable was evaluated at 2 levels, except that the modulus of subgrade reaction was evaluated at 3 levels and the initial and terminal serviceability indexes were evaluated at 1 level each.

THE PROBLEM AND APPROACH

The evaluation of rigid pavement design variables requires the use of some type of mathematical model relating the variables. If a systems approach such as that of Hudson et al. (1) is ultimately to be applicable to the model, then a system output response such as performance must be included as a variable in the model.

Selection of Model

Pavement performance criteria were developed and used at the AASHO Road Test; hence, any design models developed by using these performance data could have been used in this study. Two mathematical models for the rigid pavement design variables including the performance variable were considered. The first model is from the AASHO Interim Guide for the Design of Rigid Pavement Structures (3). Realizing the shortcomings of the Interim Guide, Hudson and McCullough (4) extended the Guide to include modulus of elasticity, modulus of subgrade reaction, and a term for pavement continuity that would include continuously reinforced concrete pavement.

Hudson and McCullough's extension of the Interim Guide was selected for use in the study described here because it was the best available mathematical model based on performance and it contained the desired design variables. The model is as follows:

$$\log \Sigma W = -9.483 - 3.837 \log \left[\frac{J}{S_X D^2} \left(1 - \frac{2.61a}{Z^{1/4} D^{3/4}} \right) \right] + \frac{G}{\beta} \qquad (1)$$

where

ΣW = number of accumulated equivalent 18-kip single-axle loads;
J = coefficient dependent on load-transfer characteristics or slab continuity;
S_X = modulus of rupture of concrete at 28 days, psi;
D = nominal thickness of concrete pavement, in.;
Z = E/k;
E = modulus of elasticity for concrete, psi;
k = modulus of subgrade reaction, psi/in.;
a = radius of equivalent loaded area = 7.15 in. for Road Test;
$G = \log\left(\frac{P_o - P_t}{P_o - 1.5}\right)$;
P_o = serviceability index immediately after construction;
P_t = terminal serviceability index assumed as failure; and
$\beta = 1 + \frac{1.624 \times 10^7}{(D + 1)^{8.46}}$.

Approach

A sensitivity analysis is a procedure that determines the change in a dependent variable caused by a unit change in an independent variable. A sensitivity analysis can be used to evaluate a whole system of variables and interactions among the variables that

compose the system. The rigid pavement design variables were evaluated in this research by means of a sensitivity analysis that determined the change in pavement life caused by changes in the variables. However, the unit of study for each variable was chosen to represent statistical variations observed in actual engineering practice. The analysis involved the levels of the variables given in Table 1.

TABLE 1

VARIABLES AND LEVELS FOR SENSITIVITY ANALYSIS

Variable	Level		
	Low	Medium	High
Modulus of elasticity, E	$2.0(10)^6$		$5.5(10)^6$
Flexural strength, S_x	400		800
Thickness, D	6		12
Modulus of subgrade reaction, k	25	200	1,000
Continuity, J	3.20		2.33
Initial serviceability index, P_o		4.2	
Terminal serviceability index, P_t		3.0	

In a previous sensitivity study by Buick (5), the theoretical importance of design variables was evaluated by the use of an instantaneous rate of change quantified by first order partial derivatives. Buick also evaluated the practical importance with a study of the parameter variations tolerated by selected thickness change constraints and a least squares fitting of appropriate equations to parameter thickness data.

In another sensitivity analysis, McCullough et al. (6) formulated the necessary partial derivatives but used numerical techniques to evaluate the "error" in total traffic in terms of percentage change in each variable. McCullough et al. evaluated only the AASHO Interim Guide (3), whereas Buick evaluated the AASHO Interim Guide Design Method, Corps of Engineers Rigid Pavement Design Method for Streets and Roads, and the Portland Cement Association Design Method for Rigid Pavements.

For this research a full factorial of the variables given in Table 1 was evaluated. In each factorial cell, each variable was evaluated for the effect of its perturbations around the mean. In order to compare meaningful variations of a variable, the standard deviation was chosen rather than the standard unit change in the variable.

Every material property, modulus of elasticity, flexural strength, and the like has a statistical distribution with a mean and a variation or a dispersion about this mean. Therefore, standard deviations have been developed for all the design variables to characterize their variation. The development of these standard deviations is covered in the rest of the paper.

The changes in expected pavement life have been computed for variations in each variable in each block of the factorial (Fig. 1). Each block of the factorial involves a fixed level of the 7 variables. One solution for each block was made for the expected pavement life for the mean values in the factorial. Solutions were then run with each of the 7 variables allowed to vary, once positively and once negatively, totaling 14 additional solutions for the expected pavement life.

The changes in expected pavement life caused by these perturbations were computed in terms of percentage increase or decrease in expected pavement life. The change was computed with the following formula:

$$L_i = \frac{W(j,i \pm \Delta) - W_j}{W_j} \times 100 \qquad (2)$$

where

L_i = percentage change in expected pavement life due to a variation in design variable, i;

W_j = expected pavement life for mean values in factorial (j indicates block of factorial by number listed in Figure 1, thus j = 1, 2, . . ., 48,); and

$W(j,i \pm \Delta)$ = expected pavement life for factorial block j with variable i incremented plus or minus some change.

A positive sign on L_i indicates increased pavement life, whereas a negative sign indicates a reduction in pavement life. The meaning of the change in expected life is shown in Figure 2. Three hypothetical lines are shown. The center line represents

Flex. Stren.	Thickness	Subg. Mod.	Mod. of Elas.	Continuity	400		800	
					6	12	6	12
3.20	5.5	2(10)6	25		1	13	25	37
			200		2	14	26	38
			1000		3	15	27	39
		5(10)6	25		4	16	28	40
			200		5	17	29	41
			1000		6	18	30	42
2.33		2(10)6	25		7	19	31	43
			200		8	20	32	44
			1000		9	21	33	45
		5.5(10)6	25		10	22	34	46
			200		11	23	35	47
			1000		12	24	36	48

Figure 1. Factorial for analysis of change in pavement life.

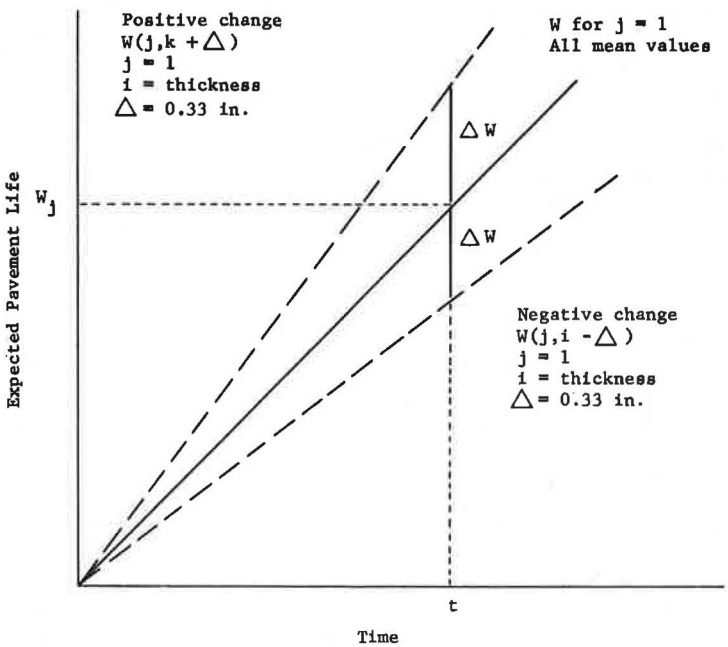

Figure 2. Graphical explanation of change in expected pavement life.

the expected pavement life for one of the factorial blocks j; e.g., j = 1 (Fig. 1). The upper line represents the expected life of a pavement with all variables fixed at that level except for one, e.g., thickness, which is increased 2 standard deviations. The lower line represents the expected pavement life for the same factorial block with a negative variation in thickness. The effects of some variations will of course be reversed; that is, an increase in the variable causes a decreased life.

FORMULATION OF DESIGN VARIABLE VARIATIONS

Highway contractors in general do not use statistical quality control in construction. Consequently, there are few exact data on expected variations in the design variables. The 2 largest sources of data for the development of the standard deviations used in this research were the permanent construction files of the Texas Highway Department and the reports on the AASHO Road Test. The authors' experience also aided in the development of some of the standard deviations. A search of the literature yielded little more than what was available through the above-mentioned sources.

Development of Standard Deviations

By using available data together with some assumptions, standard deviations were developed for each level of each variable selected for this investigation (Table 1).

Concrete Properties—Two properties of concrete were of interest in this study: (a) the modulus of elasticity (E), and (b) the flexural strength (S_X). The 2 levels of modulus of elasticity were 2.0×10^6 psi and 5.5×10^6 psi. Test data for modulus of elasticity were obtained from Shafer of the Texas Highway Department (7) and from Johnson's work (8) at the Iowa Engineering Experiment Station. Analysis of these data yielded standard deviations of 0.2×10^6 psi and 0.6×10^6 psi respectively for the low and high levels of modulus of elasticity.

Two levels of flexural strength, 400 psi and 800 psi, were involved. Data related to variation of flexural strength were obtained from several sources. The Texas Highway Department maintains permanent files of flexural strength on all concrete paving projects. Many data were used from these records (9). Hudson (10) has extended some of the AASHO Road Test work where flexural strength data were also available. Schleider reviewed large amounts of flexural strength data from the Texas Highway Department's construction files (11). Data for the 800-psi level came from all 3 sources, and the average standard deviation was 60 psi. The data for the low level of flexural strength came only from Schleider (11). The standard deviation for the low level was 45 psi.

Slab Thickness (D)—Slab thickness was involved at 2 levels of 6 and 12 in. Sample data were obtained for several other thicknesses from the Texas Highway Department (9) but were not available for these thicknesses. From these data the average coefficient of variation was obtained. The coefficient of variation was assumed to be constant. The standard deviations for the 2 thicknesses in this experiment were computed by using the obtained coefficient of variation. They are 0.165 and 0.330 in. for the 6- and 12-in. slab thicknesses respectively.

Modulus of Subgrade Reaction (k)—Although k-values are used in design, records show little evidence that agencies designing and building pavements actively measure the modulus of subgrade reaction by use of plate load tests (6). However, data were available from the AASHO Road Test (10). These data were for k-values averaging about 100 pci (pounds per cubic inch). The standard deviation for these data was 16 pci. In this investigation, k-values of 25, 200, and 1,000 were used, and the assumption was again made that the coefficient of variation would be a constant over a range of values of the parameter. The 3 necessary standard deviations were computed by using the coefficient of variation, with 15 percent coming from the AASHO data. The standard deviations calculated for the 3 levels were 4, 30, and 150 pci respectively.

Slab Continuity (J)—The slab continuity term was used by Hudson and McCullough to characterize the particular type of rigid pavement being considered. Hudson and McCullough (4) found that J = 2.20 for continuously reinforced concrete pavement. This value was based on Texas Highway Department design procedures and pavement performance. Since that time, McCullough and Treybig (12) have conducted extensive studies

on the deflection of jointed and continuously reinforced concrete pavement. Research by Treybig (13) has yielded a new J-value for continuous pavement, J = 2.33. Because this term is not a measurable material property but a pavement characteristic, its dispersion could not be determined in the normal way. Based on variability of deflection measurements and experience, standard deviations were estimated as 0.19 for continuous pavement and 0.13 for jointed pavement.

Performance Variables (P_o,P_t)—In this design method, performance is a function of the serviceability indexes. The initial serviceability index at the time of construction has never been evaluated for rigid pavements other than those evaluations done at the AASHO Road Test. Scrivner et al. (14) indicated that the average initial serviceability index on flexible pavement in Texas is 4.2. Having no better estimate for Texas, we assumed that rigid pavement for this study would have this same value. Performance studies by Treybig (15) indicate that the initial serviceability index of in-service pavements is well below the 4.5 measured at the AASHO Road Test (16). Based on a knowledge of construction variability and numerous observations of pavements under construction, the standard deviation of the initial serviceability index was estimated to be 0.5.

For the standard deviation of the terminal serviceability index, actual measurements of serviceability index were used. Measurements at the AASHO Road Test (16) as well as performance studies in Texas indicate a standard deviation of 0.3.

Discussion of Variables

The standard deviations developed for each of the design variables cannot all be used with the same confidence. Those that are true standard deviations developed from real data are thought to be good estimates of variation in service. These include the standard deviations given earlier for modulus of elasticity, flexural strength, and the terminal serviceability index.

For the modulus of subgrade reaction and slab thickness, the assumption was made that the coefficient of variation for each of the 2 respective variables would be constant for all levels of the variables in the ranges under study. Because the thickness data used (9) gave reasonable standard deviations and also a reasonable constant coefficient of variation over the range, the standard deviations for the thicknesses in this experiment are believed to be reasonable. The coefficient of variation on the k-value resulted from data recorded at the AASHO Road Test (10), which was conducted under somewhat more careful control than might be expected in the field. Furthermore, there are few data to substantiate the assumption of constant coefficient of variation, although wide variations would not be expected. The values used here should be verified in future studies.

The standard deviations of the remaining 2 variables are associated with a somewhat lower level of confidence. The standard deviations for both the initial serviceability index and the J-value are estimated and not computed from numerical data.

Variations for Sensitivity Study

Each of the design variables has some distribution. For the analysis of changes in expected pavement life, the total variation selected for each variable was either 1 or 2 standard deviations. The variation in modulus of elasticity was selected as ±1 standard deviation. The variation selected for thickness, flexural strength, and modulus of subgrade reaction was ±2 standard deviations, because 95 percent of the total variation (assuming that each variable had a normal distribution) would be included within the bounds.

The level of variation for slab continuity was selected as ±1 standard deviation because the variation was estimated rather than based on real data. The serviceability parameters were both varied ±1 standard deviation. The initial serviceability index has an upper limit of 5.0. With a mean of 4.2 and 2 standard deviations, unreasonable answers would result. For the terminal serviceability index, ±1 standard deviation was also selected. The deviation levels of all variables are given in Table 2.

RESULTS

The total expected pavement life as predicted by Eq. 1 has been determined for the factorial. Figure 3 shows the predicted pavement life for each case in total 18-kip single-axle applications. The effects of positive and negative variations in each of the variables in each factorial block have been evaluated in terms of percentage change in life.

Analysis

An analysis of variance was made on the mean values of the expected pavement life shown in Figure 3. The analysis of variance considered only 5 of the 7 factors because the initial and terminal serviceability indexes were studied only at one level. Those significant factors and interactions at selected alpha levels are shown in Table 3. All other possible interactions were insignificant.

A graphic presentation was chosen to relate the effects of variations in each variable to pavement life. Pavement life

TABLE 2

DEVIATION LEVELS OF INDEPENDENT VARIABLES

Variable	Level	Standard Deviation	Deviation Level
Modulus of elasticity, E	$2(10)^6$	$2(10)^5$	$1.8(10)^6$ $2.2(10)^6$
	$5.5(10)^6$	$6(10)^5$	$4.9(10)^6$ $6.1(10)^6$
Flexural strength, S_x	400	45	305 495
	800	60	680 920
Thickness, D	6	0.165	5.67 6.33
	12	0.330	11.34 12.66
Modulus of subgrade reaction, k	25	4	17 33
	200	30	140 260
	1,000	150	700 1,300
Continuity, J	3.20	0.13	3.07 3.33
	2.33	0.19	2.14 2.52
Initial serviceability index, P_o	4.2	0.5	3.7 4.7
Terminal serviceability index, P_t	3.0	0.3	2.7 3.3

Continuity	Mod. of Elast.	Subg. Mod.	Thickness \ Flex. Stren.	400		800	
				6	12	6	12
3.20	$2(10)^6$	25		87,000	6,432,000	1,240,000	91,918,000
		200		310,000	11,542,000	4,302,000	164,946,000
		1000		3,384,000	27,319,000	48,356,000	390,407,000
	$5.5(10)^6$	25		62,000	5,406,000	889,000	77,259,000
		200		144,000	8,271,000	2,064,000	118,198,000
		1000		567,000	14,965,000	8,106,000	213,860,000
2.33	$2(10)^6$	25		293,000	21,731,000	4,190,000	310,543,000
		200		1,017,000	38,994,000	14,533,000	557,239,000
		1000		11,432,000	92,296,000	163,370,000	1,318,957,000
	$5.5(10)^6$	25		210,000	18,265,000	3,003,000	261,013,000
		200		488,000	27,943,000	6,971,000	399,324,000
		1000		1,916,000	50,560.000	27,385,000	722,519,000

Figure 3. Predicted pavement life in 18-kip equivalencies.

TABLE 3

ANALYSIS OF VARIANCE FOR EXPECTED PAVEMENT LIFE

Combination of Variables[a]	Degrees of Freedom	Mean Squares	F-Value	Significance Level (percent)
D	1	44,961,433	161.1	1
S_x	1	43,452,302	155.7	1
S_x x D	1	33,969,002	121.7	1
J	1	16,971,287	60.8	1
J x D	1	13,267,448	47.5	1
J x S_x	1	12,822,076	45.9	1
J x S_x x D	1	10,023,472	35.9	1
k	2	8,946,193	32.0	1
k x S_x	2	6,758,959	24.2	1
k x D	2	5,269,082	18.9	1
k x S_x x D	2	3,980,810	14.3	1
E	1	3,605,810	12.9	1
J x k	2	2,639,904	9.5	1
J x k x S_x	2	1,994,450	7.2	5
E x D	1	1,740,530	6.2	5
E x k	2	1,601,046	5.7	5
J x k x D	2	1,554,808	5.6	5
E x k x S_x	2	1,209,627	4.3	5

[a]J = continuity; E = modulus of elasticity; k = modulus of subgrade reaction; S_x = flexural strength; D = thickness.

change is characterized by the percentage change in the summation of traffic loads for the performance period. The performance period is the time required for the pavement serviceability index to decrease from 4.2 to 3.0. The following are the variables analyzed and their order of importance with respect to change in expected pavement

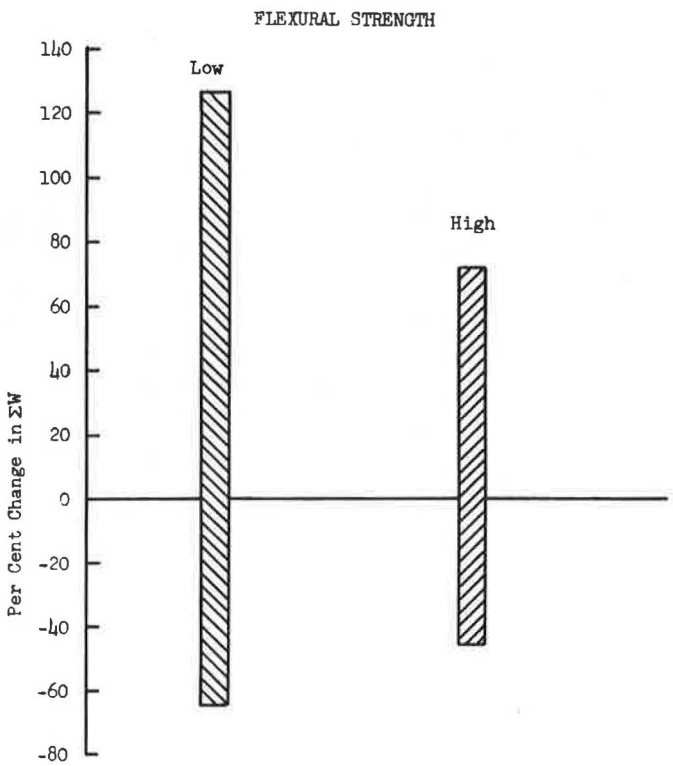

Figure 4. Effect of flexural strength variations on predicted life.

life: flexural strength, thickness, continuity, terminal serviceability index, initial serviceability index, modulus of subgrade reaction, and modulus of elasticity.

Flexural Strength—The change in predicted accumulated traffic or pavement life is more severe for the lower level of strength or lightweight concrete (Fig. 4). The change in life caused by variation in flexural strength is independent of the concrete modulus of elasticity, thickness, modulus of subgrade reaction, and slab continuity.

Thickness—The changes in pavement life caused by variations in thickness are shown in Figure 5. The positive variations in thickness resulted in longer life, while thinning the slab shortened the predicted life. The change in life that results from thickness variations is independent of the continuity and flexural strength but dependent on the concrete modulus of elasticity, modulus of subgrade reaction, and thickness. The changes in life caused by positive variations in thickness are greater per standard deviation than those caused by negative changes (Fig. 5).

Slab Continuity—Variations in slab continuity show that the change in expected pavement life is greater for continuously reinforced concrete pavement than for jointed concrete. The change in expected pavement life caused by variations in continuity of the slab is independent of all factors that were evaluated at more than one level. In actual highway engineering practice this independence may be conjectured, but for the mathematical model used here the independence does exist. Figure 6 shows the effects of variations in continuity on the change in expected pavement life for both jointed and continuously reinforced concrete pavement.

Terminal Serviceability Index—One level of terminal serviceability index, 3.0, was evaluated. The change in expected pavement life is dependent only on the level of thickness and is more severe at the higher level of thickness, as shown in Figure 7.

Initial Serviceability Index—All work in this experiment was for one level of the initial serviceability index, 4.2. It was found that change in expected pavement life due to

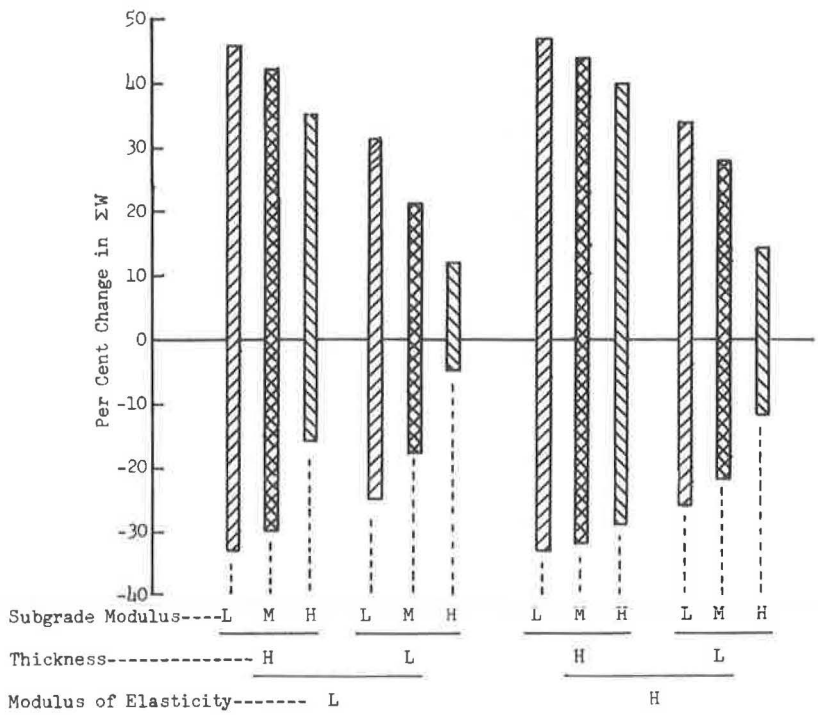

Figure 5. Effect of thickness variations on predicted life.

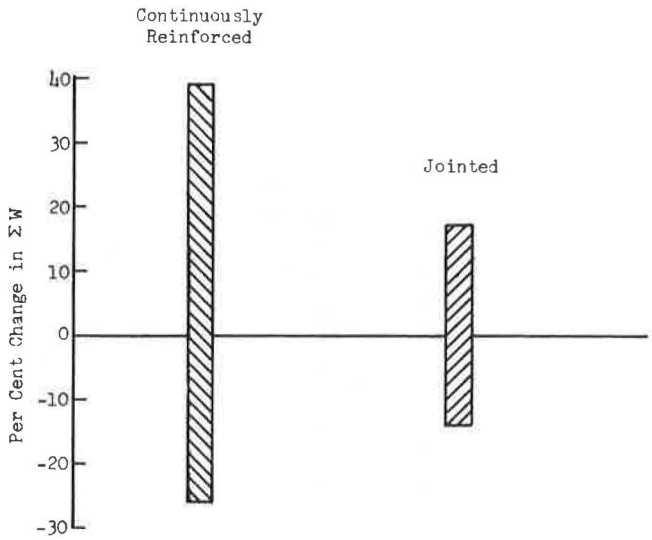

Figure 6. Effect of slab continuity variations on predicted life.

variations in the initial serviceability index depends only on the level of thickness. The change in expected life is independent of all other factors as shown in Figure 8 where the change in life for variations in the initial serviceability index is greater for the high level of thickness.

Modulus of Subgrade Reaction—The changes in pavement life due to variations in k-value are dependent on the level of the variable, modulus of elasticity, and thickness, as shown in Figure 9. They are independent of the level of flexural strength or the slab continuity. For the 2 lower levels of the subgrade modulus, the positive and negative changes in expected life are approximately equal, though they are not at the high level of the subgrade modulus. The changes in expected pavement life due to variations in

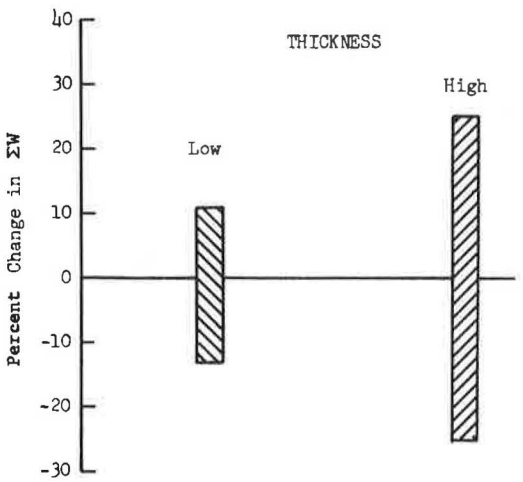

Figure 7. Effect of terminal serviceability index variations on predicted life.

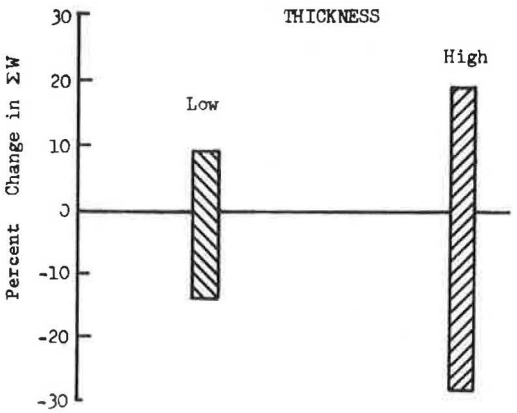

Figure 8. Effect of initial serviceability index variations on predicted life.

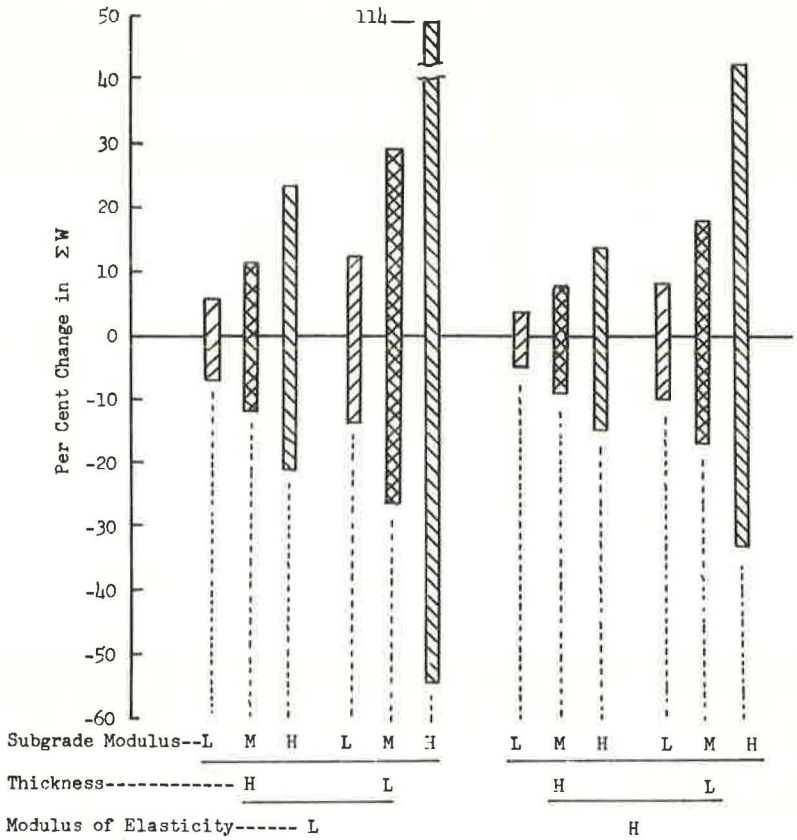

Figure 9. Effect of modulus of subgrade reaction variations on predicted life.

the modulus of subgrade reaction are much higher for the lower level of thickness than for the higher level of thickness.

Modulus of Elasticity—The change in expected pavement life is positive for a decrease and negative for an increase in the modulus of elasticity (Fig. 10). The magnitude of change in life is dependent on the level of the concrete modulus, the pavement thickness, and the modulus of subgrade reaction but is independent of flexural strength and slab continuity.

Discussion of Results

Examination of the data in Figure 3 indicates that the design equation (Eq. 1) predicts extremely high estimates of the total pavement life or accumulated traffic when combinations of variables occur at the high level. These results alone are not meaningful. The percentage change in pavement life due to variations in the factors over this entire range is useful in evaluating the importance of factors. The use of a digital computer made it a relatively simple matter to evaluate the full factorial experiment.

The analysis of variance for these data has indicated that 8 two-factor interactions and 5 three-factor interactions are significant. Thus, variations in expected pavement life other than those resulting from the main factors were not random, but were caused by a relationship between the factors. The analysis of variance indicates for the extended AASHO design equation for rigid pavement that the design variables are truly significant as are the combinations or interactions given in Table 3. The analysis of

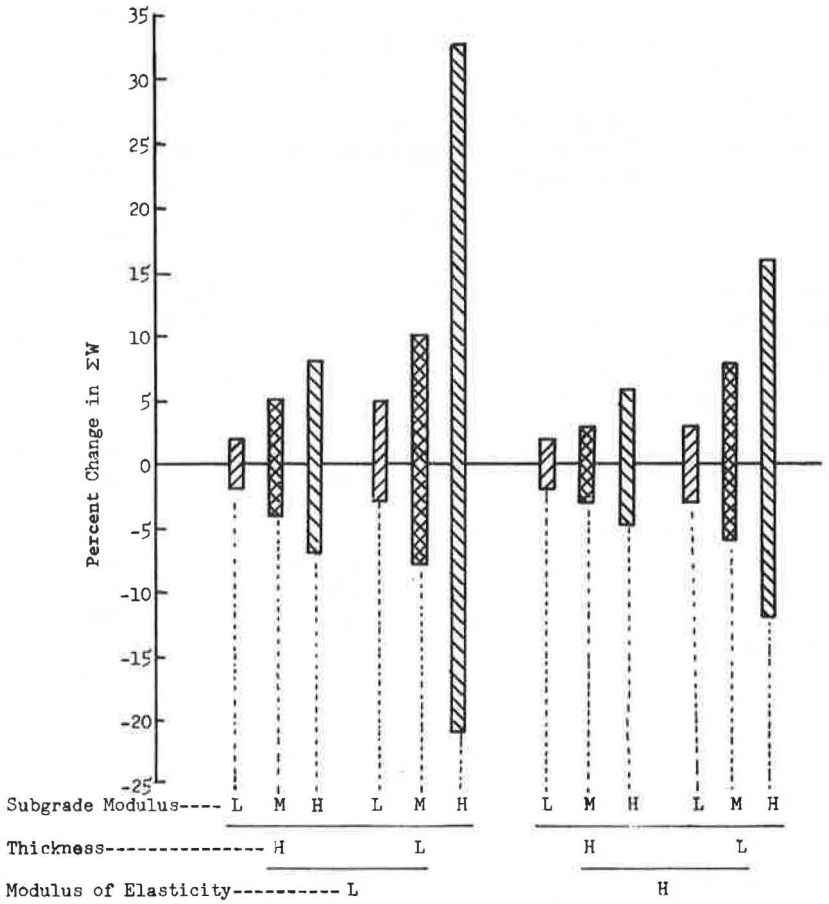

Figure 10. Effect of modulus of elasticity variations on predicted life.

variance yielded essentially the same ordering on the design variables as did the analysis of changes in expected pavement life resulting from chance variations in the design factors.

As expected and as indicated by this study the 2 most significant factors in the extended AASHO rigid pavement design equation (Table 3, Figs. 4 and 5) are the flexural strength and the pavement thickness. The analysis of variance for the mean values of expected pavement life also showed the thickness and flexural strength to be very important (Table 3). These two are closely followed by the slab continuity term. Buick found in his work (5) that, for the AASHO rigid pavement design method, the flexural strength was one of the 2 most important parameters. McCullough et al. (6) also found the effects of flexural strength to be highly significant. It appears logical that variations in the flexural strength should also be highly significant in the extension of the AASHO rigid pavement design method. Under actual construction conditions the flexural strength of the concrete has a high probability of variation (6). The magnitude of change in expected pavement life is not equal for equal magnitude of positive and negative variations in the flexural strength (Fig. 4).

The expected change in pavement service life due to overestimated thickness or deficiencies in thickness was over 20 percent in most cases (Fig. 5). The study by McCullough et al. (6) also indicates that thickness is a very significant factor. The chance

for variation in thickness is always present during construction where a section might be built thicker or thinner than the desired plan dimensions. The size of change in expected pavement life is not equal for equal magnitudes of positive and negative variations in thickness.

The slab continuity factor in this design equation does nothing more than designate the type of rigid pavement. In actual construction the continuity of continuously reinforced pavement would certainly depend on the percentage of longitudinal steel, concrete strength, and probably several other parameters. The continuity of a jointed pavement would certainly depend on joint spacings and mechanical load transfer supplied. Thus, the continuity or load-transfer term might be somewhat misleading. The variations in the load-transfer term show what might be expected in practice because of construction variations as well as variation in material properties.

Variations in the serviceability factors showed significant changes in the traffic service life, though not as great as those shown by variations in flexural strength or slab thickness. This design method indicates that the change in life caused by variations in the serviceability parameters is dependent on thickness. Buick (5), in his evaluation of relative practical importance paralleling this experiment, found the serviceability parameters to be less important than flexural strength, which agrees with the findings here.

The numerical evaluation of changes in expected pavement life in terms of percentage change in total traffic shows that, of the variables in the design equation, variations in the modulus of elasticity of the concrete have the least effect on the pavement service life within reasonable variations. Except for the high levels of modulus of subgrade reaction on the low level of thickness, all changes in expected life (Fig. 10), positive or negative, are less than 10 percent. This confirms the finding by McCullough et al. (6).

Another factor, whose variations were of little importance, was the modulus of subgrade reaction. For the factorial of this experiment only the variations at the high level of the subgrade modulus created significant changes in the expected traffic service life. This corroborates the work of McCullough et al.

CONCLUSIONS

This investigation was conducted to determine the sensitivity of pavement life as predicted by practical variations in the design variables. The conclusions are limited to the range of variables studied in this experiment and are of course only as good as the model being investigated. These findings, however, can provide reasonable information for use in design in selecting those variables requiring the most intensive study effort and those promising to yield the best improvements. This study illustrates a method that can be used to set priorities to upgrade any design model.

Based on the premise that the more important factors produce a greater change in the expected pavement life, the following conclusions are warranted:

1. The flexural strength and thickness are the most important factors whose negative variations may critically shorten pavement life.
2. The continuity factor was found to be the third most important factor.
3. The terminal and initial serviceability indexes were found to be important factors whose variations produce significant changes in the expected pavement life.
4. The modulus of subgrade reaction and the modulus of elasticity are the least important of the 7 design variables.
5. Significant interactions between the design factors do occur, indicating that the variations in the pavement life are not completely defined by the design variables alone.

Furthermore, this study shows those variables where tighter quality control restrictions are needed in order to improve life estimates.

RECOMMENDATIONS

Based on this investigation, the following are recommended:

1. Practicing highway engineers should recognize that variations in the pavement variables are real and have a significant effect on pavement life and that better quality

control of concrete flexural strength and thickness be incorporated to improve pavement performance.

2. Roughness specifications of new pavements should be updated to obtain smoother pavement and higher initial serviceability indexes.
3. In future model development, attention should be given to these variables in the priority listing presented.

ACKNOWLEDGMENTS

The work reported here was conducted jointly by 2 separate agencies: the Texas Highway Department Research Section and the Center for Highway Research, University of Texas at Austin. Special appreciation is extended to the Texas Highway Department for making available necessary data for the completion of this work.

REFERENCES

1. Hudson, W. R., Finn, F. N., McCullough, B. F., Nair, K., and Vallerga, B. A. Translating AASHO Road Test Findings—Basic Properties of Pavement Components. Materials Research and Development, Inc., Final report of NCHRP Project 1-10, March 1968.
2. Carey, W. N., Jr., and Irick, P. E. The Pavement-Serviceability Performance Concept. HRB Bull. 250, 1960, pp. 40-58.
3. AASHO Interim Guide for the Design of Rigid Pavement Structures. AASHO Committee on Design, April 1962.
4. Hudson, W. R., and McCullough, B. F. An Extension of Rigid Pavement Design Methods. Highway Research Record 60, 1964, pp. 1-14.
5. Buick, T. R. Analysis and Synthesis of Highway Pavement Design. Joint Highway Research Project, Purdue Univ., Lafayette, Ind., July 1968.
6. McCullough, B. F., Van Til, C. J., Vallerga, B. A., and Hicks, R. G. Evaluation of AASHO Interim Guides for Design of Pavement Structures. Materials Research and Development, Inc., Final report of NCHRP Project 1-11, Dec. 1968.
7. Shafer, R. W. Office memorandum on the determination of Young's modulus of elasticity for portland cement concrete, Nov. 14, 1958.
8. Johnson, J. W. Relationship Between Strength and Modulus of Elasticity of Concrete in Tension and Compression. Iowa Eng. Exp. Station, Ames, Bull. 90, May 9, 1928.
9. Concrete pavement files, Construction Div., Texas Highway Department.
10. Hudson, W. R. Comparison of Concrete Pavement Load-Stresses at AASHO Road Test With Previous Work. Highway Research Record 42, 1963, pp. 57-98.
11. Schleider, R. H. A Study of Concrete Pavement Beam Strengths. Texas Highway Department, Nov. 1959.
12. McCullough, B. F., and Treybig, H. J. A Statewide Deflection Study of Continuously Reinforced Concrete Pavement in Texas. Highway Research Record 239, 1968, pp. 150-174.
13. Treybig, H. J. Sensitivity Analysis of the Extended AASHO Rigid Pavement Design Equation. Univ. of Texas at Austin, Master's thesis, Aug. 1969.
14. Scrivner, F. H., Moore, W. M., McFarland, W. F., and Carey, G. R. A Systems Approach to the Flexible Pavement Design Problem. Texas Transportation Institute, Texas A&M Univ., Res. Rept. 32-11, Oct. 1968.
15. Treybig, H. J. Performance of Continuously Reinforced Concrete Pavement in Texas. Texas Highway Department, Res. Rept. 46-8F, July 1969.
16. The AASHO Road Test: Report 5—Pavement Research. HRB Spec. Rept. 61E, 1962.

Continuously Reinforced Concrete Pavement Observation Program in Mississippi— A Progress Report

T. C. TENG, Mississippi State Highway Department

This report covers the second year of a 5-year observation study of continuously reinforced concrete pavement construction in Mississippi. Measurements from the Desoto County and Jones County experimental projects constructed in 1961 and 1962 were continued. Their design features, data on end movement, crack width, and crack frequency, are presented and discussed. A preliminary review of the design and construction statistics and the statewide crack survey of all completed projects was made. This review indicates that in Mississippi the pouring temperatures and the design average daily traffic are not the major factors influencing crack spacing. After the early years of service, age of the pavement does not appear to be an important factor in crack spacing. The failure investigations and repair procedures are also reported. Failures, which represent a very small and insignificant percentage of the total completed mileage, were studied so that their causes could be corrected in future projects. Repair procedures were observed in the hope that a standard maintenance procedure could be established at the end of the study.

•THE DESOTO COUNTY EXPERIMENTAL PROJECT was constructed during the period from October 1960 to May 1961 in northwestern Mississippi and forms a part of Interstate 55, extending 5.3 miles southward from the Tennessee state line. This is a 4-lane highway with a median. The two parallel pavements are 24 ft wide, each containing two 12 ft traffic lanes. The upper 6 in. of the subgrade was cement-treated and compacted. A sand-gravel base course, 13 to 14 in. thick, was placed on the subgrade and the upper 6 in. of the base course was cement-treated. Two pavement thicknesses, 7 and 8 in., were used. The entire project consisted of 10 individual continuously reinforced pavements, as shown in Figure 1a. Each of the pavements terminates at a bridge or at a conventional pavement. The characteristics of the 6 pavement types are given in Table 1 (10).

The primary experimental feature of this pavement was the use of reinforced cast-in-place concrete piles as terminal anchorages to inhibit the seasonal longitudinal movements of the terminal ends of the pavement. Details of the pile anchorages are shown in Figure 1b and 1c. In order to determine the effectiveness of various sizes of pile groups, various numbers of piles were used at terminal ends of pavement, as given in Table 1 (10). The secondary experimental feature was to compare the 3 combinations of pavement thickness and steel percentage. The 4 sizes and spacings of transverse reinforcements are used for comparison also (10).

From the various field measurements, it appears that after 8 years of service, the effectiveness of using various numbers of cast-in-place concrete piles on the longitudinal movement of pavement is not statistically significant enough to identify any

Paper sponsored by Committee on Rigid Pavement Design and Committee on Maintenance of Portland Cement Concrete Pavements and presented at the 49th Annual Meeting.

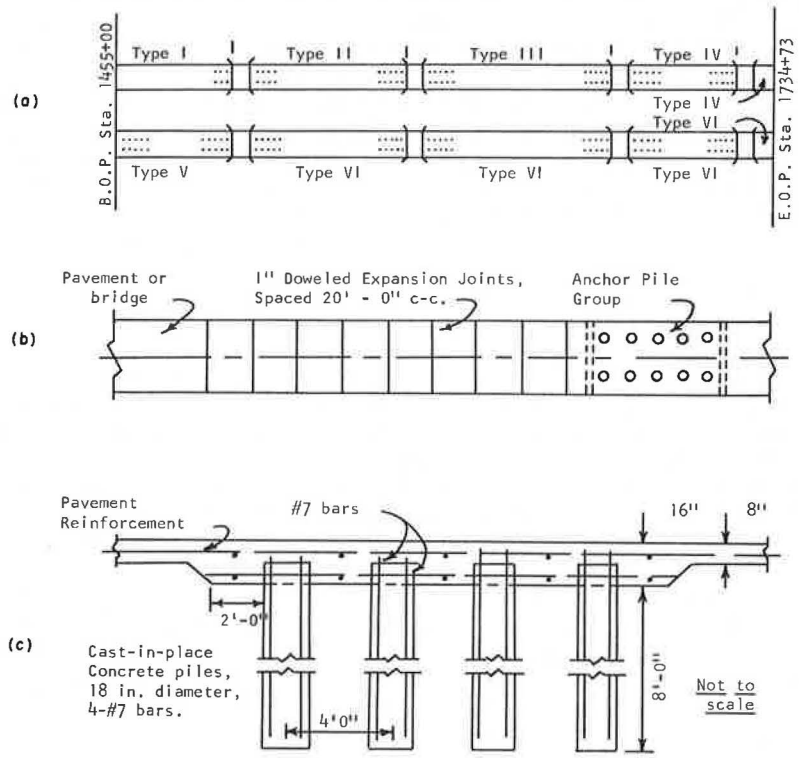

Figure 1. Details of Desoto County experimental project (10): (a) plan of design variables; (b) typical detail of end of pavement; and (c) typical detail of end of pile anchorage (3, 4, or 5 piles in line).

TABLE 1

PAVEMENT CHARACTERISTICS OF DESOTO COUNTY EXPERIMENTAL PROJECT

Type	Station Limits	Thickness (in.)	Longitudinal Reinforcement (percent)	Transverse Reinforcement	End Restraint
I	1455+00-1506+64, west	7	0.7	No. 4 bars at 24 in.	Asphalt pavement and no piles south, 6 piles north
II	1511+86-1579+68, west	8	0.6	No. 4 bars at 24 in.	8 piles south, 10 piles north
III	1586+10-1667+88, west	8	0.7	No. 3 bars at 18 in.	10 piles both ends
IV	1673+11-1720+67, west	8	0.7	No. 4 bars at 30 in.	10 piles both ends
	1725+89-1733+13, west	8	0.7	No. 4 bars at 30 in.	10 piles both ends
V	1456+60-1506+64, east	8	0.7	No. 4 bars at 36 in.	10 piles both ends
VI	1511+86-1578+90, east	8	0.7	No. 4 bars at 24 in.	10 piles both ends
	1585+32-1667+88, east	8	0.7	No. 4 bars at 24 in.	10 piles both ends
	1673+11-1720+67, east	8	0.7	No. 4 bars at 24 in.	10 piles both ends
	1725+89-1733+13, east	8	0.7	No. 4 bars at 24 in.	10 piles south, jointed pavement and no piles north

differences. The pile restrained ends (Figs. 2 and 3) showed an annual movement of ¼ to ½ in. after the first 3 years of service. It appears that cyclic action is occurring with a very slight increase in length added to the total length of pavement at the high point of each annual cycle. The same results were achieved in Illinois (5). Measurements taken in 1969 indicate that the piles were able to restrain the pavement movement to 1 in. or slightly higher after 8 years of service. A previous report (9) pointed out that the longitudinal movement does not proceed at a smooth rate from the end to some unmoving point in the interior. As the measurements do not continue to show the same occurrence, the consequence of this behavior cannot be assessed. In contrast, the 2 unrestrained ends have shown large annual movements. Figure 2 shows that in 1963 the movement was about 1½ in. from the southern end and about 1 in. from the northern end. The magnitude of the yearly cycle appears to be increasing. Measurements of the past 3 years show a movement of about 2 in.

The measurement of surface width of the selected cracks in each test section was continued, and the average crack widths are shown in Figures 4 and 5. It is obvious that no significant difference exists among various types of pavement sections. This is probably because only 2 different percentages of longitudinal reinforcement were used (0.7 and 0.6 percent). However, it appears that the overall average crack width has increased with time and is also slightly higher than the measurements obtained in Illinois (2), Pennsylvania (8), and Maryland (4).

The average crack spacing is shown in Figure 6. The different types of pavements showed a slight difference of average crack spacing after the first few years of service However, it appears to level off with time. To date, all types of pavement have an average crack spacing of about 5 ft.

The Jones County experimental project was constructed during the period from January to April 1962 in southeastern Mississippi and forms and forms a part of Interstate 59 between Ellisville and Moselle with a length of 6.77 miles. This is also a 4-lane highway with a median. The 2 parallel pavements are 24 ft wide, each containing two 12 ft traffic lanes. The upper 6 in. of the base course was cement-treated. The entire east pavement is reinforced with welded wire mesh,

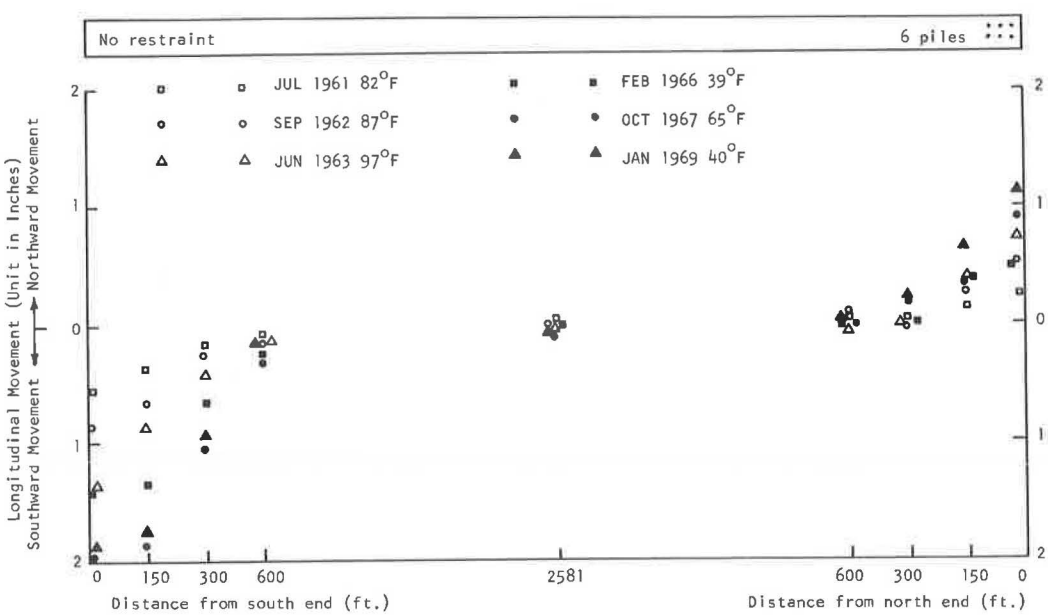

Figure 2. Measurements of longitudinal movement of Type I pavement on west roadway in Desoto County.

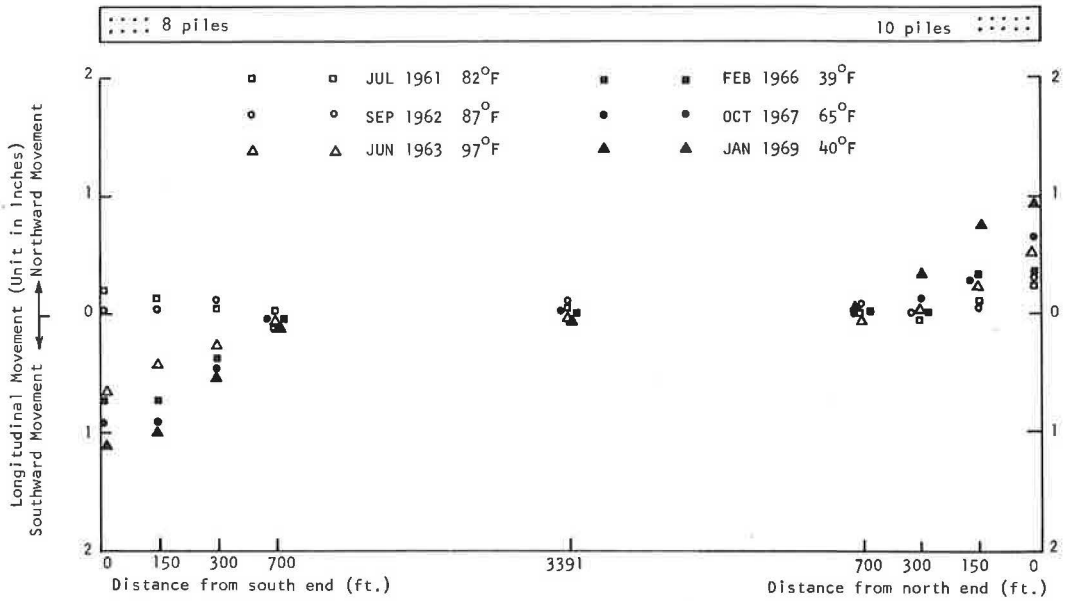

Figure 3. Measurements of longitudinal movement of Type II pavement on west roadway in Desoto County.

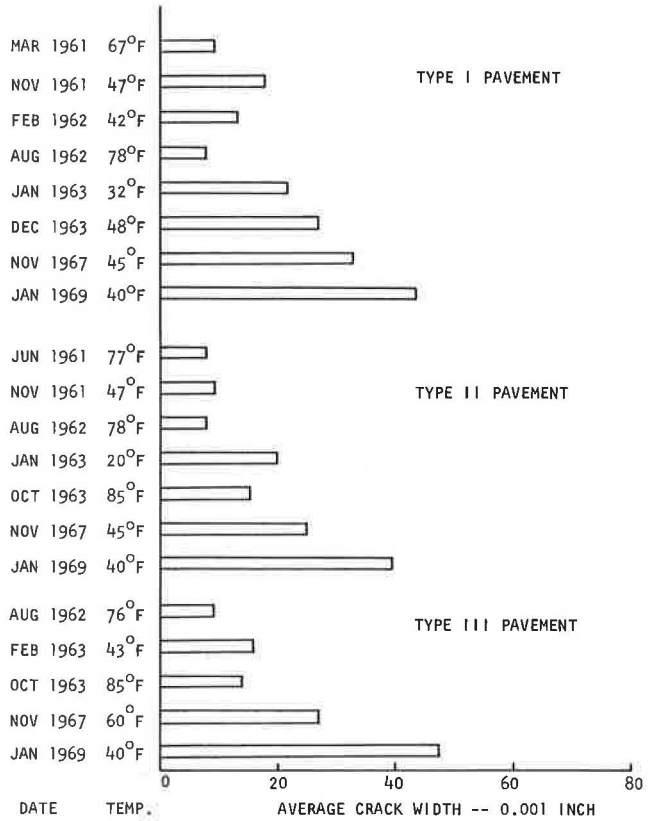

Figure 4. Average crack width of Types I, II, and III pavements in Desoto County.

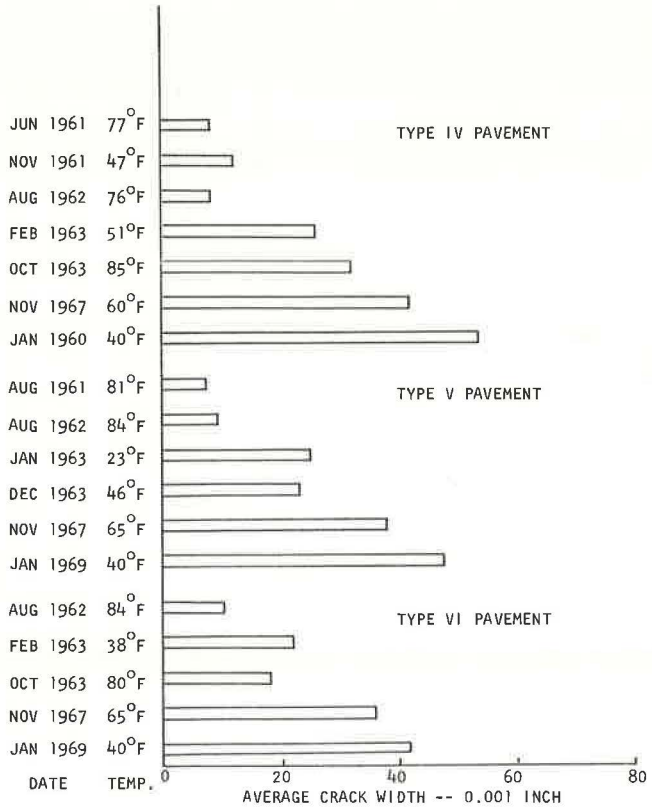

Figure 5. Average crack width of Types IV, V, and VI pavements in Desoto County.

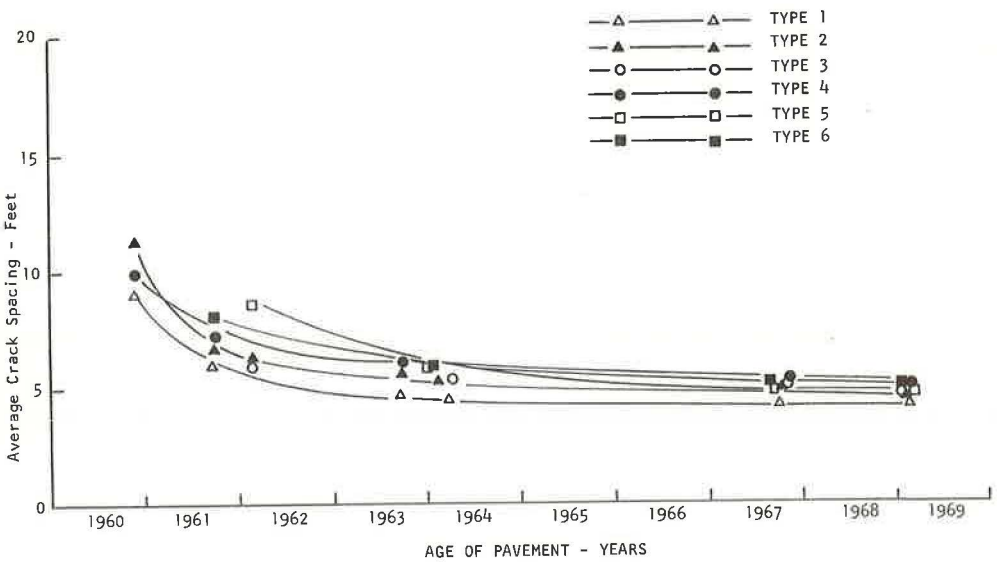

Figure 6. Average crack spacing of pavement in Desoto County.

overlapped 13 in. at the end of the 24-ft long mats. The west pavement is reinforced with No. 6 deformed bars, 40 ft long, overlapped 15 in. The entire project consisted of 6 types of continuously reinforced pavements, as shown in the upper portion of Figure 7a. The characteristics of the 6 pavement types are given in Table 2 (10). The two ends of the pavements are restrained with lug anchors, 5 at one end and 4 at the other. Typical details of the lug anchors are shown in Figure 7b, c, and d. Each concrete lug anchor extends the full width of the pavements and is cast monolithically with the concrete slab (10).

The special experimental features of this project are the comparison of 3 percentages of reinforcing steel for each of the 2 reinforcement types and the use of lug anchors as means of end restraint (10).

From the various field measurements, it appears that after 7 years of service the lug anchors were not effective in stopping all movement and in preventing growth in length. However, by comparing Figure 8 with the unrestrained ends in the Desoto County project (Fig. 2), one can easily appreciate the function of the lug anchors in

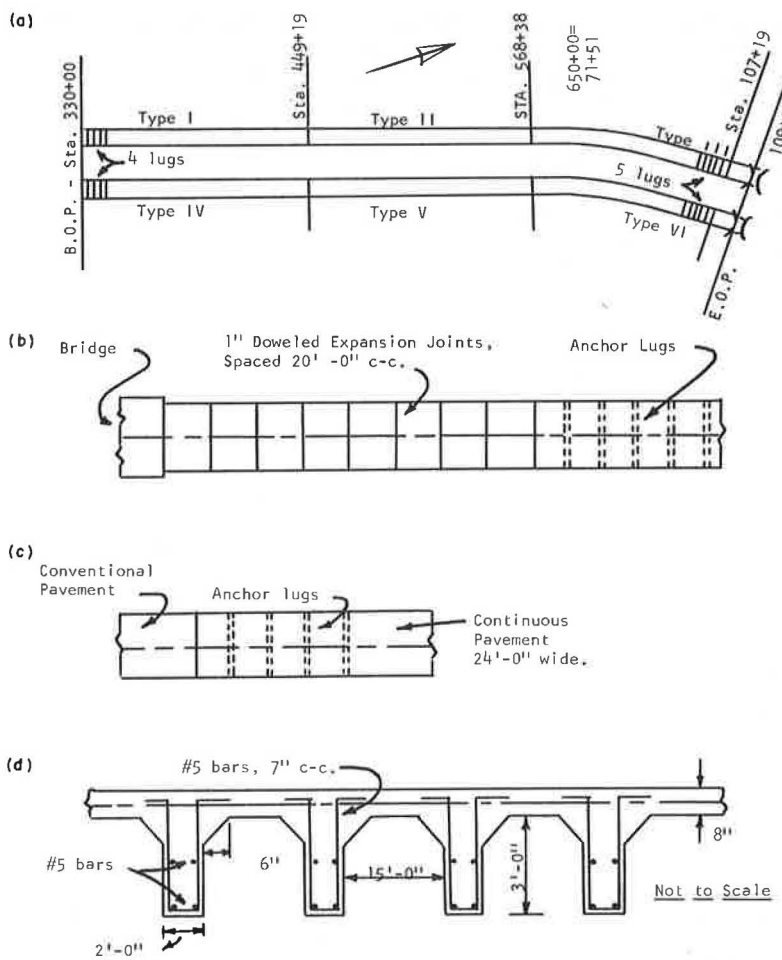

Figure 7. Details of Jones County experimental project (10): (a) plan of experiment variables; (b) pavement terminus of bridge; (c) pavement terminus of conventional pavement; and (d) details of concrete lug anchors.

TABLE 2

PAVEMENT CHARACTERISTICS OF JONES COUNTY EXPERIMENTAL PROJECT

Type	Station Limits[a]	Thickness (in.)	Longitudinal Reinforcement (percent)	Type of Longitudinal Reinforcement	Transverse Reinforcement	End Restraint
I	330+00-449+19, west	8	0.5	No. 6 bars	No. 4 bars at 30 in.	4 lugs
II	449+19-568+38, west	8	0.6	No. 6 bars	No. 4 bars at 30 in.	
III	568+38-107+19, west	8	0.7	No. 6 bars	No. 4 bars at 30 in.	5 lugs
IV	330+00-449+19, east	8	0.5	No. 5/0 wire mesh	No. 1 wire at 12 in.	4 lugs
V	449+19-568+38, east	8	0.6	No. 5/0 wire mesh	No. 1 wire at 12 in.	
VI	568+38-107+19, east	8	0.7	No. 7/0 wire mesh	No. 00 wire at 12 in.	5 lugs

[a]Equation: Station 650+00 equals station 71+51.

reducing the degree of pavement movement. To date, the end movement is still restrained to within 1 in. of its original position.

Average crack widths of the different types of pavements are shown in Figures 9 and 10. These graphs indicate that the wire mesh reinforced pavement has relatively larger cracks than the steel bar reinforced pavement. Because all the extra-wide cracks took place at the overlap, this can probably be attributed to the fact that the 13-in. overlap of the mesh was not sufficient. The percentage of longitudinal reinforcement (0.5, 0.6, and 0.7 percent) caused almost no difference in the crack width, which is increasing with time.

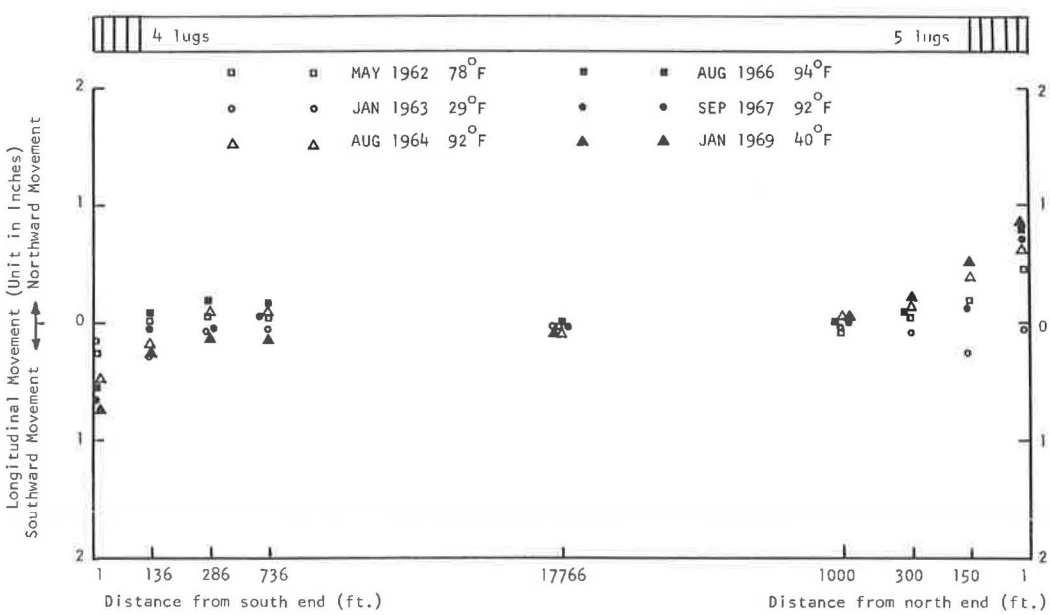

Figure 8. Measurements of longitudinal movement of pavement on east roadway in Jones County.

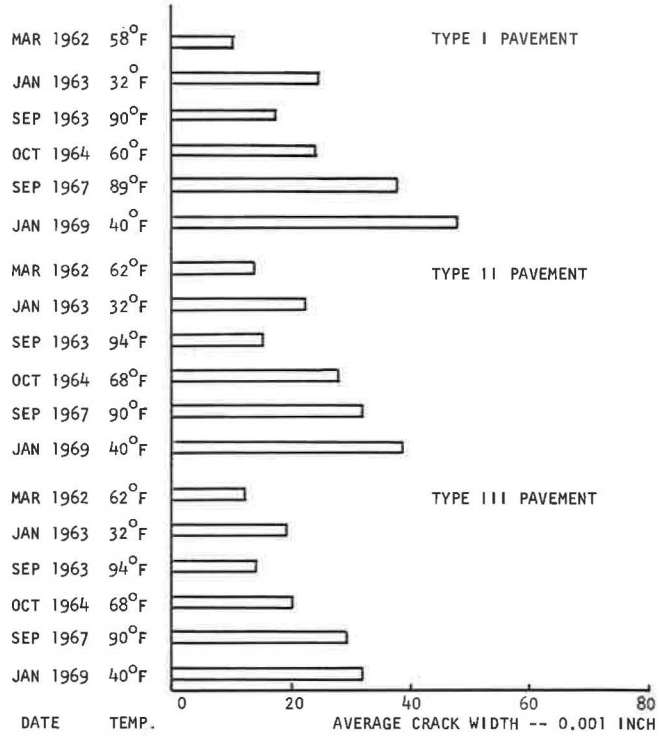

Figure 9. Average crack width of Types I, II, and III pavements in Jones County.

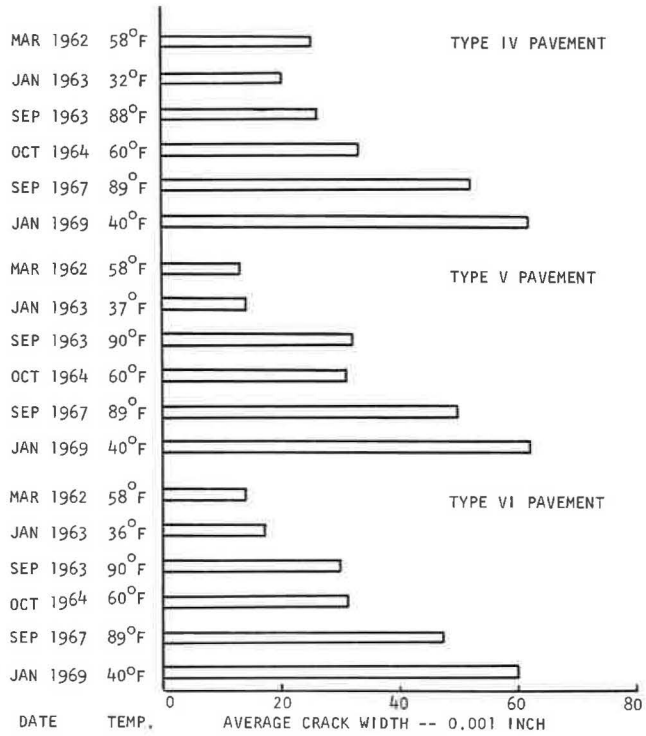

Figure 10. Average crack width of Types IV, V, and VI pavements in Jones County

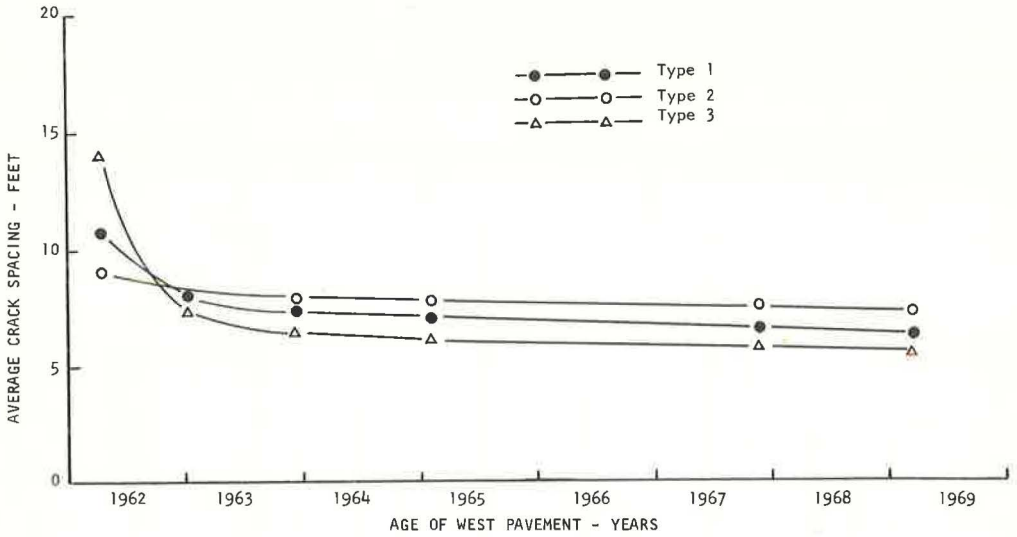

Figure 11. Average crack spacing of pavement with bar reinforcement on west roadway in Jones County.

As shown in Figures 11 and 12, the different types of pavements showed no significant difference in average crack spacing, which also appears to level off with time. To date, all types of pavements have an average crack spacing between 5 and 6 ft.

SOME STATEWIDE DESIGN AND CONSTRUCTION STATISTICS

From the research findings of the Desoto and Jones Counties experimental projects and the recommendations of the American Concrete Institute (1), Mississippi has gradually established its standard design criteria for continuously reinforced concrete

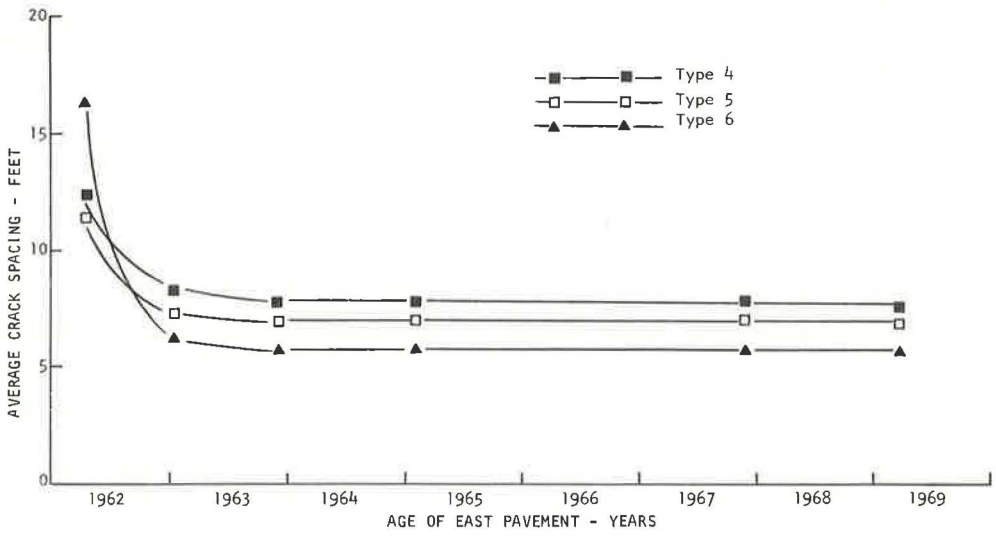

Figure 12. Average crack spacing of pavement with wire reinforcement on east roadway in Jones County.

TABLE 3

TYPES OF STANDARD STRUCTURE DESIGN

Type	Thickness (in.)	Longitudinal Reinforcement (percent)	Type of Longitudinal Reinforcement	Transverse Reinforcement
CRP-1	8	0.581	No. 5 bars at 6½ in.	No. 4 bars at 30 in.
CRP-2	8	0.611	No. 6 bars at 9 in.	No. 4 bars at 30 in.
CRP-3	8	0.581	No. 5/0 GA wire at 3 in.	No. 1 GA wire at 12 in.

pavement. As suggested by the American Concrete Institute (1) and according to the minimum criteria for federal-aid roads established by the Bureau of Public Roads, 8 in. uniform slab depth has been used for all projects.

Three types of structure design were adopted as standard: CRP-1, CRP-2, and CRP-3 (Table 3). In order to comply with the recommendations of the American Concrete Institute (1) and results from the Desoto and Jones projects, efforts were made for these 3 structure types to have a 0.6 percent longitudinal reinforcement. About 15 projects were constructed using these 3 standards during 1962-63. Since then only type CRP-1 has been used. As shown in Figure 13, 49 projects have been completed to date.

For longitudinal steel, 3 lap lengths, 15, 18¾, and 20 in., were used in the past 8 years. Presently, a 20-in. lap length is used as the standard.

At the construction joint, longitudinal bars are required to extend a minimum length of 5 ft. No additional steel was installed at the construction joints on 5 projects built during 1962-63. Since then, No. 5 deformed bars, 5 ft long, placed at 6½ in., were used as additional steel following the recommendation of the Concrete Reinforcing Steel Institute.

The same type lug anchors used in the Jones County experimental project (Fig. 7) were adopted as standard. For the first 5 years of practice, 5 lug anchors were used for bridge ends and 4 lug anchors for pavement ends. Since 1967, 4 lug anchors have

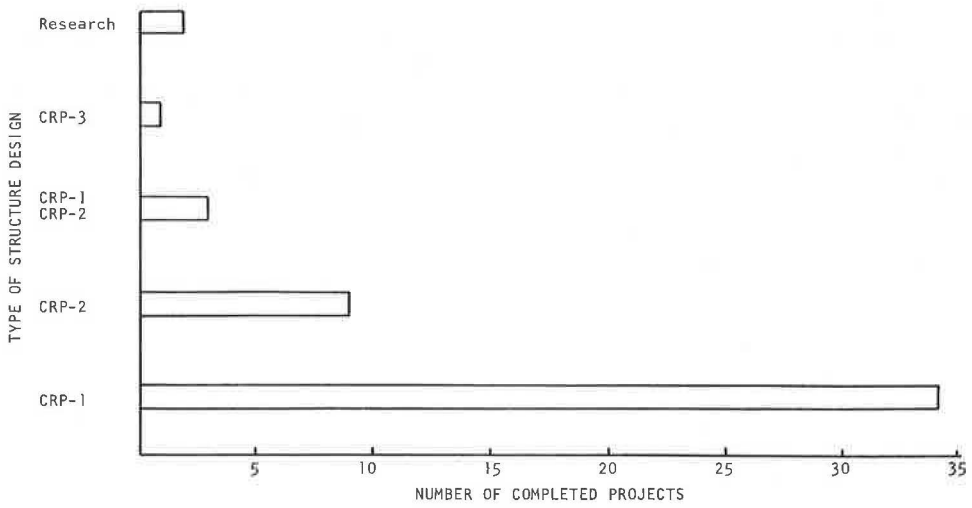

Figure 13. Structure type of completed continuously reinforced concrete pavement projects.

TABLE 4

CRITERIA FOR SUBBASE AND DESIGN SOIL TREATMENT FOR 8-IN. CONTINUOUSLY REINFORCED CONCRETE PAVEMENTS ON 6-IN. CEMENT-TREATED BASE

Subbase and Design Soil Treatment	CBR 1	CBR 2	CBR 3	CBR 4	CBR 5	CBR 6-10	CBR 11-15	CBR 16-20
Subbase, in.	1	1						
Design soil, in.	8	8						
Subbase, in.	4	1	1	1	1			
Design soil, in.	6	6	6	6	6			
Subbase, in.	14	9	7	6	4	1	1	1
Design soil, in.	0	0	0	0	0	0	0	0

Note: Design soil with CBR of five or less shall be lime or lime-cement treated, except where there are only a few short isolated sections in which case granular material may be substituted. According to past experiences, the boxed areas indicate preferred design criteria. The subbase mentioned here is actually an untreated portion of the base course.

been used for both bridge and pavement ends because the continuing measurements from the Jones County experimental project do not indicate any difference in pavement movement between 4- and 5-lug anchor installation.

Strength for the concrete is not specified. However, it is a general practice in the field that the concrete should provide a modulus of rupture of 525 to 550 psi at 7 days and 700 psi or more at 28 days when tested by the third-point method. For the 49 completed projects, 6 brands of cement were used including 46 projects with Type I cement and 3 projects with Type II cement. Fine aggregate for the concrete varies from 30 to 34 percent. The water-cement ratio ranges from 0.650 to 0.720 and the slump from 1.5 to 2 in.

Almost all of the 49 completed projects have soil-cement base and lime or lime-cement-treated subgrade. The present design procedures for base and subbase are based on CBR and traffic load. Mississippi law requires single axles not to exceed 18,000 lb, tandem axles spaced 4 ft through 7 ft apart not to exceed 32,000 lb, and gross vehicle weights not to exceed 73,280 lb. The design criteria are given in Table 4.

One of the major efforts of this research study is to compile design and construction statistics from all the completed projects and try to correlate them with the general performance of the pavements. To date the design and construction files are completed, and an attempt has been made to set up a system to collect pavement roughness data. This statewide pavement roughness survey is scheduled to begin during the early part of 1970. Once the pavement roughness information becomes available, the design and contruction statistics will be incorporated with it to make the performance analysis.

In reviewing the construction statistics, an effort was made to determine if any relationship existed between crack spacing, pouring temperatures, and design average daily traffic. The crack survey is also a statewide effort. Ten percent of the total length from each project was picked at random for this purpose, but none of the random samples was near construction ends. Readings were taken from the edge of the roadway by visual observation. Any visible crack, large or small, was counted and recorded. Figure 14 shows that the pouring temperatures and the design average daily traffic do not appear to dominate the crack spacing, and this is in general agreement with the findings in most other states. It is also interesting to note that the age of the pavement, after a few years of service, is not an important factor influencing the crack spacing. Plans have been made, however, to pick individual projects in the future from different construction seasons for detailed analysis.

It has been stated that the crack spacing on the Desoto County and Jones County experimental projects averages from 5 to 6 ft, whereas Figure 14 indicates that the crack spacing of all other projects constructed afterward averaged about 3 to 5 ft. This difference is due to a different method of counting the cracks (6, 9). In the 2 research projects, only those cracks extending all the way across the pavement were counted. On the other 47 projects, any visible cracks, large or small, were counted.

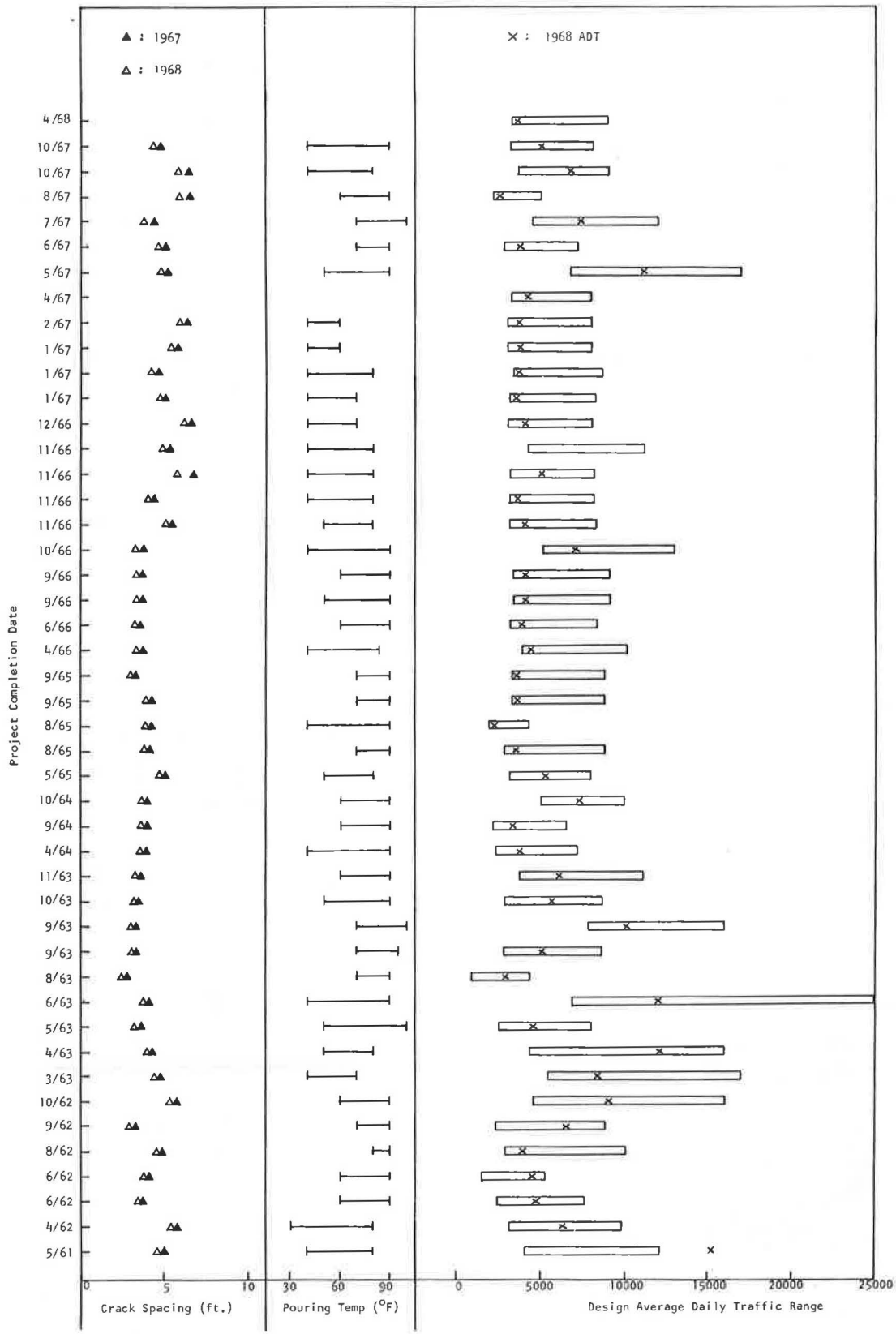

Figure 14. Crack spacing, pouring temperatures, and design average daily traffic range of completed continuously reinforced concrete pavement projects.

FAILURE INVESTIGATIONS

Failure investigation is also one of the major objectives of the research study. Various types of failures were studied, and the information obtained was submitted to all operating divisions and districts in the hope that the causes of the failures could be corrected in any future projects. For a proper perspective on the continuously reinforced concrete pavement construction in Mississippi, it should be emphasized that the total length of these failures only constitutes a very small and insignificant percentage of the total mileage of continuously reinforced concrete pavements in the state. Reported hereafter are the failures that have been investigated since the study was initiated.

I-55 Experimental Project in Desoto County

Eight small surface deteriorating areas were found that did not appear to be related to design, construction, or traffic. Severe cracking is developing in the deteriorating area. This can be easily observed from the exudation of the whitish-colored substance from these cracks during or after wet weather (Fig. 15).

To study the cause of these surface deteriorating failures, pH and sulfate content tests have been conducted on water and soil samples taken from the roadside ditches and the immediate vicinity. On the concrete sample taken from the surface of the pavement, microscope and X-ray technique were used to study the sulfur content, wet quantitative analysis was made to determine the cement content, and petrographic examination was made to study the aggregate reactivity. Results from these tests and examinations provided no substantial clues to explain the surface deterioration. It is felt that another approach should be employed to study the cause of these surface failures. At this time, the detailed procedure remains to be determined.

I-59 Experimental Project in Jones County

The southbound lane with the bar reinforcement is performing very well. However, on the northbound lane with smooth mesh reinforcement, 10 repairs have been made on extra-wide cracks that spalled badly. Four more of these extra-wide cracks (Fig. 16) are scheduled to be repaired in the future. All of these cracks occurred at the laps of the wire mesh, because of insufficient lap of 13 in. The 13-

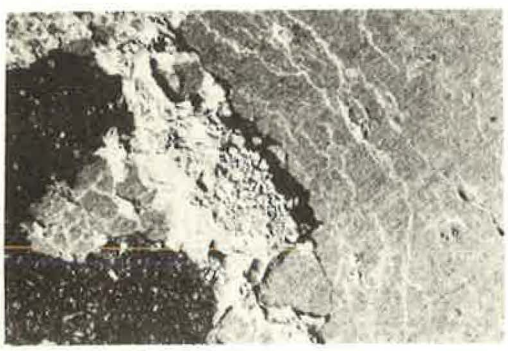

Figure 15. Exudation of whitish-colored substance from cracks around deteriorating area on I-55 in Desoto County.

Figure 16. Extra-wide cracks on I-59 in Jones County.

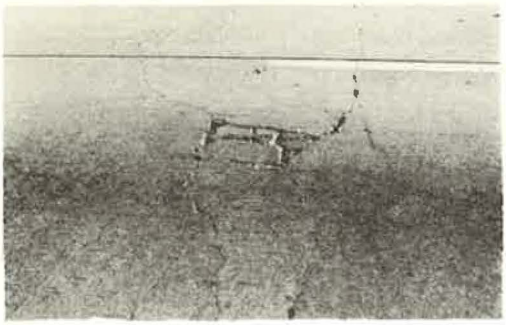

Figure 17. Typical failure on I-20 in Warren County.

Figure 18. Cores taken in failure area on I-20 in Warren County.

in. overlap was one of the experimental features. Both the Bureau of Public Roads and the Mississippi State Highway Department wanted to determine whether the 13-in. overlap was sufficient.

I-20 in Warren County

Four failures took place between closely spaced transverse cracks but are not related to cuts, fills, transitions, profile, or terrain (Fig. 17). Ten other locations have been spotted where failures may occur. Pavement coring investigation disclosed inferior honeycombed concrete or hollow spaces in the lower half and no bond with the steel (Fig. 18).

During paving operation, the placement spreader frequently left void areas of about a square yard or more at random locations (Fig. 19). Concrete flowed into these void areas from the finishing screed that carried a load of concrete of inferior quality. It appears that these construction faults are the cause of failures on this job. To prove the point, plans have been made to watch several new paving jobs. Void areas will be located and watched. Coring investigation will be made if necessary.

I-55 in Madison County

By mistake the wire-mesh overlap was increased to 46-54 in. instead of the designed 28 in. at every first lap ahead of the construction joint. The Concrete Reinforcing Steel Institute recommended increasing construction joint steel by one third. But, in this job, extra steel bars 5 ft long, which doubled the reinforcement, were used across all construction joints to hold them tight. However, this was not effective because the joints opened up, admitting water. The steel was rusted badly 4 to 6 in. on each side of the joint.

Figure 19. Void area left by placement spreader during paving operation.

To date, 11 failures (Fig. 20) have been experienced ahead of these construction joints in the direction of paving. Coring investigations show sound concrete in failed areas, but loss of bond with the steel occurred, probably because of overstress. However, the exact cause remains to be determined as the research develops. At present mesh reinforcement

Figure 20. Typical failure on I-55 in Madison County.

Figure 21. Defective area on I-59 in Pearl River County.

has been discontinued as an alternate in continuously reinforced concrete pavements.

I-59 in Pearl River County

Eight small deflective areas were found where cracking, crumbling, and distingration of concrete pavement took place (Fig. 21). Tapping the pavement at these areas with a hammer produced a hollow sound. Coring investigation disclosed that the top 2 in. of concrete was dense and solid, while the rest of the material down to the soil cement base crumbled readily. It is possible that these circular failures were due to the use of some dry and harsh or improperly mixed batches that should have been discarded.

US-82 in Leflore County

One failure was found on the east side of the construction joint, which divides 2 construction periods. Paving east of the joint began 5 months after paving west of the joint was completed. The failure, at a 30 deg angle across the entire project, is found on top of the lapped splices (Fig. 22). A few cores taken at random within the failure spot show an excellent quality of concrete but were broken at the middle where the steel is located.

A close observation, made during the repair operation, indicated that the failure was not caused by construction and that the concrete was in good condition. Presence of the failure, which coincided with the lapped splices, suggested that it may be due to, at least in part, the very high tensile stresses in the steel ahead of the construction joint that caused a decrease in bond at the splice where the concrete was poured almost 5 months later. It is possible that the serious slab separation at the failure spot was preceded or accompanied by progressive reduction in bond between the closely spaced cracks.

Figure 22. Failure on top of lapped splices on US-82 in Leflore County.

I-55 in Carroll County

Serious pavement distortion occurred causing void spaces between pavement and subgrade. Many transverse and diagonal cracks developed (Figs. 23 and 24).

Figure 23. Transverse and diagonal cracks on I-55 in Carroll County.

Figure 24. Void spaces of 2.5 in. between pavement and subgrade on I-55 in Carroll County.

The major reason for such pavement distortion was attributed to the fact that water-bearing sand and silt strata existed within a highly expansive zilpha clay area. Because of the transverse and diagonal cracks in the pavement and void spaces under the pavement, serious failures could have occurred when loads were applied. Therefore, recommendation was made that all the void spaces be filled before the highway was opened to traffic.

I-20 in Hinds County

One failure spot was found on a fill section of this pavement that was constructed in 1967 (Fig. 25). Field investigation indicated that the failure was caused by a slight settlement of the embankment.

I-55 in Copiah County

One blowup type of failure took place on this section of pavement that was constructed in 1966 (Fig. 26). During paving operation, the machine broke down for 30 min at this spot during the hot midday October weather. No construction joint was made while the paving machine was being repaired. From the inferior concrete that was found at the failure spot, it is evident that the delay of construction without a construction joint caused a weak spot that failed when high stresses developed.

Figure 25. Failure caused by embankment settlement on I-20 in Hinds County.

REPAIR OBSERVATIONS

No special efforts have been made to recommend repair procedures at this stage of the research study. It is felt that giving the district offices complete freedom in making repairs will help to

accumulate the experience of the district and project offices, which should be very beneficial in establishing a standard maintenance procedure. However, detailed observations are being made of various repair methods used by different districts. Specific recommendations will be made at the end of the study. The following discussion concerns the repairs that have been observed to date.

One district in south Mississippi, on pavement with mesh reinforcement where extra-wide cracks occurred at the laps of the wire sheets, made repairs by first making 2 saw cuts 30 to 50 in. apart with the failure in the center. The cuts were 1 in. deep after which a jackhammer was used to remove the concrete down to the reinforcement. After the concrete was removed and the area brushed clean, ½ in. reinforcing bars, 24 in. long, were placed and welded to the mats (Fig. 27). Following the welding, the entire repair zone, concrete and steel, was coated with epoxy glue (E-Poxtite Binder, Code 2385-B). Mixing of concrete was accomplished at the job site by using high-early-

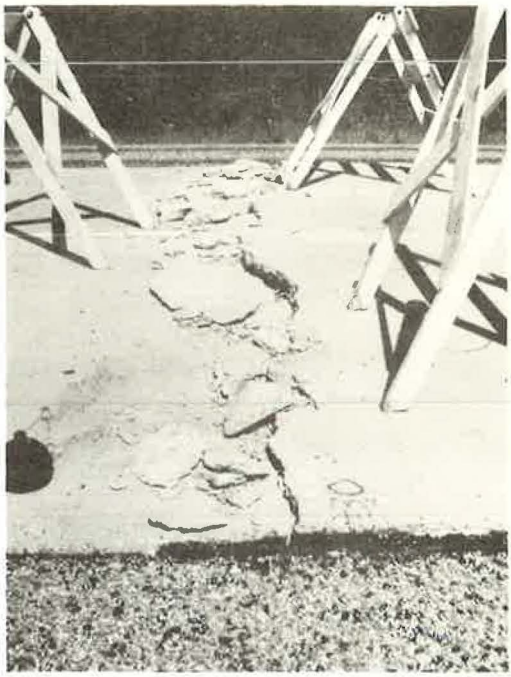

Figure 26. Failure on I-55 in Copiah County.

Figure 27. Patch ready for replacing concrete on I-59 in Jones County.

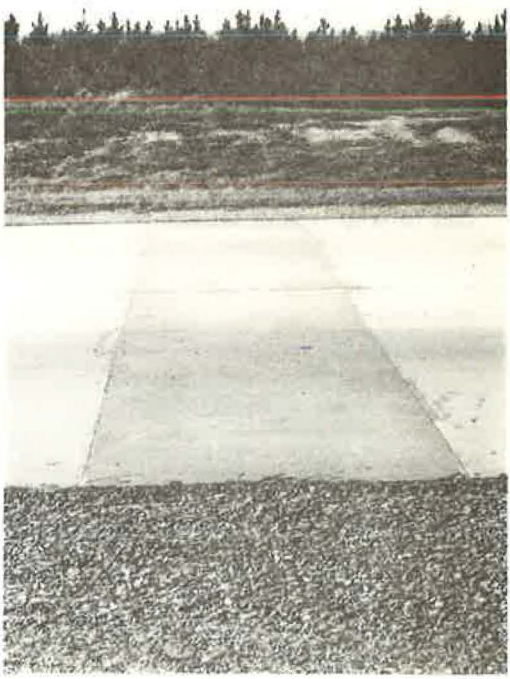

Figure 28. Complete patch 5 years after repair on I-59 in Jones County.

strength cement. A vibrator was used to ensure good placement, and the usual finishing practices were followed. The fresh concrete was covered by wet burlap while curing. Ten locations were repaired in this manner in 1962, and they still look good (Fig. 28).

On the same section of pavement, another repair procedure was tried on 4 locations in the early part of 1967. A narrow strip of concrete about 18 in. with the extra-wide crack in the center was removed down to the treated base. The continuity of the reinforcement was broken by removal of the rusted steel (Fig. 29), and 3¼-in. wood filler was installed to function as an expansion joint (Fig. 30). These procedures are against the theory of continuously reinforced concrete pavement and failure is expected again. Figure 31 shows the pavement 8 months after the repair and partially confirms the expectations.

One district in central Mississippi made repairs on pavement with mesh reinforcement where failures occurred ahead of the construction joints in direction of paving by removing a minimum of 7 ft of pavement ahead of the construction joint for full lane width. The concrete was removed by using a jackhammer first to the depth of the steel reinforcing mesh. Then the steel was cut at the center of the patch to give access for the jackhammer to remove the lower half of the pavement. This was a slow process, requiring care to prevent damage to the steel and the cement-treated base. The extra steel

Figure 29. Rusted steel removed from extra-wide cracks on I-59 in Jones County.

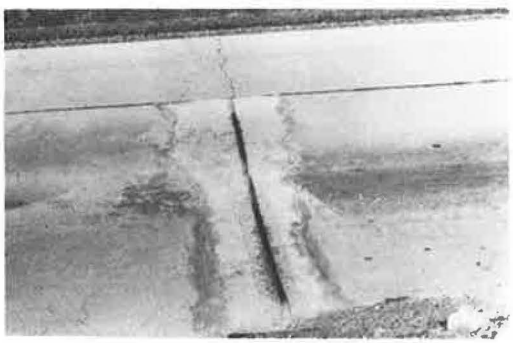

Figure 30. Expansion joint installed on I-59 in Jones County.

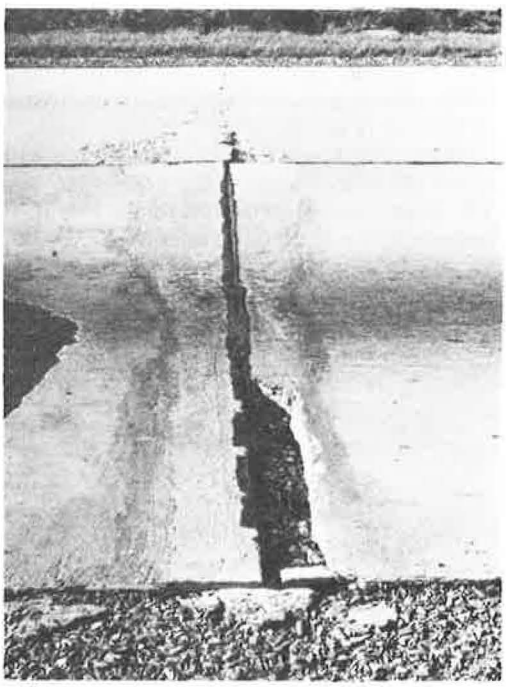

Figure 31. Eight months after repair on I-59 in Jones County.

Figure 32. Patch ready for replacing concrete on I-55 in Madison County.

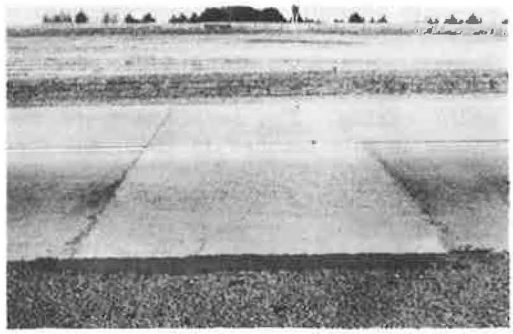

Figure 33. Patch poured in afternoon 8 months after repair on I-55 in Madison County.

bars at the construction joint were removed, except at one joint, where they were left in as a further experiment. To date, no difference in the performance of these repairs has been observed. The reinforcing mesh was brushed clean and placed back, and ½-in. reinforcing bars, 30 in. long, were placed across the mesh and tied to the mats (Fig. 32). Ready-mixed concrete, containing 6.5 sacks of cement per cubic yard, was ordered from a local batch plant for all patch jobs. A vibrator was used to ensure good placement, and the usual finishing practices were followed. Six repair operations were made in this manner in April 1967. Five poured in the afternoon still look good (Fig. 33), but the one poured in the morning failed completely (Fig. 34).

Failures that occurred in north Mississippi at the beginning of a new section on the first lapped splices (constructed 5 months later than the connected section) were repaired with bar mat reinforcement as follows.

Two saw cuts, 4 ft and 23 ft 3 in. extending eastward from the construction joint, were made across the pavement to include the entire failure spot. Between these 2 saw cuts, the pavement was cut into large pieces with sizes varying from 3 by 5 by 10 ft. Each piece was lifted up by hydraulic crane for inspection to explore the cause of failure (Fig. 35).

After the large pieces of concrete were lifted out, a jackhammer was used to remove the remainder of the concrete, and the area was brushed clean. At the saw cut 4 ft from the construction joint, it was found that the bond was loose and might cause failure in the future. Therefore, the decision was made to remove the remainder of

Figure 34. Patch poured in morning 8 months after repair on I-55 in Madison County.

Figure 35. Investigation during repair on US-82 in Leflore County.

TABLE 5

TEMPERATURE AND MEASUREMENTS OF PATCH OPENING BETWEEN TWO ENDS ON US-82 IN LEFLORE COUNTY

Time	Temperature (deg F)	Opening Between Two Ends	
		Feet	Inches
8:30 a.m.	72	23	3
1:20 p.m.	85	23	2 1/8
2:20 p.m.	87	23	2 1/8
3:20 p.m.	90	23	2
4:20 p.m.	90	23	1 15/16
4:55 p.m.	90	23	1 15/16

Figure 36. Complete patch 3 months after repair on US-82 in Leflore County.

the pavement all the way to the construction joint. On the next morning, the entire area was again brushed clean, and No. 5 deformed bars were placed as longitudinal reinforcement with sufficient length to provide a 20 in. overlap at both ends. The steel was welded at the 2 ends of the lap for a length of 3 ft. No. 4 transverse bars were placed on chairs and tied to the longitudinal bars in accordance with the pattern of the original bar mats. At 1 p.m. it was found that the steel buckled about 1 in. from its normal position. The steel was then relieved at the east end. The length between the 2 ends were measured at different times during the day (May 30, 1968); results of these measurements and the corresponding temperatures are given in Table 5. The steel was welded back about 5 p.m. because the measurements indicated no change at 4:20 p.m. and 4:55 p.m. The fact that the steel buckled during the hottest part of the day seems to be one of the explanations for the failure that occurred at the previously mentioned repair job poured in the morning. The fresh concrete apparently was not strong enough to overcome the tremendous buckling force caused by the expansion of the 2 ends.

Before pouring the concrete, the 2 ends were coated with epoxy glue. At 6 p.m. class AA ready-mixed concrete was ordered from a local batch plant for the repair. Vibrators were used to ensure good placement. The fresh concrete was covered by wet burlap while curing, and the existing pavement, from both ends, was kept wet to a distance of 100 ft during the curing period. The compressive strength of the fresh concrete was 5,359 psi at the end of the third day. The section was repaired on May 29-30, 1968, and opened to traffic on June 3, 1968. To date, it is still in excellent condition (Fig. 36).

ACKNOWLEDGMENTS

Material presented here is taken from a research project being conducted by the Mississippi State Highway Department, in cooperation with the U.S. Department of Transportation, Federal Highway Administration, Bureau of Public Roads. The opinions, findings, and conclusions expressed in this paper are those of the author and not necessarily those of the Mississippi State Highway Department or the Bureau of Public Roads.

The author wishes to express his tanks to H. V. Mahan of the Mississippi State Highway Department for valuable advice and guidance gained from his many years of experience in highway construction, and to J. O. Coley for his excellent field work and many valuable suggestions. Thanks are also due to B. F. Wallace, who read the earlier draft and made many constructive comments.

REFERENCES

1. Second Progress Report—Continuously Reinforced Concrete Pavements. American Concrete Institute Committee 325, 1962.

2. Burke, J. E., and Dhamrait, J. S. A Twenty-Year Report on the Illinois Continuously Reinforced Pavement. Highway Research Record 239, 1968, pp. 197-211.
3. Design and Construction of Continuously Reinforced Concrete Pavement. Continuously Reinforced Pavement Group, 1968.
4. Lee, A. Maryland's Two Continuously-Reinforced Concrete Pavements—A Progress Report. Highway Research Record 5, 1963, pp. 99-119.
5. Lindsay, J. D. A Ten-Year Report on the Illinois Continuously Reinforced Pavement. HRB Bull. 214, 1959, pp. 22-40.
6. Manifold, G. D. Final Report on a Study of an Experimental Continuously Reinforced Concrete Pavement, Interstate 59, Jones County, Mississippi. Eng. Exp. Station, Univ. of Mississippi, 1966.
7. Interim Base Design. Mississippi State Highway Department, 1962.
8. Shaffer, R. K., and Jensen, C. D. Continuously-Reinforced Concrete Pavements in Pennsylvania—A Six-Year Progress Report. Highway Research Record 5, 1963, pp. 83-98.
9. Spigolon, S. J. Final Report on a Study of an Experimental Continuously Reinforced Concrete Pavement, Interstate 55, Desoto County, Mississippi. Eng. Exp. Station, Univ. of Mississippi, 1962.
10. Spigolon, S. J. Behavior of Experimental Continuously-Reinforced Concrete Pavements in Mississippi. Highway Research Record 60, 1964, pp. 140-153.

Minnesota Department of Highways Flexible Pavement Design—1969

F. C. FREDRICKSON, P. J. DIETHELM, and D. M. ZWIERS, Minnesota Department of Highways

A new flexible pavement design was developed from the Minnesota Department of Highways AASHO Satellite Test Program on 50 selected roadways. The design emanated from the study of the effects of pavement section characteristics, subgrade soil strength, climate, and loading and distribution of traffic on the performance of flexible pavements. The pavement section characteristics studied include thickness, composition, strength, and quality. The stabilometer R-value is used to evaluate the subgrade soil strengths. Climatic effects were determined by measuring seasonal changes in strength of selected roadway structures throughout the state by means of the Benkelman beam. The loading and distribution of traffic is determined in terms of summation of equivalent 18-kip single-axle loads. The PSI system developed at the AASHO Road Test is used in a modified form to evaluate performance. The modification involves use of BPR-type of roughometer data in place of the slope variance component of the equation. A design chart is developed that shows the required gravel equivalent thickness dependent on embankment R-value and equivalent 18-kip single-axle loads.

•THE METHOD presently used for flexible pavement design in Minnesota uses either average daily traffic (ADT) or heavy commercial average daily traffic (HCADT), along with a designation of 5-, 7-, or 9-ton spring axle loads to categorize traffic. The AASHO soil system is used to classify the subgrade soil in order to vary the required base thickness from sections designated for an A-6 soil. The relative strengths of the layers in the pavement section are indicated by granular equivalent factors. The procedures and levels of thickness required have been established based on experience and performance evaluation on Minnesota highway pavements for the past 30 years. Past experience resulted in establishment of standard cross sections showing thickness of various materials for varying traffic volumes and load restrictions. Tables 1 and 2 give a portion of these design standards and the method of application for various subgrade soils. Table 3 gives the gradation requirements of the materials given in Tables 1 and 2. Varying amounts of crushed particles are required depending on the class of material selected.

For the past 5 years the Minnesota Department of Highways has been conducting a research project (Investigation 183) that has the purpose of studying the performance of Minnesota flexible pavements and applying the results of the study to the design of flexible pavements. The results and methods developed at the AASHO Road Test have been used to define performance and to study and evaluate 50 Minnesota test sections.

The background material and analyses are found elsewhere in a study by Kersten and Skok (1). A committee of Minnesota Department of Highways personnel and of Kersten and Skok (1) was formed in August 1968 to consider the present Minnesota flexible pavement design in light of the results and conclusions in the report.

The procedure recommended by the committee is presented in this summary of the Investigation 183 report. The procedure is dependent on the correlation between

Paper sponsored by Committee on Flexible Pavement Design and presented at the 49th Annual Meeting.

TABLE 1

FLEXIBLE PAVEMENT DESIGN

Axle Load (ton)	Heavy Commercial Average Daily Traffic (HCADT)	Average Daily Traffic (ADT)	Wearing		Binder		Bituminous Base		Bituminous-Treated Base		Aggregate Base				Total Thickness of Granular Equivalent	
			Specification	Thickness (in.)	Specification	Thickness (in.)	Specification	Thickness (in.)	Specification	Thickness (in.)	Class	Thickness (in.)	Class	Thickness (in.)	Base (in.)	Pavement (in.)
5		<400	2321	1½							5	3	3	5	7	9
7		<400	2331	1½							5	4	3	6	8½	11½
7		400-1,000	2331	1½			2331	1½			5	3	3	8	12	15
9	<150	<1,000	2331	1½			2331	1½			5	5	3	9	14½	17½
9	150-300	1,000-2,000	2341	1½	2341	1½	2331	1½			6	5	3	8	14	21
9	300-600	2,000-5,000	2341	1½	2341	1½	2331	1½	2204	4 rich or	6	6	4	6		
													3	6	18	25
9	600-1,100	5,000-10,000	2351	1½	2341	2	2331	3½	2204	4 lean or	6	5	4	6		
													3	6	21	29
9	>1,100	>10,000	2351	1½	2341	2	2331	4½	2204	4 lean			4	6	24½	32½
													3	8		

Note: These design thicknesses apply only for A-6 subgrade soils. Use the following methods to adjust the design thickness for other classes of subgrade soils:

1. Bituminous base, bituminous-treated base, and aggregate base thicknesses are converted to an equivalent thickness of aggregate base (denoted as granular equivalent, GE) by using the granular equivalent factors listed as follows. The sum of these quantities for each design is listed under the column headed "Total Thickness of Granular Equivalent, Base (in.)".
2. Select the appropriate soil factor corresponding to the AASHO soil classification of the subgrade soils. The soil factor is applied to the "Total Thickness of Granular Equivalent, Base (in.)" in adjusting to the granular equivalent base thickness required for subgrade soils other than A-6 soils. Apply this adjustment to the thickness of the base (Classes 3 and 4) only.
3. This adjustment is made algebraically by using the following formula:

$$\text{Adjusted base thickness (Classes 3 and 4)} = \text{base thickness (Classes 3 and 4)} + \frac{(\text{Total Base GE} \times 100 - \text{Total Base GE})}{0.75}$$

TABLE 2

GRANULAR EQUIVALENT AND SOIL FACTORS

Material	Specification	Granular Equivalent Factor	AASHO Soil Class	Soil Factor (percent)
Plant-mix surface	2341, 2351	2.25	A-1	50-75
	2331	2.00	A-2	50-75
Plant-mix base	2331, 2341, 2351	2.00	A-3	50
Road-mix surface	2321	1.50	A-4	100-130
Road-mix base	2321	1.50	A-5	130+
Bituminous-treated base				
Rich	2204	1.50	A-6	100
Lean	2204	1.25	A-7-5	120
Aggregate base				
Classes 5 and 6	3138	1.00	A-7-6	130
Classes 3 and 4	3138	0.75		
Selected granular material (<12 percent passing No. 200 sieve)		0.50		

pavement spring deflections and the number of equivalent 18-kip single-axle loads ($\Sigma N18$) that the pavement can withstand before the present serviceability index (PSI) of the section will drop to a PSI of 2.50. Because the pavement section is still relatively intact at a PSI of 2.50, this level is appropriate for considering required maintenance. The performance equation suggested is from the AASHO Road Test and is shown by Kersten and Skok (1) to be appropriate for Minnesota conditions. The other factors for establishing the design procedure use the thicknesses of the surface and base layers along with the Hveem stabilometer R-value of the embankment soil to calculate the spring deflection of the pavement section. The equations used are obtained from the spring recovery study of Investigation 183 on a number of the Minnesota test sections. The relationships developed are those for Minnesota Department of Highways Standard Specification 2331, 2341, or 2351 bituminous mixtures and Class 3, 4, 5, or 6 base materials. It is also assumed that adequate drainage has been designed for the section and the layers will be placed under present Minnesota Department of Highways density specification.

DESIGN PROCEDURE

As mentioned previously, the design procedure involves the R-values of the soil, $\Sigma N18$, granular equivalent factors of each layer, and Benkelman beam deflections. Each of these factors will be discussed briefly as they relate to the design procedure.

Hveem Stabilometer R-Value

The design procedure presented in this report is for flexible pavements that are being built starting with the embankment soil. The method consists of sampling the

TABLE 3

MATERIAL GRADATION REQUIREMENTS

Sieve Size	Total Percent Passing						
	Class 3	Class 4	Class 5	Class 6	2331	2341	2351
2 in.	100	100					
1 in.			100	100			
¾ in.			90-100	90-100	100	100	100
⅜ in.			50-90	50-85	65-95	65-90	70-80
No. 4	35-100	35-100	35-80	35-70		50-70	50-65
No. 10	20-100	20-100	20-65	20-55	35-65	35-55	35-55
No. 40	5-50	5-35	10-35	10-30	10-35	10-30	15-30
No. 200	5-10	4-10	3-10	3-7	1-7	1-7	4-8
Maximum 200/40 ratio	50	40	40	40			

proposed construction area to determine the predominant soil type and establishing the AASHO classification and strength of representative soil samples in the laboratory. The strength is determined by using the stabilometer R-value as a criterion. The procedure to be used for determining the R-value is contained in Wolfe's work (3).

The use of R-value as a criterion for analysis of soil strength was recommended after consideration of the several practical methods of soil tests and classification systems. The best correlation was established between field E-modulus and R-value in Investigation 183. This relates field conditions to the laboratory test results. The results of this study indicate the best correlation was obtained by using the R-value determined at an exudation pressure of either 200 or 240 psi.

The stabilometer R-value test is not considered to be the ultimate test for evaluating the strength of an embankment soil, but it is the most practical test available at this time.

Equivalent 18-kip Axle Loads ($\Sigma N18$)

The loading on a highway pavement is composed of applications of a distribution of axle loads of various weights. At the AASHO Road Test, sections of highway were subjected to repetitions of the same load and the performance of the pavement structure was evaluated. Using this performance information, the relative effect of various loadings on a pavement structure can be calculated. The relative effect of various loadings can then be used to convert each load repetition to an equivalent number of repetitions of a base load. Using an equivalent axle load of 18-kips, the equivalent load effect may be considered by summing up all equivalent loads applied over a design period. A program has been set up for the Minnesota Department of Highways computer that makes it possible to predict $\Sigma N18$ for design purposes and also the $\Sigma N18$ that have been on a section since it was built. Traffic can be predicted for any number of years into the future, so staged construction may be utilized if desired.

Granular Equivalent Factors

The pavement sections obtained for a new design procedure have minimum thicknesses of surface and base materials. These thicknesses are essentially the same as those in the design method currently in use by the Minnesota Department of Highways. The present Minnesota design procedure uses the granular equivalent concept to define the pavement structure. The granular equivalent is defined by Eq. 1:

$$GE = a_1D_1 + a_2D_2 + a_3D_3 + \ldots \quad (1)$$

where

GE = granular equivalent thickness, in.;
$a_1, a_2, a_3, \ldots$ = constants defining the relative effect of the given layer; and
$D_1, D_2, D_3, \ldots$ = thickness of individual layers, in.

For the granular equivalent in Minnesota the constant "a" for a Class 5 or 6 base material is taken as 1.00 and the other constants rate the strength of the various other materials relative to the granular bases. The constants thus define the equivalency between layers. Table 2 gives a list of these factors presently used for the Minnesota flexible pavement design procedure. These factors have been set up primarily from experience in Minnesota and other locations.

It has been with the elastic theory that pavement deflections can be predicted if the elastic properties of the materials are determined under the same conditions of test as in the field (3, 4, 5). An equation of the form shown in Eq. 2 can be fitted to the elastic theory prediction of deflection.

$$\log d = a_0 - a_1D_1 - a_2D_2 - a_3 \log E \quad (2)$$

where

d = deflection, 0.001 in.;
D_1 = surface thickness, in.;
D_2 = granular base thickness, in.;
E = elastic modulus of embankment soil, psi; and
a_0, a_1, a_2, a_3 = constants determined from multiple regression analysis.

The spring deflections measured on the spring recovery test sections (Investigation 183) have been correlated with the thickness of the pavement layers and the strength of the embankments by using the model of Eq. 2. For each test section, the spring Benkelman beam deflection for 1965, 1966, and 1967 surface, base, and subbase thickness and log R (rather than log E, which is related to log R) were put into the computer. By means of a mathematical operation, known as multiple regression analysis, values of a_0, a_1, a_2, and a_3 were determined such that the equation best fits the data points. Equation 2 is rewritten and Eqs. 3, 4, and 5 result from using the data obtained during 1965, 1966, and 1967 respectively.

$$\log d_{SR} = 3.125 - 0.070 D_1 - 0.027 D_2 - 0.024 D_3 - 0.601 \log R \quad (3)$$
when $r^2 = 0.95$, and standard error = 15 percent;

$$\log d_{SR} = 2.781 - 0.056 D_1 - 0.016 D_2 - 0.019 D_3 - 0.507 \log R \quad (4)$$
when $r^2 = 0.85$, and standard error = 15 percent; and

$$\log d_{SR} = 2.733 - 0.056 D_1 - 0.019 D_2 - 0.025 D_3 - 0.416 \log R \quad (5)$$
when $r^2 = 0.80$, and standard error = 17 percent.

In Eqs. 3, 4, and 5, $\log d_{SR}$ = spring Benkelman beam deflection, 0.001 in. using a 9-ton axle load, and r^2 = correlation accuracy, 1.00 equaling perfect fit. The other terms are as described in Eq. 2.

As previously defined, the equivalency for granular base is assigned a value of 1.00. The granular equivalency for bituminous surfacing is then determined by dividing the surfacing constant, a, by the granular base constant, a_2. For the lower base equivalency, a_3 is divided by a_2. Table 4 gives a listing of layer equivalencies implied by Eqs. 3, 4, and 5.

Generally, the equivalencies found from deflections measured or estimated during the spring in Minnesota for sections on plastic embankment soils are somewhat lower than those calculated from the Road Test data. This reflects the wider range of materials in the Minnesota sections as opposed to the constant materials at the Road Test.

The granular equivalencies given in Table 4 appear to be liberal in comparison with those presently used and given in Table 2. These limited data, however, will not be used to change the present granular equivalencies until further evaluation of the equivalencies has been made.

TABLE 4

EQUIVALENCIES BETWEEN SURFACE AND BASE MATERIALS USING EQUATIONS DEVELOPED FROM MINNESOTA SPRING RECOVERY TEST SECTIONS

Year	Equivalency Factors		
	Surface	Base (Classes 5 and 6)	Base (Classes 3 and 4)
1965	2.59	1.00	0.89
1966	3.50	1.00	1.20
1967	2.95	1.00	1.32

Performance Prediction

At the AASHO Road Test, Benkelman beam deflection tests were run on each of the test sections periodically. The deflections were run to determine the variation in strength of the sections and to see if the strength of the pavement measured in the field could be used to predict the performance of the sections.

Four equations were developed relating deflection to performance. The equation best suited to Minnesota conditions is shown as Eq. 6, which uses a PSI of 2.5.

$$\log (\Sigma N18)_{2.5} = 11.06 - 3.25 \log d_S \quad (6)$$
$$\text{when } r^2 = 0.78, \text{ and standard error} = 0.21,$$

where

$(\Sigma N18)_{2.5}$ = summation of equivalent 18-kip axle loads to a PSI level of 2.5;
d_S = Benkelman beam deflection taken during the spring period, 0.001 in.; and
r^2 = squared correlation coefficient.

Figure 1 shows a plot of Eq. 6, which is a straight line on a semi-log plot. Also plotted in Figure 1 is a line indicating the standard error of Eq. 6. This line is one standard error below the "best-fit" line and indicates the level above which 5/6 of the data points occur when they reach a PSI of 2.5.

In order to see how well Eq. 6 relates to Minnesota conditions, spring deflections measured on the spring recovery test sections are plotted against ΣN18 of the test section through 1966. The spring deflections have generally been consistent for the 4 spring periods in which testing has been performed. As more data are obtained, it will be possible to see if the deflections tend to increase or decrease with age and condition of the pavement.

The deflections on roads that have been restricted during the critical spring period have been reduced accordingly. For instance, if a road has been restricted to 7-ton axle loads during the spring, the measured 9-ton deflection is reduced by 7/9 to obtain the deflection for 7-ton axle load. The linear relationship between deflection and load for normal loads used on highway sections is justified by Kersten and Skok (1) and Huculak (6). Using the data adjusted in this manner, it has been recommended that the "best-fit" line from the Road Test represented by Eq. 6 be used for design purposes.

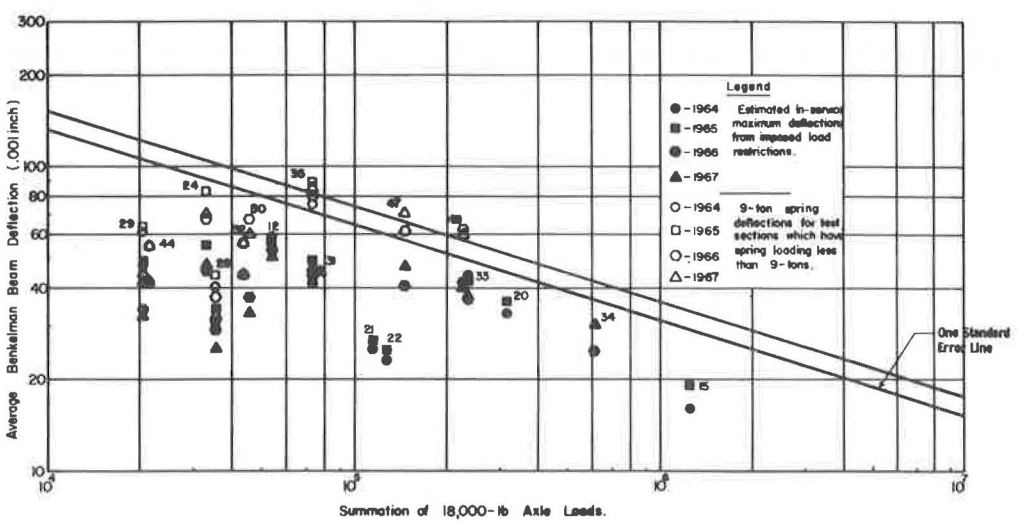

Figure 1. Variation of measured spring deflections with total equivalent 18-kip axle loads through 1966.

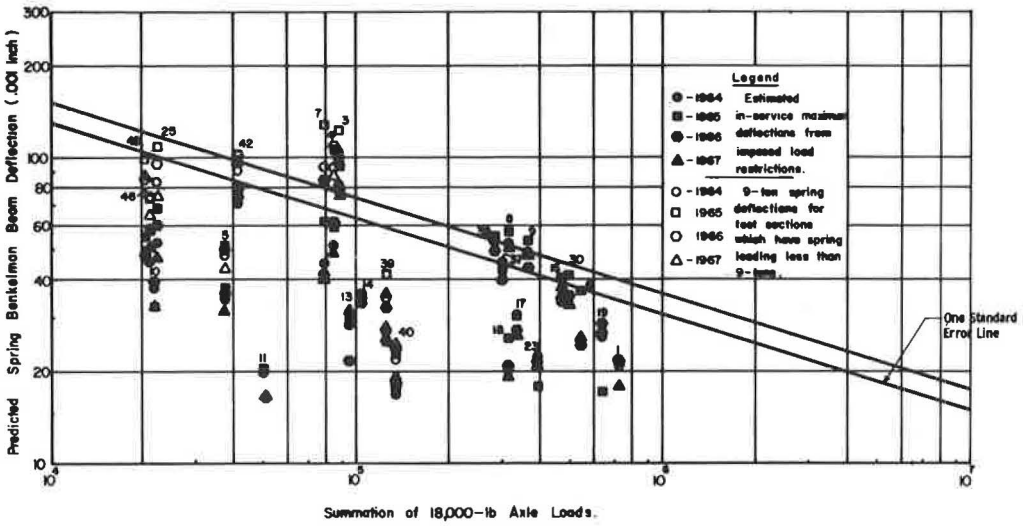

Figure 2. Variation of predicted spring deflections with total equivalent 18-kip axle loads through 1966.

By using the relationships developed from the spring recovery program, spring deflections have been estimated for the test sections on which deflections have not been run during the spring period. These estimated spring deflections for each year are plotted against $\Sigma N18$ through 1966 and are shown in Figure 2. The deflections on sections that have axle load restrictions during the spring period have been appropriately reduced as indicated previously.

The position of the points in Figures 1 and 2 suggests that the line representing Eq. 6 could be used to predict the $\Sigma N18$ that a pavement can withstand under a given level of spring deflection. If the serviceability of the test sections is determined periodically in future years, it will be possible to see whether another line would be more appropriate than the line represented by Eq. 6. If all of the sections are observed to PSI of 2.5, it will be possible to establish more precisely a trend line for Minnesota conditions.

The advantage of using a strength test such as Benkelman beam deflection to predict performance is that all localized conditions such as drainage and poor quality base material are evaluated. Using only thickness as an evaluation does not make this possible.

New Design Development

The present granular equivalent factors (Table 2) are justified further by Kersten and Skok (1) and are used in the new design procedure. In order to develop the design procedure based on granular equivalent thicknesses, it was necessary to correlate deflections to thickness and R-value by using an equation of the form of Eq. 7 (similar to form of Eq. 2):

$$\log d_S = a_0 - a_1 (GE) - a_2 \log R \qquad (7)$$

where

d_S = spring deflection, 0.001 in.;
GE = granular equivalent thickness using the coefficients in Table 2; and
R = stabilometer R-value.

Equation 8 resulted from the correlation using the maximum deflections measured on the spring recovery test sections during the spring of 1967.

$$\log d_S = 2.587 - 0.0230\,(GE) - 0.306 \log R \qquad (8)$$
when $r^2 = 0.73$ and standard error = 17 percent.

Equation 9 resulted from the correlation using spring deflections calculated from deflections run on all the test sections throughout the summer of 1967.

$$\log d_S = 2.799 - 0.0219\,(GE) - 0.521 \log R \qquad (9)$$
when $r^2 = 0.80$ and standard error = 28 percent.

The squared correlation coefficient for Eq. 9 is somewhat higher than that for Eq. 8. This is because there is a wider range of granular equivalents and R-value represented for Eq. 9. However, the error in predicting deflection is about 11 percent higher using all of the sections.

Equation 5 is the result of the correlation using the same deflection data but allowing the coefficients on thickness to be determined from the correlation. The standard error is about the same, but the squared correlation coefficient is somewhat higher. This indicates that using the various granular equivalent coefficients does not appreciably affect the error in predicting spring deflection.

It is felt that Eq. 9 should be used to predict deflections from granular equivalent and R-value of the embankment soil because it has been derived from a wider range of independent variables. Each year as more data are accumulated relating these variables, the relationship represented by Eq. 9 can be improved.

For relatively high traffic roads (more than 90,000 ΣN18 for design life), the design recommended is obtained by using Eqs. 6 and 9. When these equations are combined and the spring deflection relationship (Eq. 9) is substituted in Eq. 6, Eq. 10 results.

$$\log (\Sigma N18)_{2.5} = 11.06 - 3.25\,[2.799 - 0.0219\,(GE) - 0.521 \log R]$$

Rearranging and solving for GE results in

$$GE = 1.40 \log (\Sigma N18)_{2.5} - 2.38 \log (R) - 2.75 \qquad (10)$$

Even though there is some error involved with estimating deflection from granular equivalent and R-value in Eq. 9, it is felt that Eq. 10 is appropriate for design because (a) the deflection used for determining strength is the average value plus 2 standard deviations and thus represents close to the weakest condition of the pavement section, and (b) the deflection-performance equation is a line that includes all of the sections considered through 1967. All of these sections to the left of this line are performing well except for TS 50 as indicated in Figures 1 and 2. A number of sections have exceeded the performance predicted by this relationship, which is the "best-fit" line through the AASHO Road Test deflection-performance data. Part of the continuing evaluation of Minnesota flexible pavements will be the verification of these equations.

For low-traffic roads, Eq. 10 is assumed to be appropriate until the spring design deflection goes up to 0.075 in. Huculak (7) states that a light traffic road can withstand repeated applications of deflections up to this magnitude. To establish minimum designs for 9-ton loads the respective R-values along with the 0.075-in. deflection are substituted into Eq. 10 to predict a granular equivalent necessary to limit the deflection. To establish minimum designs for a road to be limited to a 7-ton maximum spring axle load, an allowable 9-ton deflection is $\frac{9}{7}$ (0.075) in. = 0.096 in. This deflection with the respective R-values yields the minimum granular equivalent thicknesses using Eq. 10. Justification for using a linear ratio of the loads to predict deflections under other loads can be found in Huculak's work (7) and Chapter 12 of Investigation 183. According to this criterion, a section designed by this procedure could withstand 9-ton axle loads during the critical spring period if the R-value is 30 or greater.

Figure 3 shows a semi-log plot of the required granular equivalent thicknesses dependent on embankment R-value and ΣN18. The thicknesses shown are a combination

of present Minnesota Department of Highways design plus a plot of Eqs. 6 and 9. The thicknesses of the upper layers can also be obtained from data given in Table 5. Thicknesses of Class 3 and 4 materials will vary depending on the R-value obtained.

DESIGN METHOD

The following method is recommended to design an appropriate flexible pavement:

1. Determine R-value of embankment soil to be used for design by running appropriate laboratory tests.
2. Determine ΣN18 by having a traffic analysis made. ΣN18 will be the total number of equivalent 18-kip axle loads to be sustained by one design lane of the pavement during the design life.
3. Enter Figure 3 with the values of R and ΣN18 (from steps 1 and 2 preceding) and read off granular equivalent (GE) from the left side.
4. Divide total GE (from step 3) into GE thicknesses of the various materials shown in Figure 3.
5. Convert GE thickness (from step 4) to actual thickness of material by using GE factors given in Table 2 (actual thicknesses are also given in Table 5).

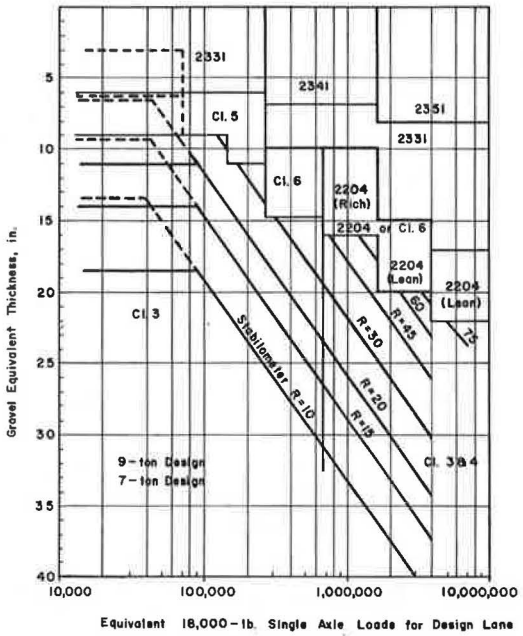

Figure 3. Required granular equivalent thickness dependent on embankment R-value and ΣN18.

6. If desired, substitution of material with higher equivalencies as given in Table 2 can be made so that the total GE adds up to the total obtained as shown in Figure 3.

TABLE 5

SURFACE AND BASE THICKNESS AND GRANULAR EQUIVALENT THICKNESS PRESENTED BY SURFACE PLUS BASE (CLASSES 5 AND 6) FOR VARIOUS TRAFFIC LEVELS

Equivalent Load Category (ΣN18)	Surface		Bituminous Base		Bituminous-Treated Base		Aggregate Base		Total Thickness of Granular Equivalent (in.)
	Thickness (in.)	Specification	Thickness (in.)	Specification	Thickness (in.)	Specification	Thickness (in.)	Class	
<60,000[a]	1½	2331	—	—			3	5	6
60,000-90,000[a]	1½	2331	1½	2331			3	5	9
<90,000	1½	2331	1½	2331			3	5	9
90,000-150,000	1½	2331	1½	2331			3	5	9
150,000-250,000	1½	2331	1½	2331			5	5	11
250,000-650,000	3	2341	1½				5	6	14¾
650,000-1,700,000	3	2341	1½	2331	4 rich	2204 or	6	6	15¾
1,700,000-3,800,000	3½	2351	3½	2331	4 lean	2204 or	5	6	20
>3,800,000	3½	2351	4½	2331	4 lean	2204			22

Note: Total thickness not shown because base thickness depends on subgrade strength. The total thickness of granular equivalent required including base (Classes 3 and 4) is shown in Figure 3.

[a]7-ton design, remainder of designs are for 9 ton.

Examples of each preceding step follows:

1. Assume that a stabilometer test was run in the laboratory and resulted in R = 20.
2. Assume that a traffic analysis was made and that ΣN_{18} = 1,000,000.
3. By using the above values, a GE of 26 in. is obtained from Figure 3.
4. From Figure 3, the total GE can be divided into the following:

   2341 = 6.75-in. GE,
   2331 = 3.25-in. GE,
   Class 6 or 2204 (rich) = 6.00-in. GE, and
   Classes 3 and 4 = 10.00-in. GE.

5. By using conversion factors given in Table 2, the following values are obtained:

   2341 = 6.75/2.25 = 3 in.,
   2331 = 3.25/2.00 = 1½ + in.,
   Class 6 = 6.00/1.00 = 6 in., and
   Classes 3 and 4 = 10.00/0.75 = 13 + in.

6. Ten inches of Class 6 could be substituted for 13 in. of Classes 3 and 4 (GE is the same). Additional Classes 3 and 4 could not be substituted for the initially required 6 in. of Class 6 because Classes 3 and 4 had a lower equivalency factor.

In addition to using the design procedure for new construction, it can be applied to bituminous overlay of existing pavements. A procedure has been formulated, but will require further field study to verify the results. It is anticipated this information will be available in the near future.

REFERENCES

1. Kersten, M. S., and Skok, E. L., Jr. Application of AASHO Road Test Results to Design of Flexible Pavements in Minnesota. Highway Research Record 291, 1969, pp. 70-88.
2. Wolfe, R. E. Resistance R-Value of Embankment Soils and Aggregates for Use as Bases and Subbase. Minnesota Department of Highways, Investigation 176, 1960.
3. Kingham, R. I., and Reseigh, T. C. A Field Experiment of Asphalt-Treated Bases in Colorado. The Asphalt Institute, Res. Rept. 67-2, Jan. 1967.
4. Skok, E. L., Jr., and Finn, F. N. Theoretical Strength Considerations Applied to Asphalt Pavement Design. Proc., Internat. Conf. on Structural Design of Asphalt Pavements, Univ. of Michigan, 1962.
5. Coffman, B. S., Kraft, D. C., and Tamayo, J. A Comparison of Calculated and Measured Deflections for the AASHO Test Road. Proc. AAPT, Vol. 33, Ann Arbor, Mich., 1964.
6. Huculak, N. A. Evaluation of Pavements to Determine Maintenance Requirements. Highway Research Record 129, 1966, pp. 12-27.

Isotropy and an Asphaltic Concrete

BONNER S. COFFMAN*, GEORGE ILVES, and WILLIAM F. EDWARDS,
Department of Civil Engineering, Ohio State University

Asphaltic concrete core specimens were secured from a contract-constructed pavement in 3 orthogonal directions. These core specimens were tested in unconfined compression to determine the complex moduli at different temperatures and frequencies. Comparisons of the directional moduli indicated that the material was isotropic in compression to a first approximation at the phenomenological level. Block samples of the asphaltic concrete were taken and sawed to produce trapezoidal specimens for testing in bending to determine complex moduli. The results of these tests indicated that the linear range in bending was substantially restricted in comparison to axial compressive tests. The results of tests outside the linear range are presented. Comparisons indicated that linear complex moduli in bending and compression were the same and it was concluded that this asphaltic concrete was isotropic to a first approximation at the phenomenological level.

•CAN ASPHALTIC CONCRETE be isotropic and have the same properties in all directions? At the molecular, micro, and low macrovolume levels the answer is clearly no because the material is a mixture of different components. For structural pavement design, however, primary interest is in the phenomenological response of relatively large volumes. The work reported here is restricted to such volumes in which test specimens and measurements represent average material, and the property investigated is its response to surface forces as expressed in the complex modulus, $|E^*|$.

Previous work here indicates that asphaltic concrete is isotropic, in an engineering sense, and exhibits the same properties in tension and compression. That work was based on the concept of the complex modulus for asphaltic concrete developed by Papazian (1) with Baker (2). This concept was experimentally extended to all pavement layers, and lab-measured moduli of these were used with linear elastic theory to predict maximum deflections for in-service pavements under various truck loadings, speeds, and times of year (3, 4). Such comparisons are necessary and are directly responsive to an ultimate answer; however, they may not be sufficient. Full-scale experiments involve many and changing variables with corresponding opportunities for compensating interactions. At the same time, this evidence of isotropy and equal tensile-compressive moduli appears to be contradicted in the literature (5). Because of these anomalous indications, it was considered necessary to investigate this basic problem.

As will be noted in the differing temperatures and frequencies used in the various test series, this study was not planned for statistical analysis. The temperature differences, for example, are partly the result of the time requirements in reaching system equilibrium with ambient temperature before testing. Mostly these test differences reflect the authors' experience in using graphical techniques to normalize large quantities of 3-dimensional test data where strict statistically based comparisons are a study in their own right.

*Deceased, August 4, 1970.

Paper sponsored by Committee on Flexible Pavement Design.

COMPRESSION

Directional Effects

Specimens for this investigation were obtained by sawing or coring a never-loaded full-scale asphaltic concrete pavement section located on university farmland. This 30-ft wide and 120-ft long pavement was built in 2 lanes in 1.5-in. nominal lifts. It was constructed under contract for a full-scale investigation of fatigue involving one asphaltic concrete mix at 5 thicknesses. The design gradation is given in Table 1; construction results with the mix are as follows.

Laboratory compaction	Gyratory
Asphalt, percent	6.3
Chevron AC, penetration	60-70
Density, pcf	147
Stability, lb	3,275
Flow, in.	0.15
Filled aggregate voids, percent	83
Mix air voids, percent	3
Paver	Barber-Green
Rollers	10-ton steel tandem and rubber tired
Control	Cores and nuclear
Average pavement density, pcf (243 cores ranging from 136 to 145 pcf)	141
Average pavement AC content, percent (8 chunks ranging from 6.2 to 6.8 percent)	6.6

A plot of aggregate percentage passing versus sieve opening raised to the 0.45 power is closely linear.

The sides of cores and faces of sawed slabs showed that elongated aggregate particles tended to be oriented parallel to the plane of rolling. This is typical of local, if not all, asphaltic concrete pavements. To determine directional effects, cores were taken from the pavement in 3 orthogonal directions: vertical, horizontal in the north-south direction, and horizontal in the east-west direction (in construction, paver and roller travel was north-south, and maximum differences were expected with respect to this axis). The cored area was held to a minimum (some 6 ft square in one lane) to reduce the probability that different plant-mix batches were included in any one lift. Thirty-eight cores were taken, and 3 sets of 9 cores each were selected to represent the 3 directions.

The pavement was constructed in 5 lifts. In each core the third lift was central; i.e., in reference to core length and lab load direction, the third lift was centered transversely in vertical and parallel in horizontal cores (Fig. 1). Lifts were difficult to distinguish and some layer-centering deviations undoubtedly occurred. Core ends were sawed and strain gages mounted on the central lift (about 1.5 in. thick) with the 0.75-in. active gage length parallel to specimen and lab test-load axis. For vertical cores, 2 sets of 2 strain gages each were mounted on every core; one set facing the north-south and one facing the east-west directions, in place. For horizontal cores only one set of gages could be mounted on the third or central lift, and this set was expected to reduce the variables. The cylindrical test specimens were 3.70 in. in diameter and 7.20 in. long (each ±0.005 in.), with a height-diameter ratio of 1.95:1.

Compressive complex moduli were measured for these cores with load in the form of a haversine wave at frequencies from 3 to 200 rad/sec (radians per second) and

TABLE 1

DESIGN GRADATION

Sieve	Percent Passing	Sieve	Percent Passing
3/8 in.	100	No. 16	42
1/4 in.	81	No. 30	26
No. 4	68	No. 50	15
No. 6	64	No. 100	9
No. 8	58	No. 200	6

temperatures from 20 to 116 F. Measurements represent the steady-state condition, and the complex Poisson's ratio was not measured. Specimen loading was in unconfined compression. Loading was with MTS; amplification and recording was with CEC equipment. Specimens were encased in membranes, and temperature was controlled by circulating fluid from a water bath; however, moduli determined without membranes showed no fluid effect. Complete details of test and interpretation are given in Filon's work (7). Solution of the theoretical boundary problem of the test array is indicated by Filon for linear elasticity (7). No theoretical corrections were applied to the test data. The results of the tests are given in Table 9 in the Appendix in the form of average, standard deviation, and coefficient of variation for 9 replicate specimens; and averages are typically shown in Figure 1. All tests were within the linear range. Supporting data are omitted for brevity. Average test data were plotted as $|E^*|$ versus log ω on large family-of-curves graphs to normalize temperature differences and to interpolate for missing frequencies (the test data are not strictly amenable to analysis of variance because of these differences). Graphs of this type are normally used here in loaded pavement problems, and the following discussion is based on the data so interpreted.

For the 2 sets of gages mounted on the orthogonal sides of the vertical cores and measured simultaneously in testing, the interpreted average data are given in Table 2 and are not appreciably different from those obtained using the appended average data. The information given in Table 2 shows that moduli from the north and south facing strain gages algebraically average some 0.4 percent higher than east-west gage moduli. The difference range, for unique test conditions, is from 2.2 percent smaller to 2.5 percent larger. There appears to be no trend in the data. These differences are not significant on an accuracy of measurement basis. They cannot be distinguished on the graph (Fig. 1), and have no meaning on a practical basis. These data support the validity of instrumenting vertical pavement cores with strain gages without regard to roller travel direction. They also suggest that any effect of north-south, east-west anisotropy is small.

For the 2 sets of horizontal cores, one taken in the north-south and one in the east-west direction, Figure 1 shows no obvious difference in moduli at the scale plotted. For

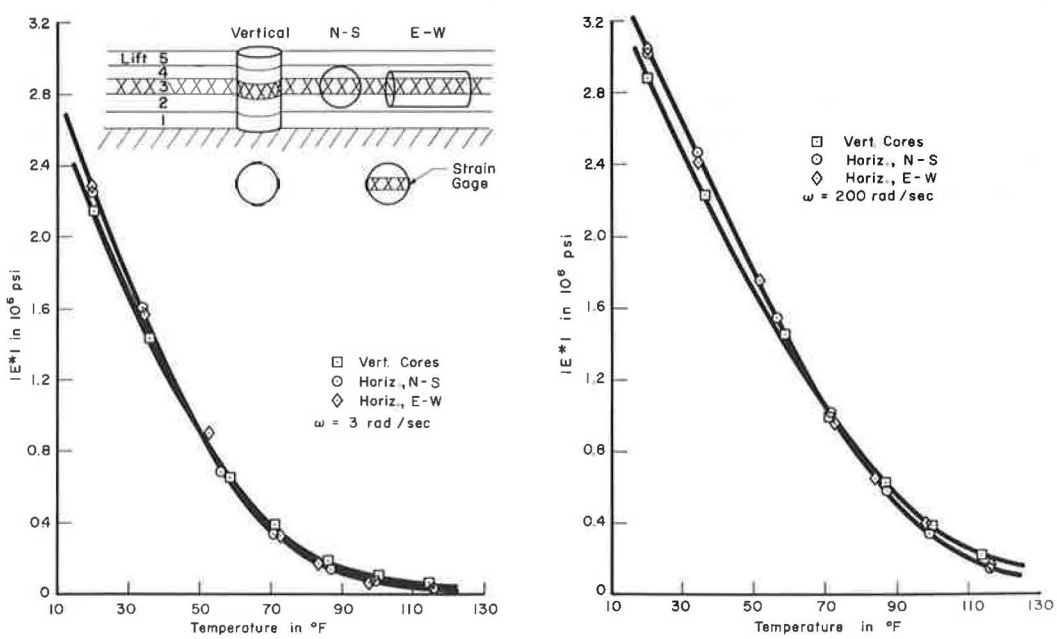

Figure 1. Complex moduli versus temperature at 3 and 200 rad/sec.

TABLE 2

PERCENTAGE N-S MODULI ARE GREATER THAN E-W—VERTICAL CORES

ω (rad/sec)	Temperature, F							
	20	36	58.5	71	86	99	114	Avg
3	0.7	0.0	-0.8	0.5	-0.6	-2.2	0.0	-0.3
10	0.3	0.3	1.2	1.4	1.5	0.0	0.0	0.7
30	-0.2	0.5	1.6	1.5	0.0	0.5	-0.9	0.4
100	-0.6	1.1	0.8	0.8	0.6	0.3	0.0	0.4
200	-0.7	1.4	0.6	0.7	2.5	0.3	0.5	0.8
Avg	-0.1	0.7	0.7	1.0	0.8	-0.2	-0.1	0.4

Note: Interpreted data.

TABLE 3

PERCENTAGE E-W MODULI ARE GREATER THAN N-S—HORIZONTAL CORES

ω (rad/sec)	Temperature, F							
	20	36	58.5	71	86	99	114	Avg
3	0.0	-0.7	2.4	0.9	2.7	4.3	11.0	2.9
10	-0.1	-0.6	5.5	3.2	4.6	5.5	12.5	4.4
30	-0.2	-1.0	4.0	3.7	4.0	7.1	13.1	4.4
100	-0.3	-1.3	4.7	3.5	4.7	6.6	11.8	4.2
200	-0.3	-1.3	4.9	3.3	3.5	5.8	1.4	2.5
Avg	-0.2	-1.0	4.3	2.9	3.9	5.9	10.0	3.7

Note: Interpreted data.

the interpreted data, the east-west cores algebraically average 4 percent larger in moduli than north-south cores over the frequency and temperature range investigated. The effect is essentially independent of frequency, as given in Table 3. For individual test conditions, this value ranges from 1 percent lower to 13 percent higher. There is no clear trend with temperature. These results are not appreciably different from those obtained by using the average data given in Table 9. For the latter, there is a trend of higher coefficients of variation with temperature. These coefficients range from below 4 percent at low temperature to below 10 percent at high temperature for each test series. On this basis the difference between moduli from the 2 orthogonal sets of horizontal cores are on the order of differences in tests of replicate specimens. Differences of this order are not particularly significant on a practical basis, as data shown in Figure 1 suggest.

Comparing moduli from the vertical and horizontal pavement cores, Figure 1 shows the trend of horizontal cores to give higher moduli at low temperatures and lower moduli at high temperatures. Table 4 gives data that relate interpreted average data of

TABLE 4

PERCENTAGE VERTICAL MODULI ARE GREATER THAN HORIZONTAL—ALL CORES

ω (rad/sec)	Temperature, F							
	20	36	58.5	71	86	99	114	Avg
3	-6	-4	3	6	21	31	66	9
10	-5	-3	-1	7	15	23	33	10
30	-5	-3	-3	6	12	18	27	7
100	-5	-2	-3	-3	10	13	29	6
200	-8	-2	-2	4	13	9	27	6
Avg	-6	-3	-1	4	14	19	29	8

Note: Interpreted data.

north-south and east-west facing gage sets mounted on vertical cores with average data of north-south and east-west horizontal cores. These data show that the effect is almost entirely due to temperature and algebraically averages some 8 percent difference. For individual test conditions, this ranges from 8 percent smaller at low temperatures to 33 percent higher at high temperatures, and this trend is consistent.

DISCUSSION OF RESULTS

It should be noted that the design of this experiment was such that a positive answer to the question "Are orthogonal compressive moduli equal?" is possible from these tests only if the 5 layers of the test cores are identical; i.e., the core layers are alike and there is no effect at lift boundaries. If these conditions are not met, the investigating test represents 2 new layered boundary problems. Theoretical solutions of these 2 problems and complete moduli data, including $|\mu^*|$ for the surrounding lifts, are necessary to a numerical solution. Such data for the lifts surrounding the instrumented lift are not directly available, and it may not be assumed that the lifts, composed of different plant batches and compaction histories, were of identical materials. Density differences could, however, be measured.

To determine if density variations were present within the cores, densities were determined by using the remaining replicate cores. These measurements used the submersion technique on the upper, middle, and bottom third of each of 10 vertical cores (referenced to pavement). Test results are given in Table 5. The density of the middle of the cores was about 2 pcf greater than that of the 2 ends, which were closely the same. The middle layer was very probably of higher modulus than the surrounding layers. This is true because, for an asphaltic concrete mix tested at 2 densities, the lower density specimens will give the lower modulus. Moduli from small density differences, when graphed, will be most easily distinguishable at the lower temperatures. Density differences with asphalt-cement content at constant compactive effort appear to give the same trend short of very high compactive efforts (8).

Because of these density and moduli complications, it is not strictly possible to conclude that the instrumented middle test layer was, or was not, isotropic. It is reassuring to note, however, that where specimen boundaries were the same and measurements were simultaneous (the 2 sets of gages on the vertical cores) no differences were found. It is believed that this similarity in layer geometry did not exist for the horizontal cores as a group. Problems were found in precisely locating the middle or third lift, and it was most likely in slightly different relative positions within the different cores as well as with respect to the strain gages. It is also of interest that the differences found are not larger and that differences of the order found can be ignored for most purposes. As was noted, and while indirect, this is consistent with the results of previous comparisons of measured and predicted deflections in which vertical cores from layered asphaltic concretes were used and homogeniety and isotropy were assumed.

For the vertical cores it appears reasonable that the less dense and less stiff surrounding layers would result in decreased measured moduli because of negative restraint. For the horizontal cores, where these softer layers were located along the sides, the same measured moduli effect would be expected. This is in analogy with the load-transfer effect of dissimilar columns of common length and deflection. Calculations for the latter case indicate errors below 10 percent for these materials. Data shown in Figure 1 suggest that the geometry effect with the vertical cores is of the same numerical order. An explanation of the clear trend of the horizontal and vertical moduli data in crossing with temperature at all frequencies (Fig. 1) is not obvious. This trend is probably the combined result of interactions between layering test-geometry differences and that of the less dense surrounding layers. If the relative percentage difference in moduli of the 2 materials is greater at high temperatures, then the 2 curves could

TABLE 5

DENSITIES FROM VERTICAL PAVEMENT CORES

Portion	Avg (pcf)	Range (pcf)
Top	141.2	139.6-142.6
Middle	143.5	142.9-144.5
Bottom	141.5	139.1-144.2

Note: Data for 10 core specimens.

be expected to cross as these data show. It should be noted, in any event, that differences in materials were small as were differences in measured moduli.

Conclusions

These tests were directed at the question of anisotropy in asphaltic concrete from a highway pavement. The complex Poisson's ratio was not measured and, for the compressive moduli, no "clean" conclusion can be reached. The conditions of the experiment were such that a clear answer was possible only if all layers or lifts had identical properties and there were no lift-boundary effects. These conditions were not met and the results of the moduli tests indicate differences, but these are not large except at the highest test temperature. The differences found appear to be consistent with the density variation in the different sections of the cores. Had the densities of the surrounding lifts been equal, it is expected that all moduli would be more nearly equal within normal statistical variations. On an engineering basis, the differences found are not considered significant for predicting strains and deflections for a layered pavement structural system. Based on the considerations discussed, it is concluded that the assumption of isotropy for compression loadings is reasonable for the asphaltic concrete of this pavement at the phenomenological level.

BENDING MODULI

This study was aimed at fatigue testing, and bending tests using trapezoidal specimens were chosen over more conventional beams. This was to minimize or avoid unsupported lengths during sampling, handling, storing, and testing, and to minimize sawing accuracy and possible inertial problems in the laboratory. The sketch in Figure 2 shows, in principle, the loading and test geometry used in which 1 side of the specimen is alternately in tension and compression. Equations in linear elasticity for this geometry are given in Timoshenko's work (9). Tests of asphaltic concrete in this geometry were first used by Bazin and Saunier, who gave solutions for the forced loading of a viscoelastic material (10). In testing, the loading system, amplification, and recording equipment was the same as those used in testing the core specimens. Temperature was controlled by circulating fluid from a water bath. Specimens were not enclosed in membranes, and fluids were water and aqueous methanol. No significant fluid effect was found in comparisons of submerged asphaltic concrete bending moduli with those obtained in air before and after submersion in these fluids.

Only deflections are readily measurable in fatigue testing. Strain gages, mounted as shown in Figure 2, risk interference with measured fatigue life. For such tests it is necessary to calibrate the apparatus (using specimens of known moduli) and desirable to theoretically solve the boundary problem represented in the test. For this study the theoretical solution was not known, and it was necessary to check the apparatus for inertial effects and to calibrate it. Checks for inertial effects were made by using aluminum specimens (Aluminum Assn. T6061-T651) of 3 machined thicknesses—0.800, 0.500, and 0.250 in. The density of the aluminum was 175 pcf, some 34 pcf greater than that of the asphaltic concrete specimens, representing a more severe test with the aluminum. Strain-based $|E^*|$ for the aluminum overall tests (at room ambient temperature) averaged 10.50 $(10)^6$ psi. Tests at 0.8 in. thickness, 100 lb force, and 9 frequencies from 3 to 21.5 cps gave random moduli values between 10.42 and 10.58 $(10)^6$ psi. Tests at 10 cps over the 3 thicknesses, with 7 loads from 36 to 135 lb, gave random moduli values between 10.42 and 10.66 $(10)^6$ psi. These measured differences are only slightly greater than those expected on precision of measurement basis, and it was concluded that inertial effects could be ignored over the range of frequencies and loads used in this study. Aluminum and plexiglass specimens of the same thicknesses were used in calibrating the apparatus for deflection-based moduli. The results of these tests showed that moduli derived from strain measurements were essentially correct and that moduli from deflection measurements were always lower. For strain-based moduli, this appears to be consistent with Saint-Venant's principle. For deflection-based moduli, the error in modulus seems to be the result of shear strain and incomplete boundary rigidity. For specimens of constant dimensions, the error is proportional to the modulus plus a

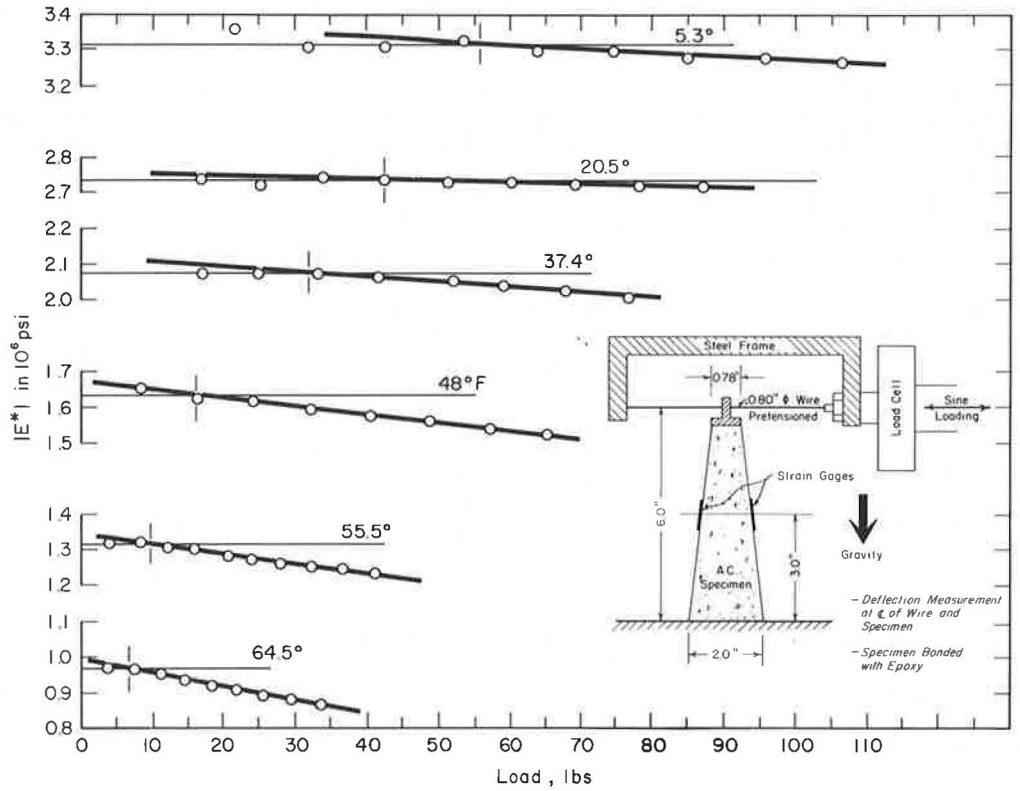

Figure 2. Linearity in bending.

constant. This proportionality was reported earlier by Taylor (with Pell) using cylindrical specimens (11). For trapezoidal specimens of varying thickness, this proportionality is with the product of modulus and thickness. Only strain measurements are used in this study of moduli determined with bending tests.

Asphaltic concrete specimens for these tests were taken from the same pavement section that furnished the cores. These were obtained in the form of block samples sawed with a 24-in., diamond-tipped blade. The 4- by 15- by 8-in. blocks were further sawed in the laboratory to obtain trapezoidal test specimens, as shown in Figure 2. After sawing, strain gages were bonded with epoxy, the specimen was bonded with epoxy (top and bottom) to steel platens, and oven-cured and annealed for over 12 hours at 135 F. Figure 2 shows that the specimen face parallel with the paper is parallel to pavement surface. In reference to the cores and pavement, measured strains (Fig. 2) were north-south for one strain gage and north-south ±12.6 deg for the other. Test specimens were about 1.90 in. constant thickness and included parts of the 2 bottom pavement lifts. Average specimen density was 142.5 pcf with a range of ±1.1 pcf. The dimensions of each test specimen were measured to 0.001 in. with dial micrometers, and the individual dimensions were used in calculations. In testing, the output of each gage was recorded in the steady-state condition. Variations between gages on the same specimen were similar to those for cores. Measurements of double amplitude were made for load and for each strain gage, and these were used in calculating moduli.

Five specimens were selected for moduli comparison tests. Test series were of 2 types: one, constant frequency with varying load to determine the linear range at 62.8 rad/sec; and, two, varying frequency with constant load (generally outside the linear range at 62.8 rad/sec). Test temperatures for both series ranged from 5.3 to 64.5 F.

The results of these tests are given in Tables 10 and 11 in the Appendix in the form of average, standard deviation, and coefficient of variation for 3 replicate tests of 5 specimens. Each strain gage was treated as a separate test.

Figure 2 shows the results of the bending tests to determine linearity at 62.8 rad/sec over the 6 temperatures investigated (Table 10). These load data are related to temperature shown in the inset of Figure 3. On the basis of these data, the linear range in bending tests is far more restrictive than in compression tests. Although not shown, the linear range as determined by bending deflection measurements cannot be distinguished from that determined by strain measurements. It should be noted that these data refer strictly to the test system and may not be extrapolated to other conditions of test or confinement as, for example, probably exist in an in-service pavement.

Figure 3 shows comparisons of vertical compressive with bending moduli over a range of temperatures and frequencies as well as linearity conditions. Compressive data are the vertical core data used in comparing directional core test results. For the comparison here it was necessary to extrapolate the compressive results to 5.3 F and to interpolate for 62.8 rad/sec data below about 56 F. Test data at 62.8 rad/sec, supplementing Table 9, are given in Table 6. Linear bending data are from Table 10, as interpreted in Figure 2. Nonlinear bending data are from graphical interpretation of the data given in Table 11. Numerical comparisons of the differences between bending and compressive moduli (vertical and horizontal north-south) for the linear tests at 62.8 rad/sec are given in Table 7.

Linear bending moduli compare with vertical compressive moduli much as they compared with all horizontal moduli (Table 4). Comparison of only north-south moduli, bending and compressive, improves this but not significantly. For the orthogonal compressive test series, it was concluded that directional effects were not significant in an engineering sense. On this same basis, the linear data given in Table 7 and shown in Figure 3 indicate no essential difference between moduli determined in compression and in bending within the normal scatter of replicate test measurements and interpretation.

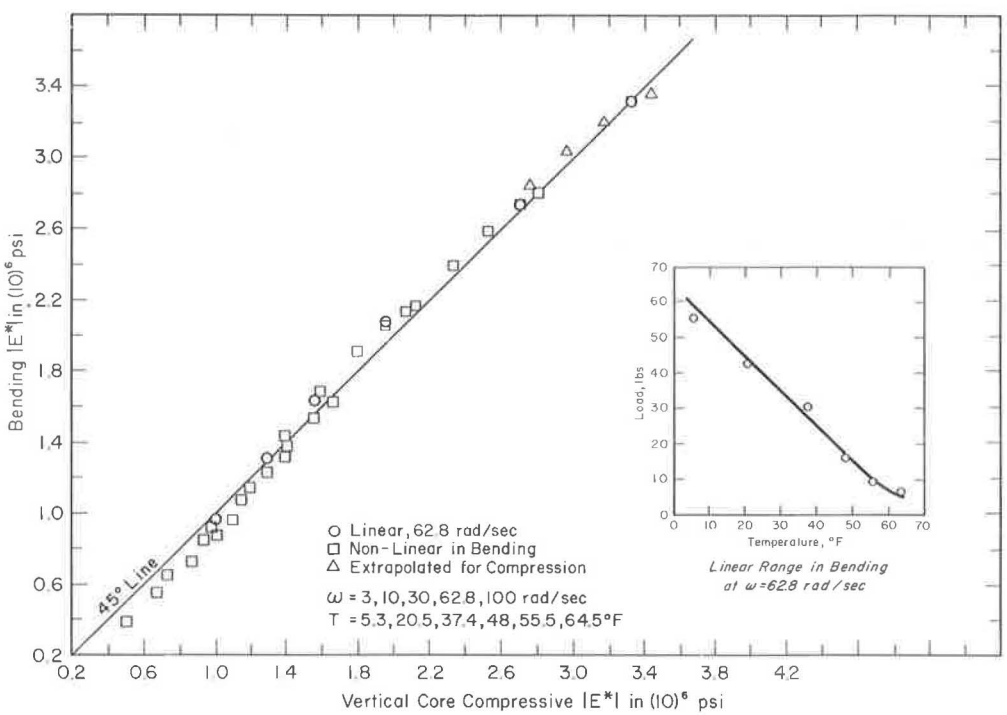

Figure 3. Comparison of compressive and bending moduli.

TABLE 6

COMPRESSIVE COMPLEX MODULI AT 62.8 RAD/SEC

Core	Gage Direction	Temp. F	Avg. $\|E^*\|$ (10^6 psi)	σ (10^6 psi)	CV (percent)
Vertical	N-S	58.5	1.194	0.052	4.3
Vertical	E-W	58.5	1.189	0.049	4.2
Vertical	N-S	114	0.135	0.008	6.2
Vertical	E-W	114	0.132	0.013	9.9
Horizontal	N-S	56	1.258	0.045	3.6
Horizontal	N-S	71	0.767	0.032	4.1
Horizontal	N-S	87	0.404	0.022	5.2
Horizontal	N-S	116	0.088	0.005	5.5
Horizontal	E-W	72	0.749	0.054	7.2
Horizontal	E-W	84	0.462	0.036	7.8
Horizontal	E-W	116	0.100	0.009	9.3

TABLE 7

PERCENTAGE COMPRESSIVE MODULI ARE GREATER THAN LINEAR BENDING MODULI

Temp. F	Bending $\|E^*\|$	Vertical Cores		Horizontal Cores N-S	
		$\|E^*\|$	Percent	$\|E^*\|$	Percent
64.5	0.966	0.985	+1.6	0.950	-2.1
55.5	1.314	1.270	-4.7	1.280	-3.9
48.0	1.634	1.545	-5.5	1.600	-1.9
37.4	2.073	1.955	-4.9	2.050	0
20.5	2.735	2.645	-2.9	2.765	1.6
5.3	3.314	3.280[a]	-1.2	3.420[a]	2.6

Note: ω = 62.8 rad/sec; $|E^*|$ in 10^6 psi; compressive data interpreted below 56 F.

[a]Extrapolated.

TABLE 8

PERCENTAGE LINEAR COMPRESSIVE MODULI ARE GREATER THAN NONLINEAR BENDING MODULI

Temp. F	Load (lb)	ω	$\|E^*\|_C$	$\|E^*\|_B$	Percent	Temp. F	Load (lb)	ω	$\|E^*\|_C$	$\|E^*\|_B$	Percent
64.5	12	3	0.502	0.394	21.0	37.4	37	3	1.390	1.440	-3.6
64.5	12	10	0.670	0.547	18.3	37.4	37	10	1.590	1.683	-5.9
64.5	12	30	0.864	0.727	15.9	37.4	37	30	1.793	1.908	-6.4
64.5	12	62.8	0.998	0.872	12.6	37.4	37	62.8	1.952	2.055	-5.3
64.5	12	100	1.095	0.958	12.5	37.4	37	100	2.060	2.138	-3.8
55.5	20	3	0.727	0.655	9.9	20.5	50	3	2.120	2.168	-2.3
55.5	20	10	0.928	0.848	8.6	20.5	50	10	2.330	2.390	-2.6
55.5	20	30	1.140	1.070	6.1	20.5	50	30	2.520	2.593	-2.9
55.5	20	62.8	1.285	1.228	4.4	20.5	50	62.8	2.695	2.725	-1.1
55.5	20	100	1.390	1.315	5.4	20.5	50	100	2.800	2.799	0.4
48.0	33	3	0.975	0.921	5.5	5.3	53	3	2.755[a]	2.847	-3.6
48.0	33	10	1.190	1.143	3.9	5.3	53	10	2.960[a]	3.030	-2.4
48.0	33	30	1.400	1.375	1.8	5.3	53	30	3.162[a]	3.200	-1.2
48.0	33	62.8	1.555	1.538	1.1	5.3	53	62.8	3.327[a]	3.314	0.4
48.0	33	100	1.660	1.624	2.2	5.3	53	100	3.433[a]	3.358	2.2

Note: $|E^*|$ in 10^6 psi; ω in rad/sec.

[a]Extrapolated.

The nonlinear data shown in Figure 3 were selected from Table 11 and are given in summary in Table 8. These data indicate that the effect of nonlinearity was not great except at the higher temperatures and lower frequencies. The same temperature effect is shown in Figure 2 in the relative rates of moduli decrease with load in the linearity tests at 62.8 rad/sec.

SUMMARY AND CONCLUSIONS

Asphaltic concrete specimens were secured from a contract-constructed full-scale pavement. Core specimens were taken in 3 orthogonal directions with the middle pave-

ment lift centered in the cores. This lift was instrumented with strain gages, and the cores were tested in unconfined compression at different frequencies and temperatures to determine steady-state compressive complex moduli. Comparison of these directional test results was not strictly valid because of theoretical considerations based on small density and thus moduli differences between pavement lifts. These differences were small and qualitatively consistent in moduli. The resulting differences were not considered significant in predicting strains and deflections for layered pavement structural systems. Based on this it was concluded, to a first approximation, that the asphaltic concrete of this pavement system was isotropic in compression at the phenomenological level.

Block samples of the same pavement were sawed to produce trapezoidal specimens for testing in bending. These specimens were instrumented with strain gages oriented to within about 13 deg of 1 of the 3 orthogonal directions previously tested but were on different pavement lifts. Linear tests in the steady-state condition at 1 frequency gave moduli results of the same order of variation from vertical compressive moduli that was found with the average of all horizontal compressive moduli. Comparisons of bending moduli with compressive moduli taken in the same direction were slightly, but not significantly, better. It was found that the range of linearity in bending was much more restrictive than that in compression and that the effect of nonlinearity was large only at low frequencies or high temperatures or both. Based on the data, it was concluded that bending and compressive moduli for this asphaltic concrete were the same within the accuracies and normal scatter of replicate test measurements present in the study. In answer to the opening question "Can asphaltic concrete be isotropic?" it is concluded that it can and, within the limitations of this study, is certainly to a first approximation at the phenomenological level.

ACKNOWLEDGMENT

This study was sponsored, as part of a larger study, by the Ohio Department of Highways in cooperation with the U. S. Department of Transportation, Federal Highway Administration, Bureau of Public Roads, and grateful acknowledgment is made of the continued interest and cooperation of representatives of those organizations. Particular recognition is due to Willis B. Gibboney of the highway department, whose thoughtful suggestions and cooperation in coordinating the field phases made this study possible. Recognition is also due to Betty Colley for typing the formidable tables. The interpretations and conclusions of this study represent those of the authors and not necessarily those of the sponsors.

REFERENCES

1. Papazian, H. S. The Response of Linear Viscoelastic Materials in the Frequency Domain With Emphasis on Asphaltic Concrete. First Internat. Conf. on the Structural Design of Asphalt Pavements, Ann Arbor, Aug. 1962.
2. Baker, R. F. A Structural Design Procedure for Pavements. First Internat. Conf. on the Structural Design of Asphalt Pavements, Ann Arbor, Aug. 1962.
3. Coffman, B. S., and Kraft, D. C. A Comparison of Calculated and Measured Deflections for the AASHO Test Road. Proc. AAPT, Vol. 33, 1964.
4. Coffman, B. S. Pavement Deflections From Laboratory Tests and Layered Theory. Second Internat. Conf. on the Structural Design of Asphalt Pavements, Ann Arbor, Aug. 1967.
5. Deacon, J. A. The Fatigue of Asphaltic Concrete. Inst. of Transp. and Traffic Eng., Univ. of Calif., Graduate rept., 1965, p. 274 and Fig. 49.
6. Coffman, B. S. Suggested Method of Test for Determining the Complex Moduli of Soils and Asphaltic Concrete in Compression. In Procedures for Testing Soils, ASTM, in press, 1970.
7. Filon, L. N. G. On the Elastic Equilibrium of Circular Cylinders Under Certain Practical Systems of Load. Philos. Trans., Royal Soc. of London, Vol. 198, Series A, May 1902.

8. Shook, J. F., and Kallas, B. F. Factors Influencing Dynamic Modulus of Asphalt Concrete. Proc. AAPT, Vol. 38, 1969.
9. Timoshenko, S. Strength of Materials, Parts I and II. D. Van Nostrand Co., Inc., New York, 1956.
10. Bazin, P., and Saunier, J. B. Deformability, Fatigue and Healing Properties of Asphalt Mixes. First Internat. Conf. on the Structural Design of Asphalt Pavements, Ann Arbor, Aug. 1962.
11. Taylor, I. F. Asphaltic Road Materials in Fatigue. Univ. of Nottingham, England, Graduate rept., Sept. 1968.

Appendix

Table 9 gives the results of compression tests of 9 replicate specimens. Tables 10 and 11 give the linear and nonlinear data from the bending tests of 5 specimens.

TABLE 9

COMPRESSIVE COMPLEX MODULI
(9 specimens, $|E^*|$ & σ in 10^6 psi)

Vertical Cores, N-S gages

ω, rad/sec	20°F Avg $\|E^*\|$	#	CV %	36°F Avg $\|E^*\|$	#	CV %	58.5°F Avg $\|E^*\|$	#	CV %	71°F Avg $\|E^*\|$	#	CV %	86°F Avg $\|E^*\|$	#	CV %	99°F Avg $\|E^*\|$	#	CV %	114°F Avg $\|E^*\|$	#	CV %
3	2.146	.078	3.6	1.432	.001	4.2	0.955	.045	6.9	0.374	.015	4.0	0.174	.009	5.2	0.089	.006	7.1	0.049	.004	6.6
10	"	"	"	"	"	"	0.842	.040	4.7	0.511	.023	4.5	0.264	.015	5.8	0.144	.011	7.2	0.072	.006	8.6
30	2.530	.080	3.2	1.873	.070	3.7	1.059	.045	4.2	0.676	.030	4.5	0.370	.020	5.5	0.198	.013	6.6	0.103	.009	8.6
100	"	"	"	"	"	"	1.287	.061	4.7	0.876	.038	4.3	0.516	.024	4.6	0.305	.017	5.5	0.160	.011	6.9
200	2.471	.109	2.8	2.251	.071	3.2	1.438	.059	4.1	0.998	.041	4.1	0.614	.031	5.0	0.384	.021	5.5	0.211	.016	7.7

Vertical Cores, E-W gages

	20°F			36°F			58.5°F			71°F			86°F			99°F			114°F		
3	2.134	.073	3.4	1.421	.076	5.3	0.955	.037	5.7	0.375	.022	6.0	0.170	.011	6.4	0.089	.007	7.8	0.050	.006	11.2
10	"	"	"	"	"	"	0.833	.047	5.6	0.508	.030	5.9	0.263	.018	7.0	0.143	.013	9.2	0.072	.008	10.7
30	2.540	.091	3.6	1.870	.067	3.6	1.056	.051	4.9	0.670	.036	5.4	0.366	.024	6.6	0.196	.014	6.9	0.102	.009	9.1
100	"	"	"	"	"	"	1.273	.062	4.9	0.872	.039	4.5	0.519	.028	5.3	0.302	.019	6.4	0.159	.013	8.5
200	2.890	.080	2.8	2.200	.103	4.7	1.433	.063	4.4	0.976	.047	4.8	0.599	.033	5.4	0.385	.026	6.7	0.210	.019	9.2

Horizontal Cores, N-S

	20°F			34°F			50°F			71°F			87°F			99°F			116°F		
3	2.257	.085	3.8	1.602	.071	4.4	0.678	.032	4.8	0.328	.018	5.6	0.139	.008	4.5	0.066	.004	6.3	0.025	.001	5.5
10	"	"	"	"	"	"	0.888	.039	4.4	0.458	.023	5.0	0.214	.010	4.6	0.105	.005	5.1	0.042	.002	4.4
30	2.711	.071	2.6	2.050	.069	3.3	1.108	.046	4.2	0.625	.027	4.3	0.314	.015	4.8	0.161	.009	5.5	0.066	.004	5.5
100	"	"	"	"	"	"	1.375	.054	3.9	0.858	.026	3.0	0.461	.023	5.1	0.255	.013	5.1	0.106	.006	5.2
200	3.018	.090	3.0	2.463	.098	4.0	1.537	.054	3.5	0.995	.040	4.0	0.570	.024	4.2	0.329	.016	5.0	0.140	.008	5.7

Horizontal Cores, E-W

	20°F			34°F			52°F			72°F			84°F			98°F			116°F		
3	2.270	.117	5.2	1.570	.099	6.3	0.982	.070	8.0	0.318	.028	8.8	0.167	.016	9.5	0.073	.007	9.2	0.028	.003	11.2
10	"	"	"	"	"	"	1.115	.079	7.1	0.451	.035	7.8	0.254	.023	9.1	0.119	.012	10.0	0.051	.005	9.1
30	2.670	.193	7.2	2.000	.111	5.5	1.342	.089	6.6	0.619	.048	7.8	0.368	.033	9.0	0.187	.012	6.3	0.075	.007	9.0
100	"	"	"	"	"	"	1.669	.092	5.7	0.840	.062	7.3	0.536	.041	7.7	0.300	.027	9.1	0.118	.011	9.4
200	3.028	.121	4.0	2.408	.125	5.2	1.745	.090	5.1	0.968	.060	6.2	0.651	.050	7.7	0.382	.032	8.4	0.155	.014	9.1

TABLE 10

LINEARITY IN BENDING, 62.8 rad/sec
(5 specimens with 2 gages, avg. of 3 repeats)
($|E^*|$ and σ in 10^6 psi)

5.3°F Avg. Load, lbs.	Avg $\|E^*\|$	#	CV %	20.5°F Avg. Load, lbs.	Avg $\|E^*\|$	#	CV %	37.4°F Avg. Load, lbs.	Avg $\|E^*\|$	#	CV %	48.6°F Avg. Load, lbs.	Avg $\|E^*\|$	#	CV %	55.5°F Avg. Load, lbs.	Avg $\|E^*\|$	#	CV %	64.5°F Avg. Load, lbs.	Avg $\|E^*\|$	σ	CV %
21.55	3.358	0.225	6.7	16.96	2.739	0.200	7.3	16.90	2.072	0.154	7.4	8.23	1.649	0.173	10.5	3.99	1.309	0.154	11.8	3.68	0.986	0.096	10.0
31.90	3.307	0.225	6.8	25.37	2.724	0.196	7.2	24.99	2.077	0.163	7.9	16.31	1.622	0.160	9.9	8.02	1.320	0.134	10.1	7.41	0.963	0.100	10.4
42.51	3.309	0.229	6.9	33.95	2.741	0.198	7.2	33.33	2.072	0.161	7.8	24.23	1.617	0.170	10.5	12.03	1.305	0.137	10.5	11.03	0.952	0.103	10.8
53.40	3.322	0.227	6.8	42.47	2.734	0.200	7.3	41.66	2.062	0.160	7.8	32.28	1.593	0.168	10.5	15.96	1.303	0.133	10.2	14.62	0.934	0.101	10.8
63.80	3.295	0.218	6.6	51.25	2.730	0.196	7.2	50.22	2.051	0.161	7.8	40.49	1.577	0.162	10.3	20.06	1.284	0.134	10.4	18.25	0.920	0.099	10.8
74.55	3.292	0.221	6.7	60.16	2.728	0.197	7.2	58.65	2.040	0.162	7.9	48.81	1.561	0.163	10.5	23.93	1.270	0.133	10.4	21.87	0.909	0.101	11.1
85.13	3.277	0.222	6.8	69.23	2.723	0.201	7.4	67.72	2.027	0.163	8.0	57.09	1.539	0.160	10.4	28.05	1.260	0.130	10.3	25.65	0.891	0.099	11.1
95.74	3.273	0.227	6.9	78.34	2.719	0.195	7.2	76.72	2.018	0.162	8.0	65.21	1.522	0.158	10.4	32.29	1.253	0.130	10.4	29.59	0.880	0.097	11.0
106.4	3.262	0.228	7.0	87.09	2.716	0.201	7.4	84.75	2.004	0.157	7.8					36.65	1.246	0.130	10.4	33.61	0.868	0.096	11.0
																41.06	1.235	0.130	10.6				

TABLE 11

VARIABLE FREQUENCY IN BENDING
(5 specimens with 2 gages, no repeat tests)
(ω in rad/sec)

Load = 52.3 lbs Linear range = 59 lbs @ 62.8 rad/sec				Load = 50.0 lbs Linear range = 44 lbs @ 62.8 rad/sec			Load = 33.3 lbs Linear range = 27 lbs @ 62.8 rad/sec			Load = 32 lbs Linear range = 17 lbs @ 62.8 rad/sec			Load = 20 lbs Linear range 10 lbs @ 62.8 rad/sec			Load = 12.2 lbs Linear range 5 lbs @ 62.8 rad/sec		
ω	Avg. |E*|	σ	CV %	Avg. |E*|	σ	CV %	Avg. |E*|	σ	CV %	Avg. |E*|	σ	CV %	Avg. |E*|	σ	CV %	Avg. |E*|	σ	CV %
0.94	2.650	0.206	7.8	—	—	—	—	—	—	—	—	—	—	—	—	—	—	—
1.57	2.747	0.208	7.6	—	—	—	—	—	—	—	—	—	—	—	—	—	—	—
3.00	2.860	0.215	7.5	2.168	0.178	8.2	1.446	0.124	8.6	.920	0.111	12.0	.655	0.082	12.6	.393	0.052	13.3
6.28	2.965	0.222	7.5	2.308	0.184	8.0	1.598	0.137	8.6	1.061	0.131	12.4	.774	0.095	12.1	.484	0.064	13.3
9.42	—	—	—	—	—	—	—	—	—	—	—	—	—	—	—	.537	0.068	12.7
12.6	3.068	0.214	7.0	2.430	0.194	8.0	1.720	0.144	8.4	1.159	0.136	11.4	.880	0.105	11.7	.581	0.072	12.4
15.7	—	—	—	—	—	—	—	—	—	—	—	—	—	—	—	.616	0.076	12.3
18.8	3.123	0.213	6.8	2.498	0.192	7.7	1.803	0.150	8.3	1.273	0.140	11.0	.975	0.112	11.5	.641	0.076	11.8
25.1	3.171	0.216	6.8	2.556	0.203	7.9	1.874	0.158	8.4	1.335	0.152	11.4	1.030	0.118	11.5	.695	0.082	11.8
31.4	3.219	0.227	7.1	2.598	0.198	7.6	1.914	0.150	7.9	1.385	0.154	11.1	1.081	0.122	11.3	.739	0.090	12.2
37.7	3.231	0.227	7.0	2.631	0.199	7.6	1.955	0.139	7.0	1.435	0.153	10.7	1.121	0.125	11.2	.776	0.095	12.2
44.0	3.250	0.226	7.0	2.664	0.193	7.2	1.991	0.157	7.9	1.463	0.151	11.0	1.153	0.126	10.9	.803	0.095	11.9
50.2	3.285	0.219	6.7	2.688	0.203	7.6	2.014	0.164	8.1	1.494	0.161	10.8	1.184	0.132	11.2	.829	0.097	11.7
56.5	3.305	0.222	6.7	2.705	0.202	7.5	2.041	0.155	7.6	1.518	0.157	10.3	1.208	0.131	11.1	.856	0.101	11.9
62.8	3.304	0.228	6.9	2.726	0.197	7.2	2.069	0.157	7.6	1.539	0.163	10.6	1.227	0.130	10.6	.873	0.102	11.7
69.1	3.316	0.226	6.8	2.731	0.203	7.4	2.077	0.158	7.6	1.558	0.160	10.3	1.245	0.131	10.7	.889	0.103	11.6
75.4	3.327	0.232	7.0	2.739	0.202	7.4	2.092	0.161	7.7	1.575	0.159	10.1	1.261	0.140	11.1	.901	0.101	11.5
81.6	3.338	0.237	7.1	2.757	0.201	7.3	2.108	0.168	7.9	1.591	0.167	10.5	1.277	0.133	10.4	.918	0.102	11.1
87.9	3.338	0.236	6.8	2.775	0.203	7.3	2.124	0.160	7.5	1.602	0.169	10.6	1.291	0.138	10.7	.930	0.105	11.3
94.2	3.338	0.229	6.8	2.774	0.210	7.6	2.132	0.160	7.5	1.614	0.169	9.9	1.305	0.140	10.7	.941	0.108	11.4
101	3.360	0.228	6.7	2.791	0.203	7.3	2.139	0.159	7.4	1.625	0.162	10.0	1.321	0.141	10.7	.956	0.108	11.2
107	3.357	0.229	6.8	2.802	0.198	7.1	2.162	0.160	7.4	1.630	0.165	10.1	1.325	0.145	10.8	.976	0.111	11.6
113	3.398	0.216	6.4	2.805	0.197	7.0	2.158	0.156	7.2	1.654	0.168	10.1	1.337	0.139	10.4	.982	0.111	11.7
119	3.374	0.223	6.6	2.808	0.200	7.1	2.163	0.171	7.9	1.656	0.168	10.1	1.347	0.138	10.3	.993	0.110	11.1

Optimum Structural Strength of Materials in Flexible Pavements

N. K. VASWANI, Virginia Highway Research Council, Charlottesville

The optimum structural strength contributed by a material to the overall strength of the pavement was studied for cases applicable to Virginia. The variables were (a) the modulus of elasticity or the thickness equivalency of the material, (b) the thickness of the material in the layer, (c) the location of the material with respect to other layers containing stronger or weaker materials and in varying thicknesses, and (d) the effect of the total pavement thickness and the depth of the material from the top of the pavement. The investigation consisted of a study of the thickness equivalencies of the materials on Interstate, primary, secondary, and subdivision roads in Virginia, and a model study. The evaluation of the highway system was quantitative, while that of the model study was qualitative only. The investigation showed that the structural strength of a pavement is decreased when a weaker layer is placed over a stronger layer or when a weaker layer is sandwiched between 2 strong layers. The investigation also showed that, when the bottom of the top layer does not bend, the stress distribution is bulb type and that, when the bottom bends, the stress distribution is fan type. Each case would therefore need a different mathematical treatment for design.

•FLEXIBLE PAVEMENT DESIGN has undergone a change, in Virginia and other states, from the basic principle of designing each successive layer stronger than the layer underneath it. Materials having a high modulus of strength, e.g., soil cement, soil lime, and cement-treated aggregate, are now commonly used. These materials are placed in subgrades or bases and at various depths and positions in relation to other layers having a low modulus of elasticity. Because of this, the structural strength contributed by a given material is affected by the arrangement of the other materials in relation to the material under consideration.

In this investigation, the manner and the degree of strength contributed by a material in such pavement systems, with respect to the strength of other materials, have been studied. Two types of studies were made:

1. Determinations of the optimum thickness equivalency values of the materials used on primary, Interstate, secondary, and subdivision roads in Virginia, where the thickness equivalency values are based on the location of the materials in the structure of the flexible pavement; and
2. Qualitative evaluation of the effect of thickness and modulus of strength of a given layer with respect to the thickness and modulus of strength of the other layers in the pavement system.

The thickness equivalency values of the materials with respect to their location in the structure were determined. The effect of the location of a given material in a pavement with respect to the other materials in the pavement system was determined, along with stress distribution patterns.

Paper sponsored by Committee on Flexible Pavement Design and presented at the 49th Annual Meeting.

PURPOSE

The main purpose of this study was to determine the structural behavior and the optimum use of a given material in a layered pavement system. It was proposed to determine the behavior and strength of the given material with respect to the modulus of strength and thickness of other layers in the system.

THICKNESS EQUIVALENCY VALUES OF PAVEMENTS IN VIRGINIA

The thickness equivalency value, a, is an index of the load-carrying capacity of a material and could be defined as the ratio of the strength of a 1-in. thickness of the material to that of 1 in. of asphaltic concrete or any other specified material.

In Virginia, different design standards are established for (a) primary and Interstate roads and (b) secondary and subdivision roads. In the case of primary and Interstate roads, the design is based on the subgrade CBR value and on traffic in terms of 18-kip equivalents. In the case of secondary and subdivision roads, the design is based mostly on traffic in terms of vehicles per day. The evaluations of thickness equivalency values for these roads were carried out as discussed in the following sections.

Primary and Interstate Roads

The evaluation of thickness equivalency values for primary and Interstate roads was based on (a) adoption of soil support values (based on CBR and soil resiliency), which would account for the regional factor; (b) traffic in terms of 18-kip equivalents; and (c) deflections. The thickness equivalency values have been reported previously (1, 2). These values were determined by multiple regression analysis.

A study of cement-treated aggregate subbases was carried out in this investigation and their thickness equivalency values, along with all the others previously determined, are given in Table 1.

TABLE 1

THICKNESS EQUIVALENCY VALUES OF MATERIALS IN FLEXIBLE PAVEMENT SYSTEM

Serial Number	Location	Material	Values	
			Primary and Interstate Roads	Secondary and Subdivision Roads
1	Surface	Asphaltic concrete	1.0	1.0
2	Base	Asphaltic concrete	1.0	1.0
		Cement-treated aggregate over dense-graded aggregate base or soil cement or soil lime and under asphaltic concrete mat.	1.0	1.0
		Dense-graded aggregate, crushed or uncrushed	0.35	0.60
		Select material I (Va. specifications) directly under asphaltic concrete mat. and over a subbase of a good quality	0.35	—
		Select material cement-treated	—	0.80
3	Subbase	Select material I, II, and III (Va. specifications)		
		In Piedmont area	0.0	0.0
		In valley and ridge area and coastal plain	0.2	0.50
		Soil cement	0.4	0.60
		Soil lime	0.4	0.55
		Select material cement-treated	0.4	0.80
		Cement-treated aggregate directly over subgrade	0.6	—

Secondary and Subdivision Roads

The evaluation of the thickness equivalency values for secondary and subdivision roads was based mainly on traffic in terms of vehicles per day. The values determined by regression analysis were based on the present design practice in Virginia (3) by correlating daily traffic with the thickness index $D = a_1h_1 + a_2h_2 + \ldots$ in the equation $\log D = P + Q \log vpd$, where D = thickness index = $a_1h_1 + a_2h_2 + \ldots$; vpd = number of vehicles per day; $h_1, h_2, \ldots$ = thickness in inches of different layers; $a_1, a_2, \ldots$ = thickness equivalency of the materials with thicknesses $h_1, h_2, \ldots$ respectively and $a_1 = 1$; and P and Q = constants of the equation. The following equation was obtained from 12 mean values:

$$\log D = 0.2 + 0.24 \log vpd$$

The correlation coefficient was found to be 0.99, and the standard error of estimate was 0.02. These values indicated a very high degree of correlation.

Effect of Depth of Cover and Pavement Thickness on Thickness Equivalency Values

The primary and Interstate roads in Virginia usually carry high volumes of traffic while the secondary and subdivision roads carry comparatively low volumes. The primary and Interstate roads are therefore stronger and thicker than the secondary and subdivision roads.

Examination of the thickness equivalency values given in Table 1 for the 2 sets of design procedures reveals the following:

1. The thickness equivalency of untreated aggregate in the base is 0.35 for primary and Interstate roads, and 0.60 for secondary and subdivision roads.
2. Similarly, the thickness equivalency values of the materials in the subbase for primary and Interstate roads are lower than the values for secondary and subdivision roads.
3. In the case of primary and Interstate roads, the thickness equivalency for the cement-treated aggregate is 1.0 for the base course and 0.6 for the subbase course.

The reason for these differences in the thickness equivalency values is the depth of the cover. In the case of primary and Interstate roads, the surfacing, binder, and base courses over the untreated aggregate would consist of asphaltic concrete varying in thickness from 4.5 to 10.5 in. Furthermore, an intermediate layer of about 6 in. of cement-treated aggregate is sometimes provided between the untreated aggregate base and the asphaltic concrete mat, which further increases the cover thickness. As compared to this thickness of cover, the cover thickness of asphaltic concrete over the untreated aggregate base for secondary and subdivision roads varies from 0 to 5 in. The reduction in thickness equivalency with an increase in cover thickness has also been pointed out by Foster (4).

In some cases it has also been found that as the thickness of the pavement decreases the thickness equivalencies of the materials increase. This is evident from the data given in Table 1, wherein the thickness equivalency values of the subbase materials in secondary and subdivision roads are higher than those of similar materials in primary and Interstate roads.

Figure 1 has been drawn on the bases of the AASHO Road Test results (3). Figure 1 shows that, as the depth of the pavement increases, the thickness index required decreases. For example, with 200,000 repetitions of the 20-kip axle load shown in Figure 1, the thickness index decreases from 3.31 to 3.14 when the pavement depth increases from 17.4 to 23.8 in.

In spite of the effect of the depth of cover and pavement thickness on the thickness equivalencies of the materials, it is found that the equation of thickness index, $D = a_1h_1 + a_2h_2 + \ldots$, holds. This equation is applicable if the thickness equivalencies of the materials are determined according to their quality or strength and their location in the pavement system. However, during study of the flexible pavements in Virginia, certain observations were made that, because of lack of data, could not be clarified. Therefore,

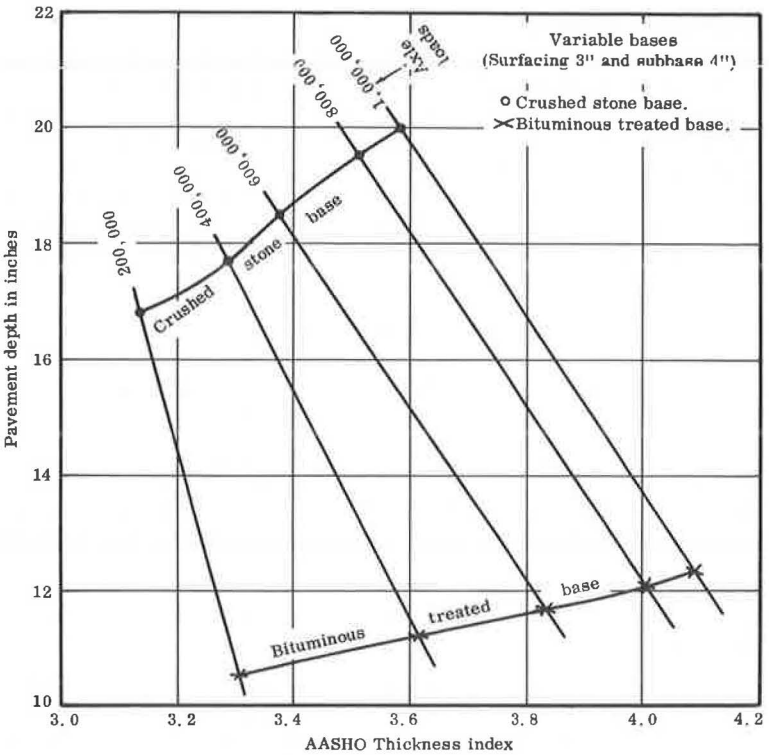

Figure 1. Thickness index versus pavement depth (3, Fig. 36).

model studies were conducted to investigate these observations. This study is discussed in the following paragraphs.

MODEL STUDIES

The study of pavements in Virginia indicated that, when the organization of the layered system deviated from that of the usual system, there was a change in the load-thickness index relationship. It was not possible to make any theoretical verification of this fact beyond certain limits. [Theoretical evaluations made on pavements in Virginia have been reported elsewhere (2).] The method of verification by models was therefore used. The object of the model studies was to obtain a qualitative evaluation of the behavior of the pavement. No quantitative or numerical evaluation was proposed or should be assumed, although numerical values are given for clarity.

In all the studies mentioned here, the models consisted of 2, 3, or 4 layers of materials arranged in varied order and in varied depths. The lowest layer consisted of a specified material—called the subgrade—having a modulus of elasticity = 1,000 psi for an infinite depth. The infinite depth of the subgrade was obtained by increasing the thickness of the subgrade layer until the load deflection ratio on the subgrade only remained almost constant. Some of the different combinations adopted are described later. All materials in the models were homogeneous, isotropic, and elastic within the testing range of load and time. All models whose results are reported were 2 dimensional on a 3-dimensional subgrade. The models were of a specified width to permit proper distribution of the load. The thickness of each layer was varied. The load was applied in the center of the model and maximum deflections were measured. The loading system on the 2- and 3-dimensional models is shown in Figures 2 and 3.

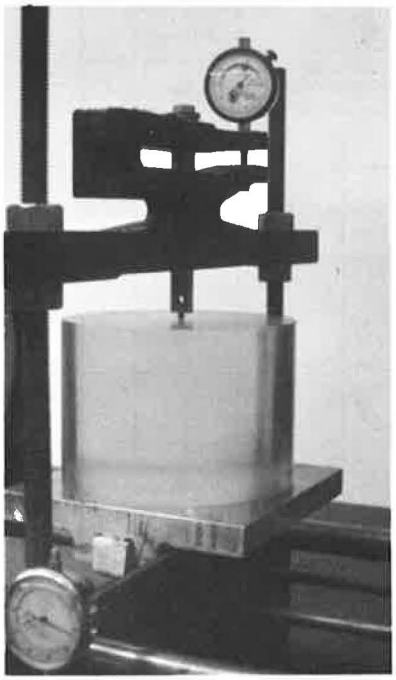

Figure 2. Loading system for 2-dimensional model.

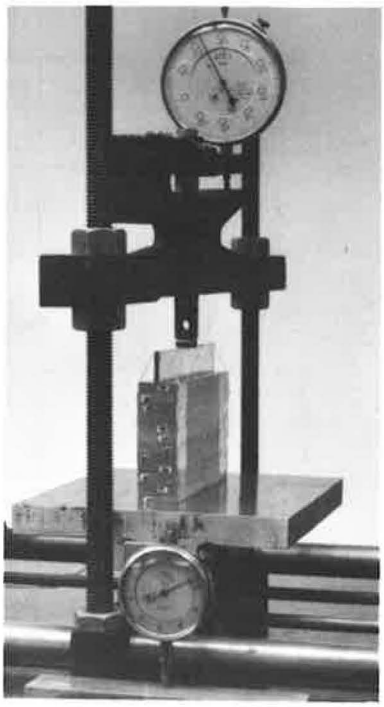

Figure 3. Loading system for 3-dimensional model.

Two Layers—Single Layer Over the Subgrade

In a 2-layer system, the modulus of elasticity of the top layer is always higher than that of its subgrade, e.g., an untreated stone or soil cement, asphaltic mat, and so forth, over a weaker soil subgrade.

In this investigation, 3 photoelastic materials having moduli of elasticity values E = 30,000, 340,000, and 450,000 psi were independently loaded while resting on a weaker subgrade having an E = 1,000 psi. A graph of load versus deflection was drawn for each of the materials with different thicknesses of the top layer resting on the given subgrade. All these curves were straight lines passing through the origin. The slopes of the curves differed from one another depending on the modulus of elasticity and the thickness of the top layer. From each of the graphs, deflection per unit load was determined. Based on the data so obtained, a curve of deflection per unit load versus thickness of the top layer was drawn for each of the materials with a given modulus of elasticity. (Deflection per unit load was adopted to enable evaluation for any given load.) Three such curves, one each for E = 30,000, 340,000, and 450,000 psi of the top layer, are shown in Figure 4.

To correlate the thickness equivalency of each of these 3 materials, the thickness equivalency of the material with E = 340,000 psi was taken as $a_1 = 1.0$. For different values of deflection, ratios of the thickness of the layer of material with E = 30,000 psi to the thickness of the material with E = 340,000 psi were determined from Figure 4. There was very little difference between these ratios. The general trend was a slight decrease in the values of the ratios with an increase in the thickness of the layer or a decrease in deflection. An average value of this ratio was found to be 0.27. Thus, this ratio is the thickness equivalency value, a_3, of the material having $E_3 = 30,000$ psi. In the same manner, the thickness equivalency value of the material having $E_2 = 450,000$ psi

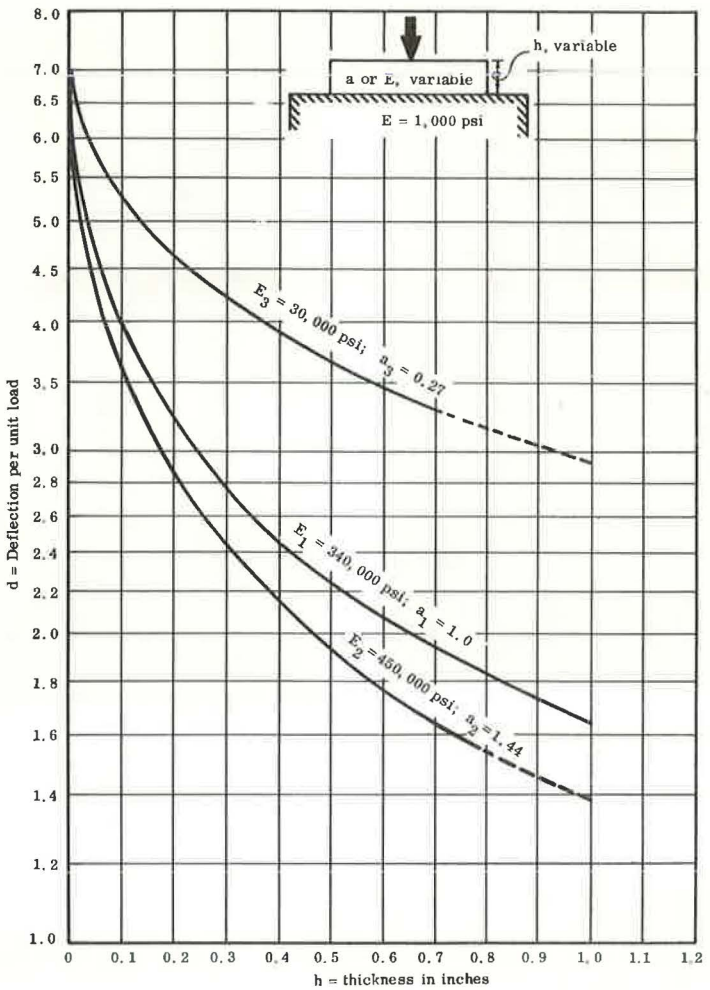

Figure 4. Deflection versus thickness (2-layer system).

was found to be a_2 = 1.40. The thickness equivalency value of the material with E_2 = 450,000 psi decreased very little with an increase in the thickness of the layer, as was observed for the material with E_3 = 30,000 psi, and hence this difference is ignored and the average value accepted. Thus, the following values for different materials were accepted for further tests:

1. For E_1 = 340,000 psi, a_1 is 1.0;
2. For E_2 = 450,000 psi, a_2 is 1.4;
3. For E_3 = 30,000 psi, a_3 is 0.27; and
4. For E_4 = 1,000 psi, a_4 was not determined, because the E value of the subgrade was also 1,000 psi.

Three Layers—Two Layers Over a Subgrade

In the 3-layer system either the top layer could be stronger than the bottom layer (e.g., an asphaltic concrete mat lying over an untreated stone base), or the top layer could be weaker than the bottom layer (e.g., stone aggregate lying over a cement-treated

subbase or an asphaltic mat lying over a portland cement concrete pavement). The model tests showed that, when a stronger layer lies over a weaker layer, the equation of log d = M + N ($a_1h_1 + a_2h_2 + \ldots$), which is based on the AASHO Road Test results and was adopted for the work reported elsewhere (5), is applicable with d = deflection, M and N = constants of the equation, and a_1, a_2, h_1, and h_2 having the same meaning as described previously.

In Figure 5, thickness index versus deflection has been drawn for the 3-layer system and the 2-layer system. The values of the 3-layer system were obtained directly from load tests, while the values of the 2-layer system were obtained from the curves shown in Figure 4, which were drawn from the load test data. Excluding the very low values of thickness index, say up to a maximum of D = 2, the graph of deflection, d, versus thickness index, D, would be a straight line. Lower values of D are ignored because pavement designs with such low values would be impractical. However, the straight-line graph shown in Figure 5 is based on a simple regression analysis of all points shown in the graph. A high degree of correlation (R = -0.97) exists between these 2 variables—deflection and thickness.

With a_1 = 1.0 for the upper layer, as determined from the 2-layer system discussed in the preceding, it was found that the thickness equivalency of the lower layer with a lower strength modulus increases as its thickness decreases, as shown in Figure 6. The increase is from a value of 0.27 as determined in the 2-layer system to 0.48 for the minimum thickness adopted. This tendency has been observed in pavements in Virginia. H. B. Seed et al. (6) have shown that resilient deformation per inch of granular base is smaller for an 8-in. base than for a 12-in. base. Resilient deformation is an inverse function of the thickness index, and hence an inverse function of the thickness equivalency. Thus, the investigation by Seed et al. also shows that the thickness equivalency of the lower layer increases as its thickness decreases. It could be concluded, therefore, that the optimum thickness value for the lower layer is the minimum thickness that could be economically provided.

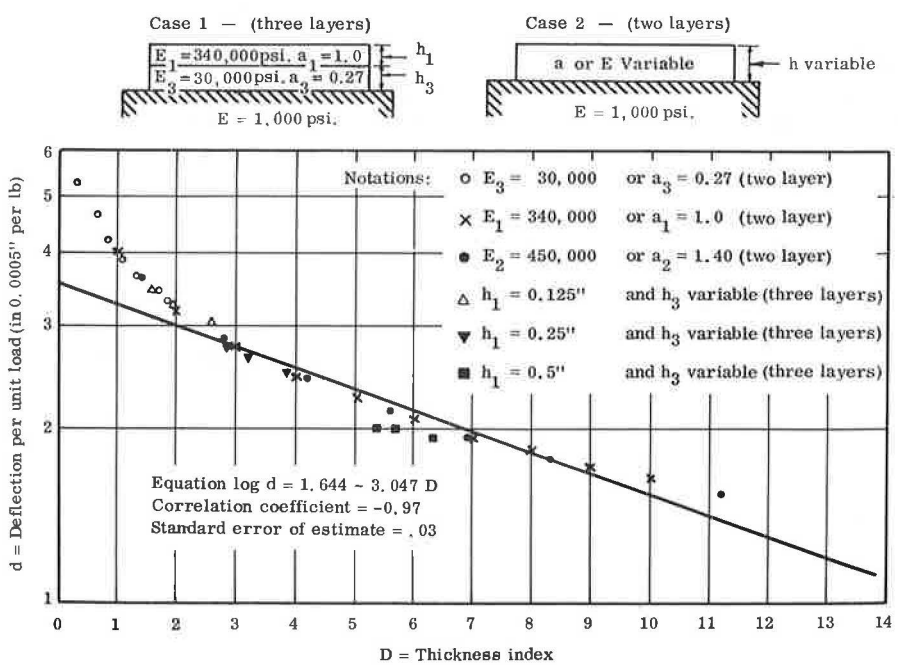

Figure 5. Deflection versus thickness index (model study).

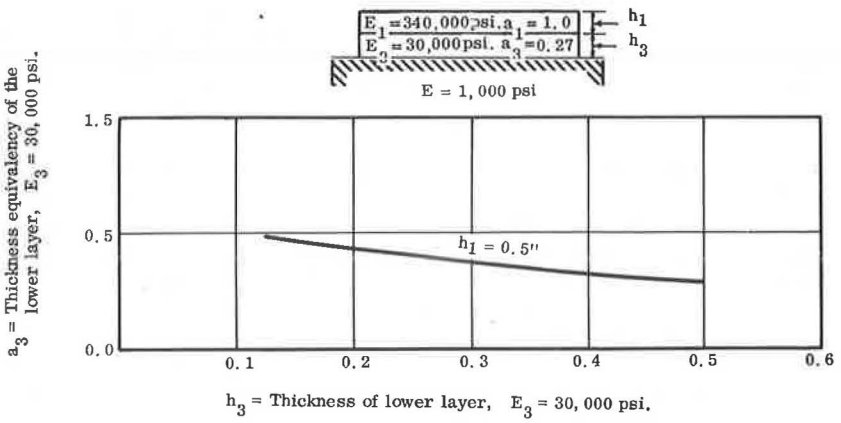

Figure 6. Weaker layer underneath a stronger layer.

In the model study, when a stronger layer was laid under a weaker layer, as shown in Figure 7, the model did not exactly fit the equation $\log d = M + N (a_1h_1 + a_2h_2 + \ldots)$ as it offered less resistance to deflection. Assuming that $a_2 = 0.27$ for the upper layer as determined from the 2-layer system discussed previously, it was found that as the thickness of the top layer increases, the thickness equivalency contributed by the lower layer decreases. This is shown in Figure 7. The reduction in the value of the thickness equivalency of the lower layer depends on the ratio of the modulus of the 2 layers and also on their thicknesses. Figure 7 also shows that the thickness equivalency of the lower layer increases as its thickness increases.

Figure 7 thus shows that the strength equivalency value, a_1, of the stronger lower layer decreases from 1.0 to 0.6, which is dependent on layer thickness if a_2 is taken as 0.27. Thus, the materials in this system remain below their optimum strengths.

Four Layers—Three Layers Over a Subgrade

In this system, if the modulus of elasticity decreased from top to bottom, no change was noticed from the fundamentals discussed in the 3-layered system with the stronger layer over the weaker layer, i.e., $\log d = a + b (a_1h_1 + a_2h_2 + \ldots)$.

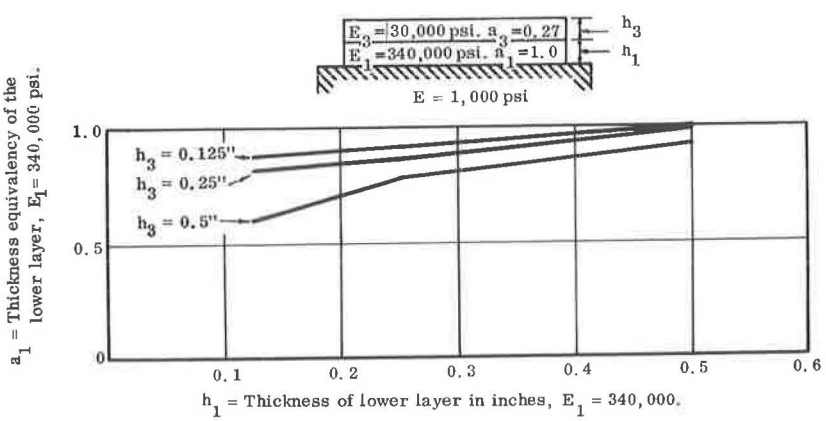

Figure 7. Stronger layer underneath a weaker layer.

The system discussed here, and which sometimes is found in practice, is the case when a weak layer is sandwiched between 2 strong layers. Two systems of sandwiched layers are discussed. In one case, the sandwiched layer had an E_4 = 1,000 psi with the sandwiching layers having an E_1 = 340,000 psi as shown in Figure 8. In the other case, the sandwiched layer had an E_3 = 30,000 psi with the sandwiching layers having an E_1 = 340,000 psi or 450,000 psi. The case of the sandwiched layer with an E_3 = 30,000 psi and sandwiching layers with an E_1 = 340,000 psi is shown in Figure 9.

In both cases the model did not exactly correspond to the equation $\log d = M + N(a_1h_1 + a_2h_2 + \ldots)$ and the following was observed:

1. Assuming that the normal thickness equivalency value is a_1 = 1.0 for the sandwiching layers with an E = 340,000 psi, the strength contributed by the weaker sandwiched layer (i.e., the values of a_2 or a_3) decreased with an increase in thickness of the sandwiching layers (Figs. 8 and 9).
2. By decreasing the modulus of elasticity of a sandwiched layer, the strength contributed by the sandwiched layer decreases considerably as compared to its normal strength and is even sometimes negative (Figs. 8 and 9).

The negative thickness equivalency value shows that the pavements are not reinforced by the sandwiched layer, but that, on the contrary, their total strength is decreased. This same behavior was observed on an experimental project in Virginia where a select soil material was sandwiched between soil cement underneath it and stone base or cement-treated aggregate and asphaltic concrete over it. The deflections as related to supposedly comparable projects were higher, and it is believed that, if this layer had not been introduced, the deflections of the pavement would have been lower. In other words, the thickness equivalency of this sandwiched material was negative, with a higher deflection thus being obtained.

This negative thickness equivalency value could be explained by the observation made on the stress distribution for weak sandwich layers. In these layers the angle of the spread of the load increases with a decrease in the modulus of elasticity of the sandwiched material. It is obvious, therefore, that the introduction of a weaker sandwiched layer provides 2 effects: (a) It spreads the load over a larger area and thus transmits very little load intensity to the underlying layer; and (b) the variation in thickness of the

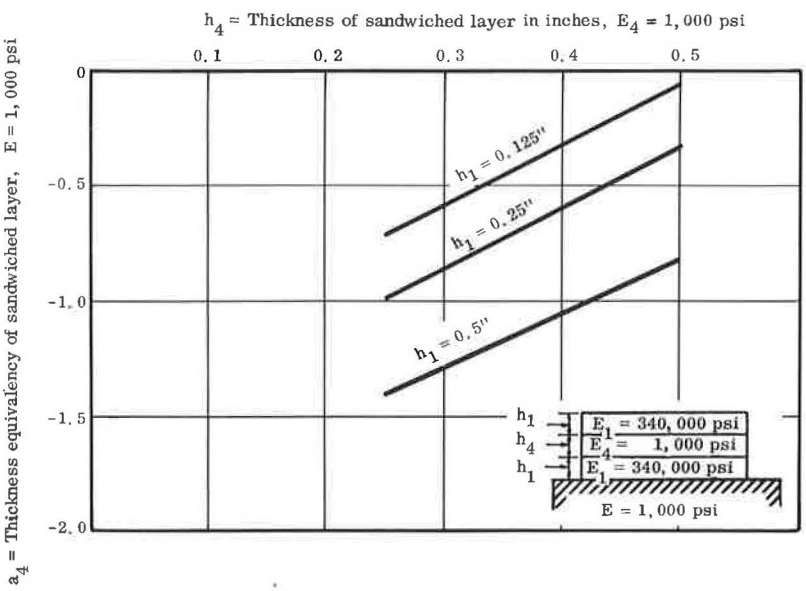

Figure 8. Weaker layer (E = 1,000 psi) sandwiched between two stronger layers.

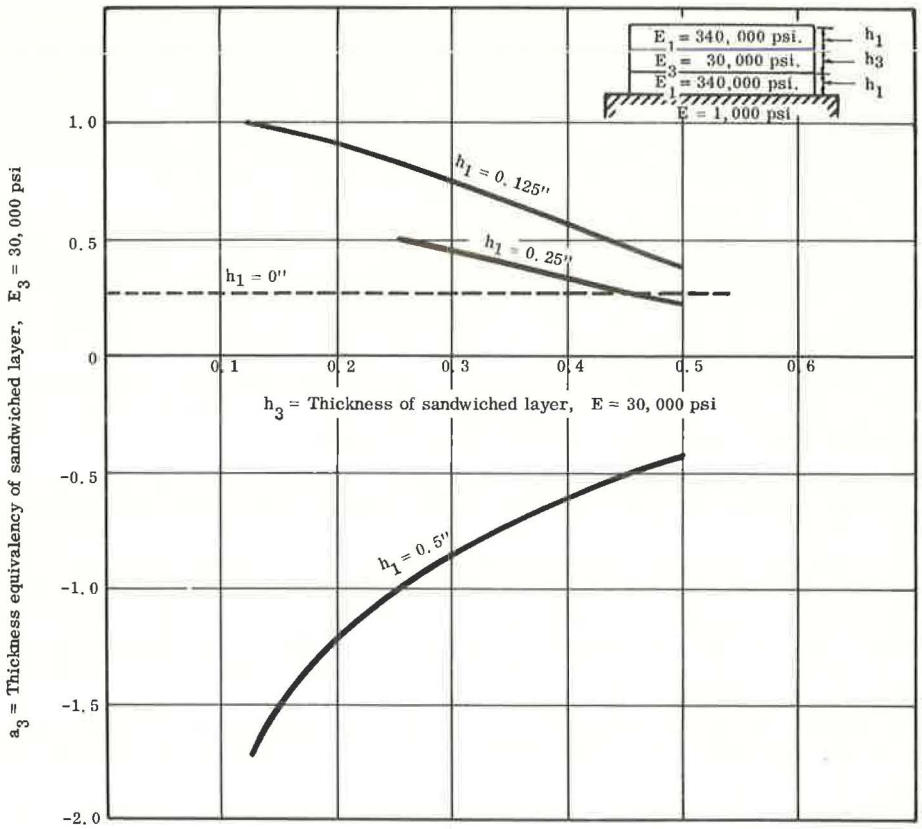

Figure 9. Weaker layer (E_3 = 30,000 psi) sandwiched between two stronger layers.

sandwiched layer does not seem to affect the system much, as long as the sandwich layer remains in compression only.

Use could be made of these 2 effects in the optimum design of pavements. For example, when the subgrade is weak or resilient, a sandwich layer system could be utilized to spread the load over a larger area. Because the load intensity transmitted to the underlying layer is small, the choice of material and thickness design of the underlying layer could be such as to provide more rigidity than strength. Further, the thickness of the sandwich layer need not be increased beyond a certain minimum.

The reduction in the overall structural strength of this type of sandwich system does not climinate its use. There are cases in which this flexible sandwich layer helps in other respects, e.g., by preventing reflection cracks in the bottom sandwiching layer from traveling into the top sandwiching layer.

Stress Distribution in Layered Systems

By means of a polariscope, the stress distributions in layered systems were determined. They were mainly of 2 types: (a) the bulb type, as shown in Figure 10; and (b) the fan type, as shown in Figure 11.

Bulb-Type Distribution—The bulb-type distribution was found in the following cases. The amount of stress and the degree of distribution depended on the thickness and the modulus of elasticity of the materials in the layered system.

1. Two-layer system—The underlying layer was a subgrade of infinite depth having an E = 30 × 10^6 psi. The overlying layer consisted of varying depths of 0.5 in. and above, and the modulus of elasticity was equal to 1,000, 30,000, 340,000, or 450,000 psi.

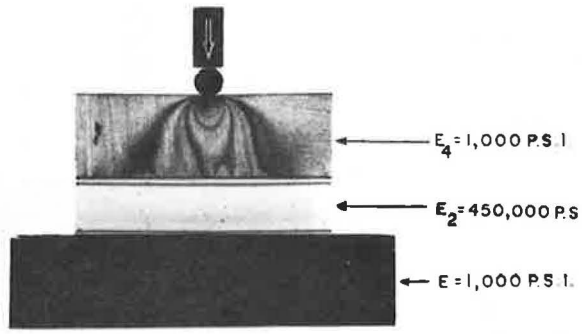

Figure 10. Stress distribution when a weaker layer lies over a stronger layer.

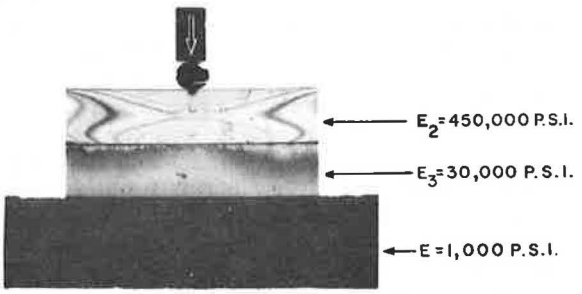

Figure 11. Stress distribution when a stronger layer lies over a weaker layer.

2. Three-layer system—The underlying layer was of infinite depth having an E = 1,000 psi. The overlying 2 layers consisted of the top layer of thickness 0.5 in. or more and an E = 1,000 or 30,000 psi. The layer below the top layer had a thickness of 0.5 in. or more and and E = 340,000 or 450,000 psi, i.e., a modulus of elasticity much higher than that of the material above it. An example of this is shown in Figure 10. The bulb-type distribution is clearly defined in the topmost layer only when the underlying layer or the layered system is very rigid.

From this it is evident that when a weaker layer, such as untreated aggregate or a combination of thin asphaltic concrete over untreated aggregate, lies over a stronger layer, such as a good quality soil cement or cement-treated aggregate, the stress distribution will be bulb type. In other words, it may be stated that, when the lower layer prevents bending of the bottom side of the top layer, the stress distribution will be of the bulb type, and Boussinesq's theory, or theories based on Boussinesq's evaluation, could be applied.

Fan-Type Distribution—The fan-type stress pattern was found in the following cases. The amount of stress and the degree of distribution depended on the thickness and the modulus of elasticity of the materials in the layered system.

1. Two-layer system—The underlying layer was a subgrade of infinite depth having an E = 1,000 psi. The overlying layer consisted of varying depths and had an E = 1,000, 30,000, 340,000, or 450,000 psi.

2. Three-layer system—Various combinations in thicknesses of 2 layers over a subgrade material of infinite depth with an E = 1,000 psi were found to give a fan-type distribution in the top layer. These combinations were as follows: The lower layer had an E = 30,000 psi, and the upper layer had an E = 340,000 or 450,000 psi; or the lower

layer had an E = 340,000 psi, and the upper layer had an E = 450,000 psi. An example of this is shown in Figure 11.

3. Four-layer system—In all the systems tried, the sandwiched layer was weaker than that of the other 2 layers. In almost all cases a fan-type distribution was observed in the top layer. In a few cases, when the ratio of the modulus of the sandwiching layers and the sandwiched layer was low and the thickness of the sandwiched layer was also low, a combination of bulb- and fan-type stress distribution was observed.

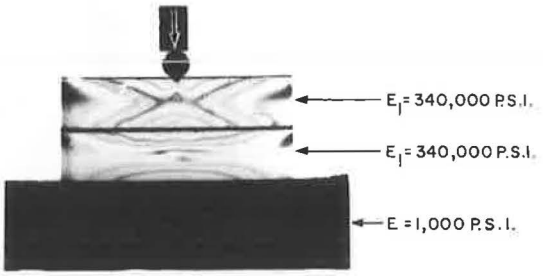

Figure 12. Effect of joint between two layers (in this case of the same modulus).

From the preceding observations, it could be concluded that, when the layer underlying the top layer has a low modulus of elasticity and the overlying layer has the same or a higher modulus of elasticity, fan-type distribution takes place in the top layer. In other words, it may be stated that, when the bottom side of the top layer bends, the stress distribution will be fan type and the design of the top layer should be based on the avoidance of failure along the shear plane as recommended by McLeod (7) and by others.

Effect of Deep Strength—The stress distribution pattern in 2 layers of the same modulus and varying depths lying over a subgrade layer was carried out with partial bond between the 2 layers that could slide over their contact surface after a certain amount of load was applied. The pattern of stress distribution in the top and lower layers was always of the form shown in Figure 12. This shows that when a certain depth of a specified material is laid in more than 1 layer and there is no perfect bond between the 2 layers the structural behavior is different as compared to that of 1 deep layer. The difference in the strength contributed depends on the thickness of the 2 layers and the

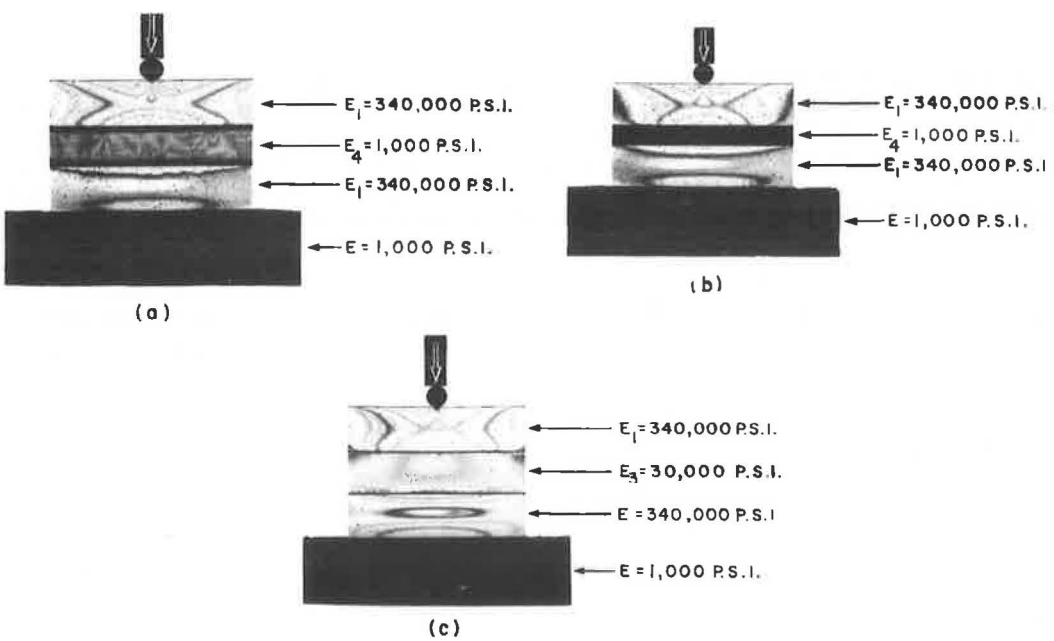

Figure 13. Weaker layer sandwiched between two strong layers (for sandwiched layer, E = 1,000 in a and b and E = 30,000 psi in c).

modulus of elasticity of the material in each. The overlying layer in combination with the underlying layer provides less structural strength than when laid in 1 depth.

Effect of Weak Sandwiched Layers—Figure 13 shows the stress distribution for 3 cases of a 4-layered system. In Figures 13a and 13b, the sandwiched layer consists of material with an E = 1,000, but the thickness of the sandwiched layer in Figure 13b is half the thickness of the sandwiched layer in Figure 13a.

No stress lines are noticed in the sandwiched layers in Figures 13a and 13b; instead, 3 horizontal bands are noticed in Figure 13a. The 2 bands near the contact surfaces with the top and bottom layers were deep brown in color, whereas the central band was light brown. In the case of thinner sandwiched layers, as shown in Figure 13b, the color was uniformly deep brown. Both Figures 13a and 13b therefore indicate uniform stress of compression with higher stresses near the contact surface. This uniform stress of compression indicates an increase in the spread of the load over the top of the sandwiched layer. Thus, it is concluded that the angle of spread of the load increases with a decrease in the modulus of elasticity of the material of the sandwiched layer.

Comparing Figures 13a and 13b, we find that under the same load there is no change in the stress distribution in the lower sandwiching layer, except in the sandwiched layer itself. This shows that the thickness of the sandwiched layer does not affect the system below the top sandwiching layer.

Figure 13c shows a sandwiched layer with a higher modulus of elasticity (30,000 psi) as compared to that shown in Figures 13a and 13b. Stress lines are visible in the sandwiched layer, and the load transfer to its underlying layer is greater than for a weaker sandwiched layer. Thus it shows that, as the modulus of elasticity of the sandwiched layer decreases, the transfer of load through the lower sandwiching layers decreases.

CONCLUSIONS

1. Investigations of satellite pavements on primary and Interstate roads of Virginia and the secondary and subdivision road designs for Virginia, coupled with model studies, have shown the following:

a. The strength contributed by a pavement could be represented by a thickness index of $D = a_1h_1 + a_2h_2 + \ldots$ as given by the AASHO Road Test results. The thickness equivalency value of the material depends on its strength and location in the pavement system.

b. The thickness equivalency value of the material decreases as the thickness of the cover increases, and vice versa.

2. The following conclusions are drawn from the model studies:

a. In the case of a single layer resting on a subgrade, the thickness equivalency of the material in the layer decreases very little with an increase in depth, and hence this variation could be ignored.

b. In a 3-layer system, when a stronger layer lies over a weaker layer (e.g., an asphaltic concrete mat over a stone base), the optimum thickness of the weaker layer is the minimum thickness one could provide economically.

c. In a 3-layer system, when a weaker layer lies over a stronger layer (e.g., untreated aggregate over treated aggregate) the structural strength of the pavement, or resistance to deflection, is less compared to when the layers are reversed.

d. When a weaker layer lies over a stronger layer and if this underlying strong layer prevents bending in the bottom side of the top layer, the stress distribution is bulb type. In such a case, Boussinesq's theory, or theories based on Boussinesq's evaluation, can be applied.

e. When a stronger layer lies over a weaker layer or over a layer of the same strength, the underlying layer permits bending in the bottom side of the top layer, and the stress distribution will be fan-type. In such a case the design of the upper layer should be based on the avoidance of failure along the shear plane.

f. In the case of a 4-layer system with a weaker material sandwiched between 2 layers of stronger materials, the strength contributed by the sandwiched layer decreases with an increase in the thickness of the sandwiching layers.

g. The strength contributed by the sandwiched layer decreases, and even becomes negative, with a decrease in its modulus of elasticity.

ACKNOWLEDGMENTS

The support of the Pavement Section of the Virginia Highway Research Council and J. H. Dillard, state highway research engineer, is gratefully acknowledged. Special thanks are given to F. C. McCormick, professor in the Department of Civil Engineering of the University of Virginia's School of Engineering and Applied Science, for allowing use of his laboratory facilities. The work was financed from highway planning and research funds.

REFERENCES

1. Vaswani, N. K. Design of Pavements Using Deflection Equations From AASHO Road Test Results. Highway Research Record 239, 1968, pp. 76-94.
2. Vaswani, N. K. Design of Flexible Pavements in Virginia Using AASHO Road Test Results. Highway Research Record 291, 1969, pp. 89-103.
3. The AASHO Road Test: Report 5—Pavement Research. HRB Spec. Rept. 61E, 1962.
4. Foster, C. R. Discussion on Nichol's paper on "A Practical Approach to Flexible Pavement Design." Proc., Second Internat. Conf. on Struct. Des. of Flexible Pavements, 1967, p. 657.
5. Vaswani, N. K. AASHO Road Test Findings Applied to Flexible Pavements in Virginia—Final Report. Virginia Highway Research Council, Charlottesville.
6. Seed, H. B., Mitry, F. G., Monismith, C. L., and Chan, C. K. Prediction of Flexible Pavement Deflections From Laboratory Repeated-Load Tests. NCHRP Rept. 35, 1967.
7. McLeod, N. W. Some Basic Problems in Flexible-Pavement Design. HRB Proc., Vol. 32, 1953, pp. 90-118.

Discussion

C. R. FOSTER, National Asphalt Pavement Association—The thickness equivalencies that Vaswani gives in his paper for untreated base and for certain other materials are lower for heavy-duty roads (primary and Interstate) than for light-duty roads. He stated that the reason for the pattern is the depth of cover. For heavy-duty roads, the untreated base would be deeper in the section than on a light-duty road.

Vaswani offers 2 elements of data to support the use of lower equivalencies for the heavy-duty roads. One element of data is Figure 1 taken from Figure 36 of the AASHO Road Test (3) and is presented with the comment "as the depth of pavement increases, the thickness index required decreases." However, thickness index is not the same as thickness equivalency, so this plot does not support a decrease in thickness equivalency with an increase in depth of cover.

Vaswani's other element of data is this statement: "The reduction in thickness equivalency with an increase in depth of cover thickness has also been pointed out by Foster." Although this appears to lend support, it really does not because we used different thickness equivalencies. Vaswani assigned unity to asphaltic concrete, whereas I assigned unity to the untreated base. My values are the reciprocal of his. If I convert my statement to the thickness equivalency as defined by him, it would have to read "an increase in thickness equivalency with an increase in depth of cover."

Figure 14 shows a plot of the data of the average thickness equivalency of the hot-mix asphalt base in the AASHO Road Test versus thickness of hot-mix asphalt base that I prepared from AASHO Road Test data (3). The 5 points for each load represent thicknesses of untreated base divided by thickness of asphalt base at serviceability indexes of 1.5, 2.0, 2.5, 3.0, and 3.5 after 1,114,000 repetitions plotted against the thickness of the hot-mix asphalt base. Adjustments were made for variations in surface

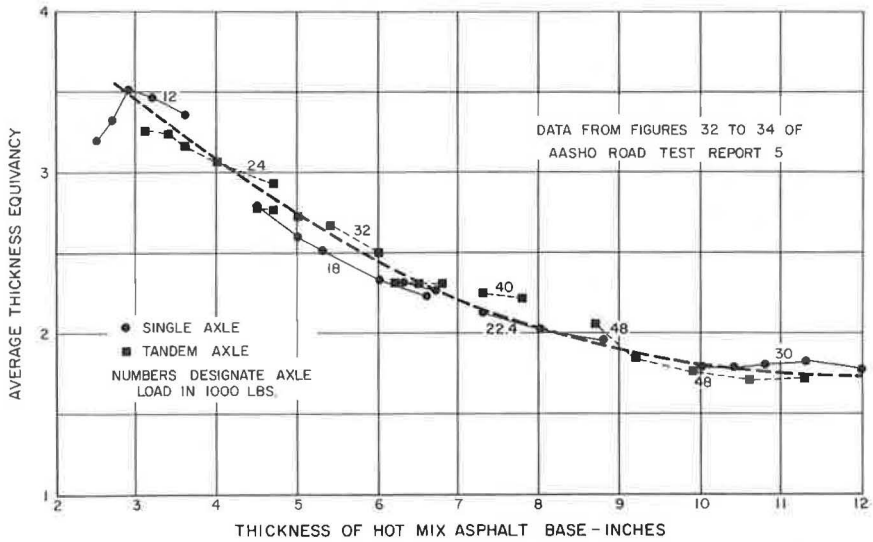

Figure 14. Average thickness equivalency versus thickness of hot-mix asphalt base.

and subbase thicknesses by using the procedures described in the report. Wheel loads not tested were interpolated.

Without question, the thickness equivalency (as I define it) in the AASHO Road Test decreased with increase in thickness of hot-mix asphalt base. A review of the variation in strength with depth in base course materials offers a reasonable explanation of the pattern shown in the AASHO Road Test.

At this point we need to define what we mean when we say strength. Strength is commonly used in reference to a breaking value such as in concrete. However, we are not concerned with this type of strength. What we are concerned with is the ability of the base course to develop strength under loading. An untreated base course will have a very small residual capacity to resist load because of tension in moisture films and surcharge of the overlying pavement, but the majority of the resistance to load is developed from the load being applied. Ability to develop strength under load is rated by the modulus of elasticity. Because the strains in the pavement are low, generally well under 1 percent, we are concerned with the modulus at low strains. The modulus of untreated base courses at low strains is highly dependent on the degree of compaction. Test data plus my observations over the years show that it is impossible to obtain a high degree of compaction and a high modulus in the first few inches of untreated base over the subgrade. Figure 15, from the Barksdale Field tests (8), shows a strong trend for the in-place CBR of the base material, both as constructed (indicated by tests outside the traffic lane) and after traffic, to increase with the height of the test above the subgrade. Since preparing this plot, which incidentally was prepared in 1943, I have observed this pattern in practically all the other test pits or trenches that I have seen cut in pavements. This pattern was vividly brought out during studies (9) conducted at the Waterways Experiment Station in the mid-1950's to develop CBR design curves for metal landing mat. An equivalency concept was used in that a given design of metal mat was rated as the equivalent of a given thickness of crushed aggregate base. With this concept, the existing CBR design curves for flexible pavements could be used to produce curves for landing mats. (Incidentally, the concept worked well, but this is not the point of discussion.) This equivalency concept was spot-checked by traffic tests. Test sections were built with mat placed on the subgrade and on 3, 6, and 12 in. of crushed aggregate base course. Although the base material was a dense-graded crushed

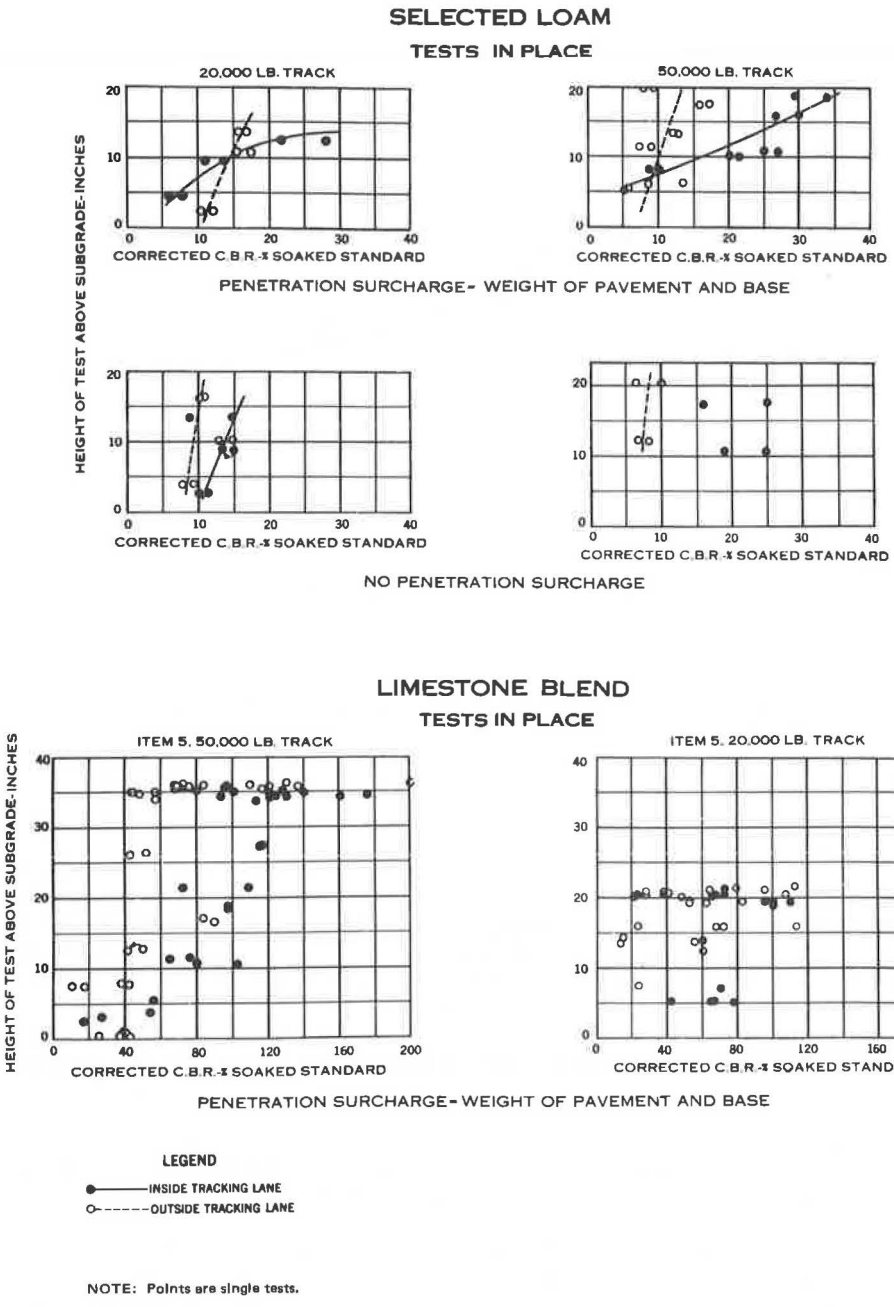

Figure 15. CBR height of test above subgrade--selected loam and limestone blend.

limestone that had developed CBR values well above 80 in other tests where thick lifts were used, it was not possible to obtain a CBR of 80 in the 3-in. sections even though these were placed on a fairly strong subgrade (CBR 14) or even in the 6-in. sections placed on a weaker subgrade (CBR 5). Average CBR values are given in the following data:

Item	Crushed Aggregate Base		
	3 in.	6 in.	12 in.
Low CBR subgrade			
Number of test sections	—	24	16
Average CBR of subgrade	—	4.9	5.8
Average CBR of base	—	50	86
Average density of base	—	144.8	145.2
Ratio CBR of base-subgrade		10.2	14.9
Medium CBR subgrade			
Number of test sections	7	15	—
Average CBR of subgrade	13.6	11.2	—
Average CBR of base	51	93	—
Average density of base	140.0	146.5	—
Ratio CBR of base-subgrade	3.0	8.3	

It should be noted that these averages represent a large number of tests. For example, a total of 24 test sections were built with 6 in. of base over the weaker subgrade. At least 3 CBR tests were made in each section. All values represent in-place tests on the as-constructed base course except for those in the 3-in. section. The as-constructed values for the 3-in. section showed wide variability. Those after a small amount of traffic (40 coverages) were much less variable, and these were used. These tests show that the in-place CBR of the base course was dependent on both the CBR of the subgrade and the thickness of the base. Apparently a large part of the variation is due to density, because there is a general trend for the CBR to increase with an increase in density. Figure 16 shows a plot of these CBR data with CBR plotted as a ratio of base CBR to subgrade CBR against base thickness. It is believed there are certain natural limits. First, if the subgrade is very strong, the ratio will probably approach 1. Also, regardless of the subgrade strength, the ratio would probably approach 1 at a base thickness slightly under 2 in., which is the diameter of the CBR piston. The data shown in Figure 16 indicate that the ratio increases slightly with a decrease in subgrade CBR and rapidly with an increase in base course thickness. Interpolated curves for subgrade CBR values of 5 and 10 are shown in Figure 16. Heukelom and this author (10) showed that in-place CBR values correlate fairly well with moduli measured in place with vibratory methods and suggested the conversion at 100 to 1 in metric units,

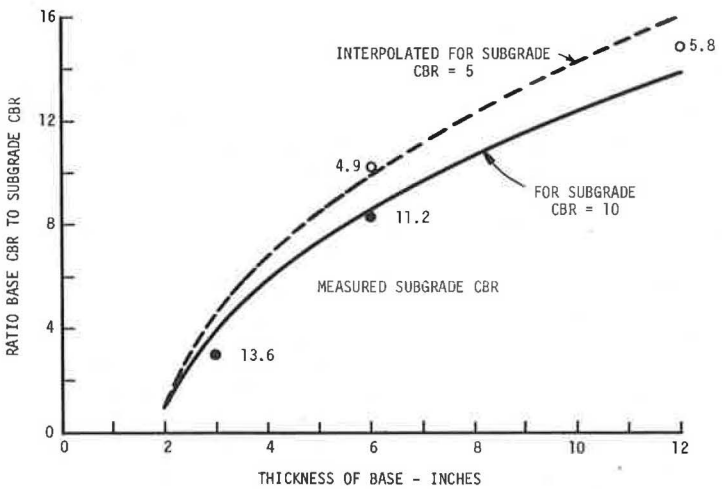

Figure 16. Ratio of base and subgrade CBR versus base thickness.

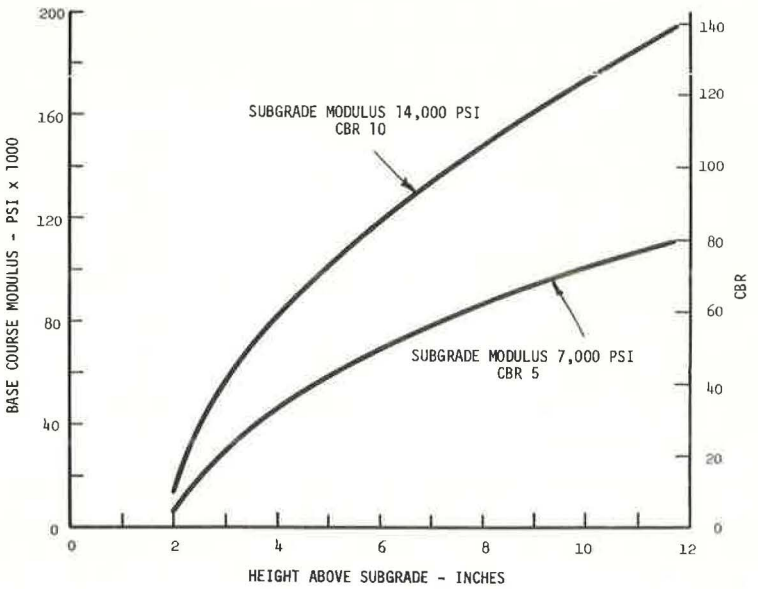

Figure 17. Base course modulus versus height above subgrade.

which is approximately 1,400 to 1 in English units. Applying this conversion factor (CBR x 1,400 = moduli in psi) to subgrades with CBR values of 5 and 10 and to the ratios shown in Figure 16 produces the variation in moduli with subgrade moduli and base course thickness shown in Figure 17. This plot shows that the base course modulus will increase rapidly with height above the subgrade, being quite low directly above the subgrade and quite high when substantial thicknesses of base are used.

Treated base courses, such as hot-mix asphalt base and cement-treated bases, develop stiffness by cementation, and the moduli at low strains are not so dependent on compaction as untreated base courses. The modulus of a given hot-mix asphalt base will also vary according to rate of loading and temperature. Because we are concerned mainly with moving loads, rate of loading is not of primary concern except that persons running laboratory tests should use rates of loading comparable to those experienced on the road.

The temperature within a hot-mix asphalt base course at any one time is a complex function of heat flowing in and heat flowing out. However, the average temperature (average for year) at the bottom of a thicker base would be a little lower than the average for a thinner base. Thus, the modulus of a hot-mix asphalt base could be expected to increase a little with depth. For the purpose of this illustration, however, we will assume that the average modulus is constant with depth.

We have no in-place data on the modulus of hot-mix asphalt pavement, so we have to depend on laboratory tests and inference. Values reported in the literature range from 200,000 to 2,000,000 psi. The performance of hot-mix asphalt base under traffic implies, at least to me, a modulus in the range of 1,000,000 to 1,500,000 psi, and for the following illustration I have used a value of 1,250,000 psi.

The layered theory of pavement design presented by Burmister (11) in 1943 shows that the stress induced in a given subgrade under a given condition of load is primarily a function of the thickness and moduli of elasticity of the overlying layers. A base with a high modulus of elasticity would transmit a lower stress to the subgrade than a low modulus base of equal thickness. To state this in another way, a given thickness of low modulus base would transmit the same stress to the subgrade as a lesser thickness of high modulus base. Thus, the ratio of the elastic modulus of one base course to the elastic modulus of another base course is a form of thickness equivalency.

The data shown in Figure 17 can be used to show that the ratio of the modulus of hot-mix asphalt base to the modulus of untreated base decreases with thickness of untreated base. For example, assume that a subgrade has a CBR of 5 and thicknesses of untreated base of 6 and 12 in. For the 6-in. base the modulus would be about 7,000 psi at the bottom and about 70,000 psi at the top for an average of 38,500. The hot-mix asphalt base course modulus of 1,250,000 psi is about 32 times that of the untreated base. For the 12-in. thick untreated base, the average modulus would be about 60,000 psi and the ratio to 1,250,000 psi would be about 21. To date we have no correlation between thickness equivalencies and ratio of moduli of base courses; but because the ratio decreases with an increase in thickness of untreated base, it could be expected that the thickness equivalency would also decrease with an increase in thickness of untreated base.

Although the preceding statement is literally true, a clearer concept is obtained if the situation is related to height above the subgrade. Figure 18 shows this for pavement sections with 6 and 12 in. of untreated base. The sections on the left have untreated base and those on the right have hot-mix asphalt base. In each case there is a 2-in. surface course. The hot-mix asphalt base is separated into 1-in. increments, and a line is drawn from the top and bottom of each increment to the amount of untreated base to which the increment is equivalent. No claim is made that the equivalencies assigned to each increment of hot-mix asphalt base are correct; they were selected merely to illustrate the situation. In the upper part of Figure 18 (the 6-in. untreated base) the first inch of hot-mix asphalt base above the subgrade is shown as being equivalent to 3.5 in. of untreated base and the second inch is shown as being equivalent to only 2.5 in. of untreated base. The reason, reference again to Figure 17, is that the modulus of the untreated base increases with height above the subgrade resulting in a decrease in ratio of moduli with increase in height above subgrade. In the lower part of Figure 18 (the 12-in. untreated base) the first inch of hot-mix asphalt base is still equivalent to 3.5 in. of untreated base and the second inch is equivalent to 2.5 in., the same as for the 6 in. of untreated base. But because the untreated base is getting stronger with increase in height above the subgrade, the equivalency for each increment of hot-mix asphalt base decreases with height above the subgrade. As a result, the average equivalencies decrease with the total thickness of base. This is the reverse of the pattern given by Vaswani, so in my opinion his conclusion 1b is invalid.

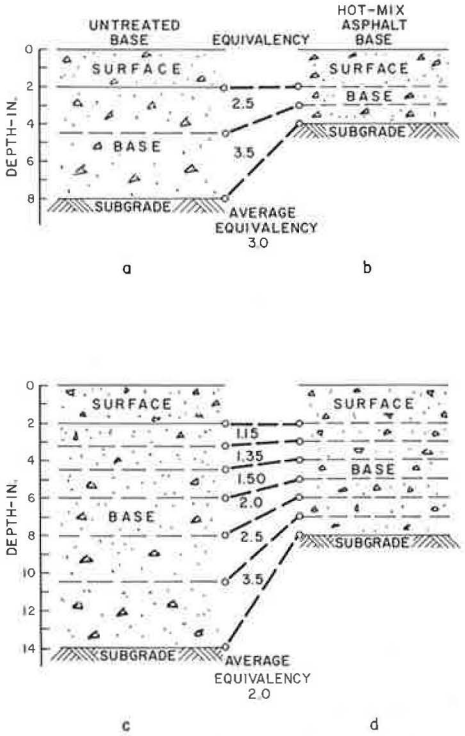

Figure 18. Thickness equivalency, base course, and height above subgrade.

I think that the model studies reported by Vaswani deserve special attention, particularly those in which a weak layer is sandwiched in between 2 strong layers. I have investigated 2 cases of heavy-duty roads consisting of a strong subbase, a relatively thin layer of untreated base (4 in. in one case and 7 in. in the other), and a fairly thick asphalt layer that cracked badly under very low deflections. I believe that the untreated base was not developing an adequate modulus under the low strain involved with the result that the asphalt layer was badly overstressed. I have seen many other cases of distress where I think this situation occurred.

References

8. Service Behavior Test Section, Barksdale Field, Louisiana. U. S. Army Corps of Engineers, Little Rock, Oct. 1944.
9. Criteria for Designing Runways to Be Surfaced With Landing Mat and Membrane-Type Materials. U. S. Army Engineer Waterways Experiment Station, Vicksburg, Miss., TR3-539, April 1960.
10. Heukelom, W., and Foster, C. R. Dynamic Testing of Pavements. ASCE Trans., Vol. 127, 1962, p. 425.
11. Burmister, D. M. The Theory of Stresses and Displacements in Layered Systems and Application to the Design of Airport Runways. HRB Proc. Vol. 23, 1943, pp. 126-154.

N. K. VASWANI, Closure—Reference is made to the second paragraph of Foster's discussion. Technically, there is no difference between the application of thickness equivalency values as determined for Virginia and described in this paper and the strength coefficient values given in the AASHO Road Test results. They are both nondimensional quantities indicating the relative strengths contributed by the materials in the pavement. Thus, in the AASHO Road Test results, the strength coefficient values of 0.44 for asphaltic concrete, 0.14 for untreated stone base, and 0.11 for subbase material have the same application in design principles as do the Virginia thickness equivalency values of 1.0 for asphaltic concrete, 0.35 for untreated stone base, and so on. Furthermore, these values show that, in the AASHO Road Test results, 1 in. of asphaltic concrete provides the strength equivalency of 0.44/0.14 = 3.1 in. of untreated stone base. Similarly, thickness equivalency values in the Virginia method indicate that 1 in. of asphaltic concrete is equal in strength to 1.0/0.35 = 2.9 in. of untreated stone base.

In reference to paragraphs 3 and 4 of the discussion, the AASHO Road Test results are based on a model equation in which the strength contributed by a layer is given by a x h where a is the strength coefficient or thickness equivalency of a material in a layer h inches thick. Based on this model equation, if a layer of untreated stone base contributing a strength equal to a_3h_3 is to be replaced by a layer of, say, asphaltic concrete, one has to apply the equation $a_1h_1 = a_3h_3$, where a_1 and h_1 are the strength coefficient (or thickness equivalency value) and thickness of the asphaltic concrete layer respectively.

Foster assumes that $a_3 = 1$; hence, in Figure 14, $a_1 = h_3/h_1$ and thus the graph in this figure is for a_1 versus h_1. This graph shows that, as h_1 increases, a_1 decreases. This is why Foster concludes (11) "...there is a decrease in thickness equivalency with an increase in thickness of the hot mix asphalt base...." This statement supports my conclusion that the thickness equivalency decreases with an increase in the thickness or depth of the pavement or the depth of cover.

Except for the last 3 paragraphs, the remainder of Foster's discussion concerns his valuable investigations and observations. In the third from last and second from last paragraph, Foster presents arbitrarily chosen values of the modulus with which I beg to differ. Based on my investigation, I feel that for the same pavement strength a 12-in. thickness of untreated base will have a lower thickness equivalency value than a 6-in. layer of the same material in the base. The values of E = 35,000 psi contributed by the 6-in. untreated stone base and E = 65,000 psi contributed by 12 in. of untreated stone base—to provide the same strength—appear to be illogical. If the strength values were reversed, which should be the case, Foster would come to the same conclusion as given in my conclusion 1b.

In reference to the last paragraph of Foster's comments, I am pleased to note that my observations on a weak sandwich layer between 2 strong layers in the model studies have proved to be consistent with the results of the observation made by him. But this observation may not always hold true. Because, as shown in Figure 9 with lower thicknesses and an insufficiently low modulus of elasticity of the sandwich layers, the thickness equivalency value of the sandwich layers increases. Thus, in Figure 9 the 2 curves

above the dotted line having $h_1 = 0$ show that the sandwich layer has contributed toward the increase in the thickness equivalency value of the sandwich layers. It has also been noted in pavements in Virginia that a 6-in. stone aggregate base sandwiched between 6 in. of cement-treated aggregate subbase and 6 in. of asphaltic concrete on top has given very good results. This investigation, in fact, shows that very carefully designed sandwich layers would offer economical designs. If proper care is not taken, poor results are likely to be obtained, as was proved in one of the experimental projects in Virginia in which a weak layer of select material was sandwiched between a cement-treated subgrade underneath it and a stone base and asphaltic concrete layer over it. The deflections in this case were more as compared to the deflection obtained by our design method based on the AASHO Road Test results.